Temporal and spatial variation of erosion processes in the Illgraben, an alpine debris flow catchment

Temporal and spatial variation of erosion processes in the Illgraben, an alpine debris flow catchment

Diploma thesis at the Department of Environmental Sciences (UWIS) at the Swiss federal institute of Technology Zurich in cooperation with the Swiss Federal Institute for Forest, Snow and Landscape Research (WSL) and the Institute of Environmental Engineering (IfU) at the Swiss federal institute of Technology Zurich.

Author:
Corina Gwerder
Rebmoosweg 35
5200 Brugg
gwerderc@student.ethz.ch

Supervised by:
Dr. Alexandre Badoux (WSL)
Dr. Brian McArdell (WSL)
Dr. Peter Molnar (ETHZ)

January, 2007
Department of Environmental Sciences (UWIS) at the Swiss federal institute of Technology Zurich (ETHZ)

Cover picture the Illgraben catchment, view from the north to the south (WSL)

Abstract

For this thesis, temporal and spatial variations of sediment erosion processes in a steep catchment were analyzed. Erosional processes include both hillslope and gully erosion, and also mass movement processes that are dominated by debris flows. Debris flows are a very destructive form of rapid mass slope movement in mountainous areas and typically arise where the rapid onset of water flow mobilizes unconsolidated debris mantling steep slopes.

The Illgraben catchment (9.5 km^2), situated near Susten (Leukerbad) in canton Valais, is characterized by a very high degree of sediment transport activity and shows rapid dynamic landscape changes and evidence of significant erosion events, including frequent large debris flows. In addition to the high degree of geomorphic activity, the relatively easy access and abundant instrumentation make it an ideal place for such a project.

In contrast to the current research on the debris fan, this thesis is directed at the catchment. The overall goal was a better understanding of the erosion processes operating in the Illgraben catchment, their location and in particular the magnitude and timing of surficial erosion on typical geomorphic sub-systems in comparison to well-constrained estimates of the total sediment exported from the catchment.

Analyses of the character and behavior of the geomorphic or landscape systems and how they are geomorphically connected provided a platform to interpret the overall sediment transfer processes operating in the Illgraben catchment. The main focus was determination of sediment yield and temporal changes in the areas of the various systems, which can be used to infer the nature of the coupling relationship among them. Following a recent advance in the literature, a distinction was made between coupled- and decoupled systems, where the decoupled system was divided further in three subsystems (grassland, forest and decoupled erosion). The analysis of the character and sediment transport rates of those systems was done with field work, where hillslope erosion was measured using a standard silt fence technique, aerial- and ortho-photography work combined in a GIS environment, petrography composition of debris flow sediments and their source areas, and climate and precipitation information.

Analyses of aerial photographs from years 1959, 1999 and 2004 showed changes inside of the decoupled system, but the spatial relation between the coupled- and decoupled system stayed almost constant. Within the decoupled system, an increase of forest and decoupled erosion area as well a decrease of grassland was measurable. The increase in the area of the forest subsystem corresponds with the natural afforestation related to landscape use changes that has been observed all over Switzerland. How much of the increase of the decoupled erosion area is related to changes in the landscape use or climate warming (and the associated higher precipitation intensities) could only be speculated. Using climate observations from the Sion station, a trend towards warmer temperature was evident, but a trend towards a higher number of precipitation events with a high intensity could not be discerned using the available daily precipitation sums from stations Sierre, Hérémence and Grimentz.

In the coupled system, only the overall erosion rate for the catchment was determined. The mass discharge rate was calculated from the weight, height, and velocity of debris flows at a force plate situated near the basin outlet. While large temporal fluctuations have been reported in the coupled system (e.g. periods of aggradation and degradation of on the order of a few meters), they were not investigated in this work. The erosion rate in the coupled system was calculated to be three orders of magnitude larger than the values measured in the decoupled system, and therefore the coupled areas contributed more than 99% of the sediment leaving the catchment. The sediment transport rate in the coupled system is strongly related to rainfall intensity (McArdell and Badoux, in Prep).

Variability in the rate of measured sediment transport in the decoupled systems was explored using rainfall intensity and other parameters. The decoupled system surprisingly showed almost no correlation with precipitation as in the coupled system where every precipitation event during the measurement period with an intensity larger than 2 mm/10 min at Pluviometer 3 (one of the automatic precipitation stations in the catchment) was associated with debris flow occurrence. The sediment amount in the silt fence plots depended mainly on the vegetation layer, slope angle, grain size composition and the measurement interval, where the missing correlation with precipitation in the decoupled system could be due to the relatively small precipitation amounts during the measurement period, a lack of surface runoff in the decoupled system related to large soil infiltration capacities, etc.

Additional analyses from a collaborative and parallel project at the Univ. of Bern provide complimentary evidence which supports the work in this thesis, such as the conclusion from the petrographic analysis of the sediment in the coupled system which indicates that more than 60% of the sediment output came from approximately 6% of the entire catchment area. Also, the volume of sediment delivered by the Illgraben to the Rhone River is estimated to be more than 20% of the yearly Rhone sediment budget.

The division into a coupled- and decoupled system as well as the subsequent independent observations clearly showed large differences in landscape connectivity and demonstrated the utility of this approach for interpreting the distribution of geomorphic processes occurring in this catchment and may be applicable to other steep Alpine catchments.

Acknowledgements

This diploma thesis in Environmental Science (UWIS) was established at the Swiss Federal Institute of Technology Zurich (ETHZ) under the supervision of Dr. Peter Molnar (ETHZ) and the Swiss Federal Institute for Forest, Snow and Landscape Research (WSL) under the supervision of Drs. Alexandre Badoux and Brian McArdell.

I would like to express my special thanks to my supervisors Dr. Alexandre Badoux, Dr. Brian McArdell and Dr. Peter Molnar. They all guided my studies and left me a lot of freedom to follow up my own ideas.

Beside my supervisors I found a very component advisor in Prof. Fritz Schlunegger at University of Berne. He suggested many new ideas and approaches for this thesis and embedded my work into current research topics.

Due to the collaboration with the University of Berne, I could benefit from the cooperation with David Schnydrig, a master student in Prof. Schlunegger's group, regarding several studies. I would like to thank David Schnydrig for this motivating teamwork as well as for his patience and endurance with the orthophotography software.

Finally, I would like to thank all my installation helpers, field workers, computer- and software supporters and manuscript readers: Kari Steiner, Christian Frischknecht, Christoph Graf, Leslie Hsu, Dirk Rieke-Zapp, Corinna Wendeler, Patrick Thee, François Dufour, Lydia Ziltener, Annemarie Schneider, Nicolas Merky, Thomas Scheuner, Margrit Gwerder, Kurt Gwerder and Massimilano Zappa (see A.6.2). I apologize to anyone who may have been forgotten in this list.

Table of Contents

Figures and tables

Figures

Tables

1 Introduction

1.1 Motivation

Soil erosion and the occurrence of landslides are among the major environmental problems and natural hazards in an alpine environment. The loss of soil from a field, the breakdown of soil structure, the decline in organic matter and nutrient, the reduction of the available soil moisture as well as the reduced capacity of rivers and the enhanced risk of flooding and landslides all are erosion processes. In all regions with steep relief and at least occasional rainfall, debris flows occur in addition to surface erosion processes. Their high flow velocity, impact forces, and long run out, combined with poor temporal predictability, cause debris flows to be one of the most hazardous landslides types. During the last decades the hazard was intensified due to land use change, deforestation and climate change that all lead to an accumulation of natural disasters. In a recent example, more than 1000 people were swept away by the mudslides that buried villages at the foot of Mayon volcano, 330 km south of Manila, in December 2006 (statement by Red Cross). Efforts to better understand the initiation and behavior of debris flows as well as in adapted safety measures are needed.

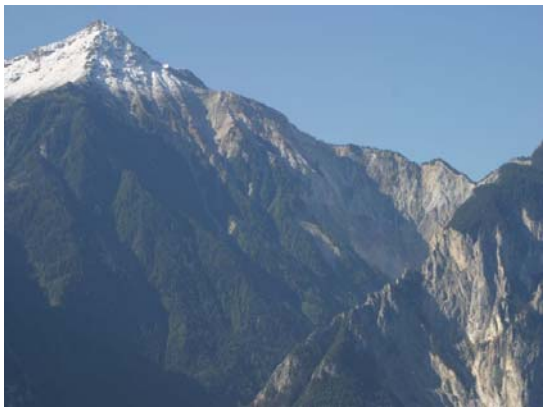

Figure 1-1 Illgraben catchment with the Illhorn, view from north to south (Corina Gwerder)

Figure 1-2 Illgraben catchment, view from south to north (Corina Gwerder)

At the Swiss Federal Institute for Forest, Snow and Landscape Research (WSL), the Avalanche, Debris Flow and Rockfall Research Department has been operating several debris flow observation stations in the Swiss Alps for the last six years. The results gained at these investigation areas and from laboratory studies contribute to a better comprehension of debris flow behavior in mountain catchments. Working at the Illgraben (Figure 1-1 and Figure 1-2), the research unit benefits from frequent debris flow activity, with easy accessibility and good infrastructure.

I became acquainted with the Illgraben and the processes that occur in this catchment during a practical training in the Debris Flow Group of the WSL (a subunit of the Avalanche, Debris Flow and Rockfall Research Department) and was fascinated by this natural process. Subsequently, I was given the opportunity to carry out a diploma thesis in this catchment which offered me the possibility for a more specific examination of this interesting topic.

1.2 Scope of the study

1.2.1 Problem

The Illgraben catchment is one of the most active debris flow catchments worldwide. Its impressive catchment and fan, with the Pfyn-forest, are component of the Swiss geography classes, where the impressive debris flows are dreaded for a long time. Due to frequent events as well as the proximity of the channel to settlements and infrastructure, the Illgraben also offers an interesting site for scientific investigations. Since this century many researches are done at the debris fan, debris flow behavior and different instrumentations shed light on their properties (composition, flow depth, density, velocity, volume, forces etc.). However, very little was known about the initiation of a debris flow, and/or on their origin or composition. Largely, that due to inaccessibility resulting from steep slopes, wildness, roughness and difficult accessibility (Figure 1-3). Now attention to a better understanding of the initiation and triggering processes in order to receive an integral comprehension of the entire debris flow process that happen in the Illgraben and sediment movement in steel catchments in general.

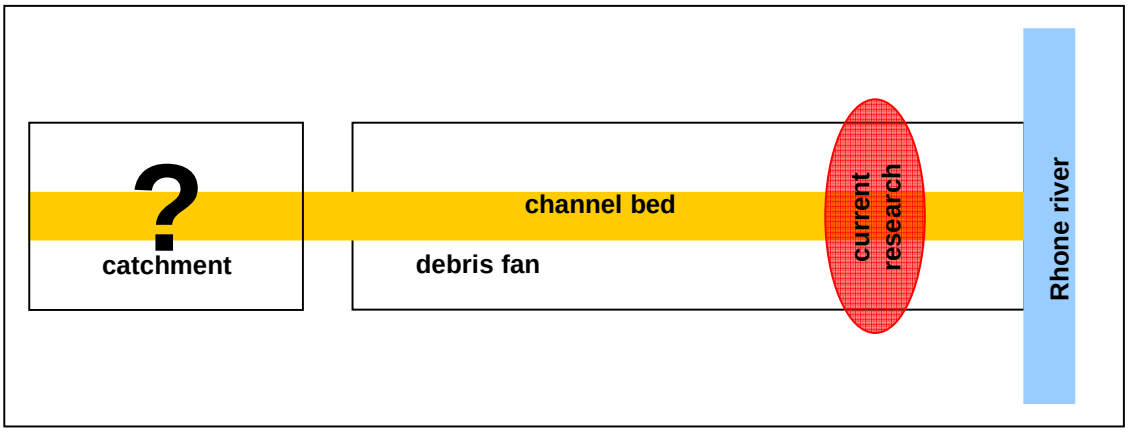

Figure 1-3 Schematic view of the knowledge of erosion processes in the Illgraben catchment (Corina Gwerder)

1.2.2 Goal

The goal of the present thesis is to investigate the erosion processes that take place in the Illgraben catchment. In addition to a general assessment, a general view and a better understanding of the erosion processes that happen in the catchment is necessary. Temporal and spatial variations of the erosion processes as well as the influence of variations in the landscape connectivity on the erosion behaviour are investigated. The results were gained using different methods. For the examining temporal and spatial variation of erosion, aerial photography observations and field experiments were applied. Specifically, the following questions are addressed at the Illgraben catchment:

- Analysis of landscape compartments: How large were the fractions of forest, grassland and erosion areas compared to the entire catchment area in 2004, 1999 and 1959?
- What is the slope angle distribution in the different subsystems (forest, grassland, decoupled erosion) and systems (coupled, decoupled)?
- Did some recognizable area changes take place and how can they be explained?
- What are the process rates in the coupled and decoupled hillslope subsystems (forest, grassland, decoupled erosion)?
- Is it possible to explain observed differences between the process rate measurements on decoupled hillslopes as a function of e.g. precipitation, grain size distribution, slope angle and different land cover (forest, grassland, decoupled erosion, etc.)?
- How strongly or efficiently were the two subsystems coupled, do they correlate? How much has the coupled system differed from the decoupled system in its additions, reactions and processes? How was the catchment connectivity in the Illgraben catchment in 2004, 1999 and 1959? How strong was the change in and among individual subsystems (forest, grassland, decoupled erosion and coupled system) during the periods 1959-2004, 1959-1999 and 1999-2004?
- How large is the yearly sediment output of the catchment?
- Where is the debris flow initiation area located?

The examination of all these questions will help to acquire a better knowledge and understanding of the erosion processes going on in the Illgraben catchment (Figure 1-4).

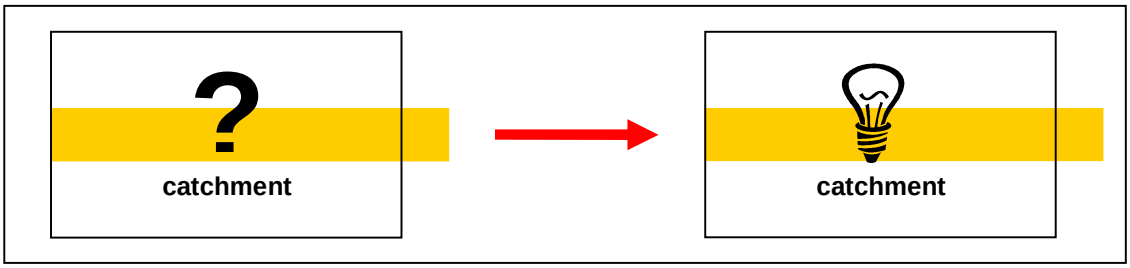

Figure 1-4 Schematic view of the coal of this thesis in the Illgraben catchment

1.2.3 Hypothesis

There are different hypotheses that will be verified among others in this thesis:

1. There is a strong influence of the grain size distribution, slope angle and the vegetation layer on erosion processes.
2. There are differences in the erosion process rates between the subsystems forest, grassland and decoupled erosion.
3. On the silt fence plots, higher erosion rates are expected during periods including intense precipitation events than during periods with little precipitation.
4. Different behaviors and processes are expected between the coupled- and decoupled systems.
5. Higher sediment rates and outputs are expected in the coupled system than in the decoupled one.
6. A high sediment output from the coupled areas in the northern catchment side is expected.
7. An increase in size of the coupled system at the expense of the decoupled system during the last 45 years is expected.
8. An increase in size of the decoupled erosion subsystem during the last years is expected.

1.2.4 Structure

In Chapter 2 the theoretic background of hydrogeomorphology, landscape connectivity, erosion and debris flow are presented.

The study area, its characteristics and history, other studies and instrumentation, geology, morphology, vegetation and soil as well the climate are presented in Chapter 3.

Chapter 4, “Data and methods”, contains all data used and explanations of the applied methods: Field work, aerial photographs, process rates and sediment budget as well the distributions and characteristics.

Chapter 5 contains the results with corresponding discussions about climate, the silt fence measurements, the aerial photography work, and the petrographic composition of the coupled sediment output as well a summary of all results.

In Chapter 6 the conclusion and perspectives are presented where the thematic conclusions, the possibilities and limits of the applied methods and the perspectives are listed.

2 Background

2.1 Hydrogeomorphology

As we work to predict social, economic, climatic or environmental changes, we recognize the need to appraise notions of connectivity, whether examined in terms of human-human interactions, human-landscape interactions, or interactions within the landscape itself (Brierley, 2006). In a catchment, different processes and interactions of hydrological and geomorphological character occur and influence each other. In the past, the hydrologic and geomorphic processes operating in catchments have typically been assessed separately. Today many research projects link various hydrologic and geomorphologic processes. This linkage among different processes leaded to an interdisciplinary science called hydrogeomorphology (Sidle and Onda, 2004). Knowledge of coherences between hydrological and geomorphologic processes is important for the comprehension of the entire system, its characteristics and phenomena (Figure 2-1). Catchment-specific knowledge of landscape character, behaviour, connectivity and evolution provides a physically-based platform to address effective management (Brierley, 2006). For example, at a location threatened by a natural hazard, where a mitigation concept should be developed, it is necessary to consider all the relevant processes occurring.

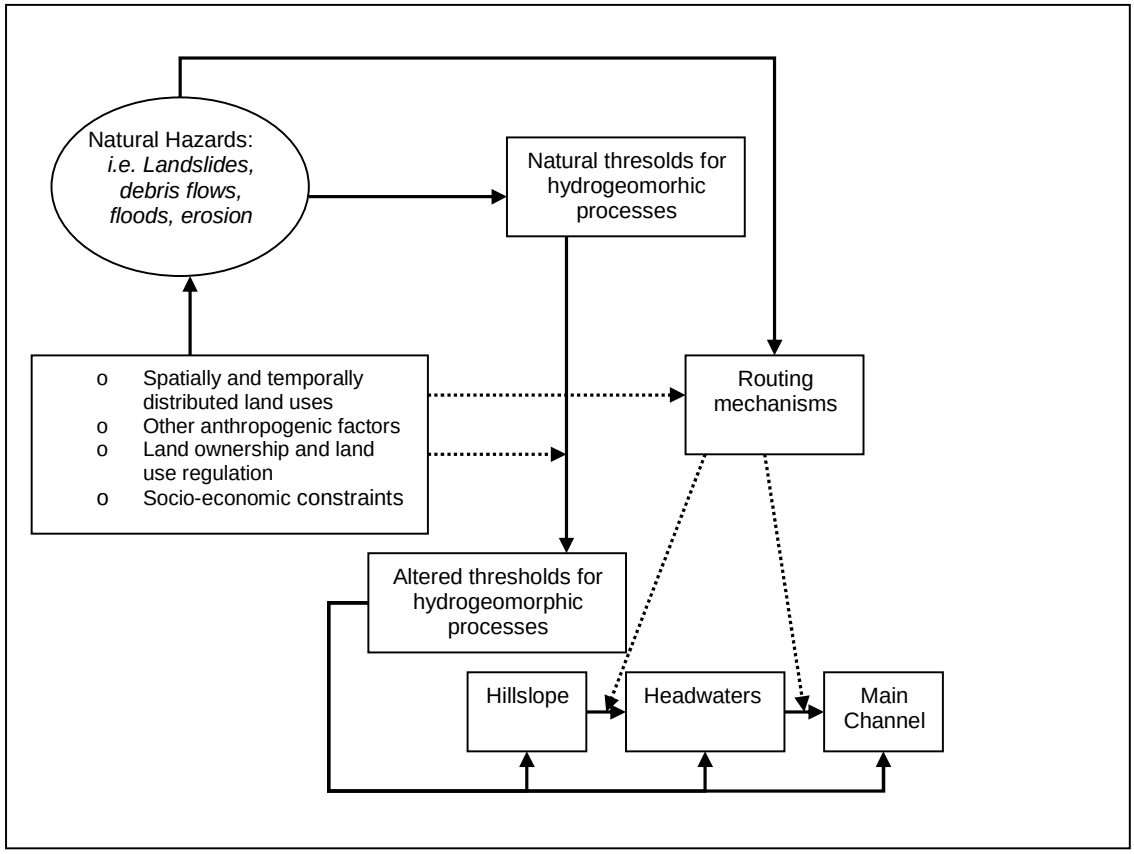

Figure 2-1 A linked system for assessing the effects of land use and other external factors, as well as the interactions with natural hazards, on hydrogeomorphologic processes across various spatial and temporal scales in drainage basins. Solid arrows represent compartmental connections; broken arrows represent process transfer or routing links (Sidle and Onda, 2004).

2.2 Landscape connectivity

2.2.1 Catchment-scale connectivity

Analysis of the character and behavior of landscape compartments, how they fit together and the connectivity among them, provides a platform to interpret the operation of geomorphic processes in any given system (Hooke, 2003). The way in which landscape systems fit together in a catchment influences the operation of physical fluxes, and the way in which responses to disturbance are mediated over time. These relationships reflect the connectivity of the landscape (Brierley, 2006). Knowledge of the degree of connectivity between landscape systems is important to explain the behavior of the entire system. Understanding coupling relationships must be framed in the context of landscape history to appraise the sensitivity of different parts of catchments to disturbance (Brierley and Fryirs, 2005). At any position in the landscape, systems may be coupled (connected) or decoupled (disconnected) (Figure 2-2) over differing timescales (Harvey, 2002).

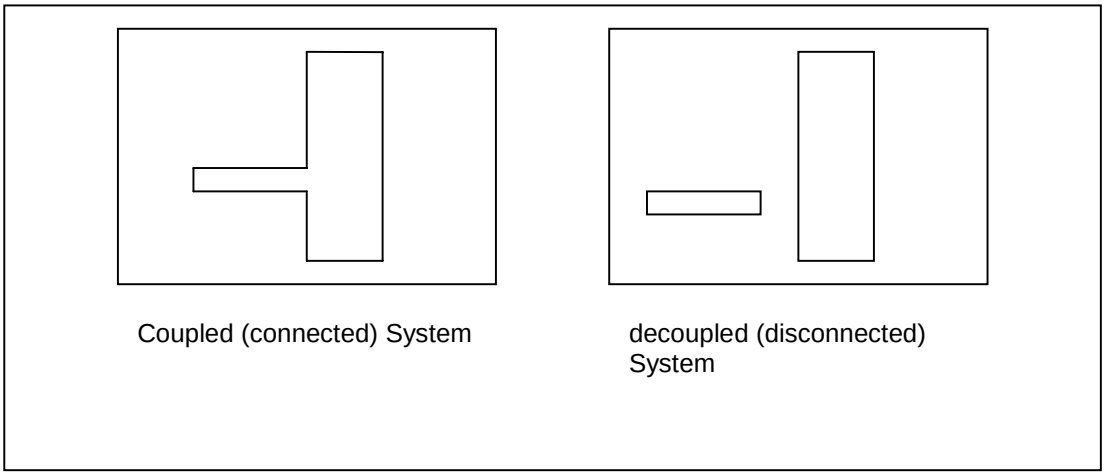

Figure 2-2 Schematic example for a coupled and decoupled System

2.2.2 Connectivity and sediment delivery

There are many factors that influence slope sediment delivery. Some of these relate to topography and soil conditions (the nature of the land surface and include slope angle, surface roughness and infiltration capacity). Others relate to the nature of runoff, volume and duration. These factors determine the forces or amount of energy available for erosion and sediment transport (section 2.3). Furthermore, spatial scale and the topological relationships between different parts of the land surface that have a strong influence on sediment delivery. Because connectivity within and between systems affects the extent and rate of transfer of mass and energy through a catchment, the focus on connectivity provides a basis to identify sensitive parts of the landscape, thereby assisting or enhancing prediction of geomorphic change (Fryirs, 2001).

The *sediment delivery ratio* (SDR) is defined as the ratio of total catchment erosion transported from the basin (Milliman and Syvitski, 1992). It provides a measure of catchment scale connectivity. Temporal variability in SDR within a catchment can be explained through analysis of differing forms of connectivity (Brierley, 2006). Impediments to sediment movement within a catchment restrict the rate of sediment transfer from the area upstream of that point. These impediments disconnect the entire system and determine the area of a catchment that has the potential to directly contribute sediment to the channel network under given flow conditions. This area is referred to as the *effective catchment area*.

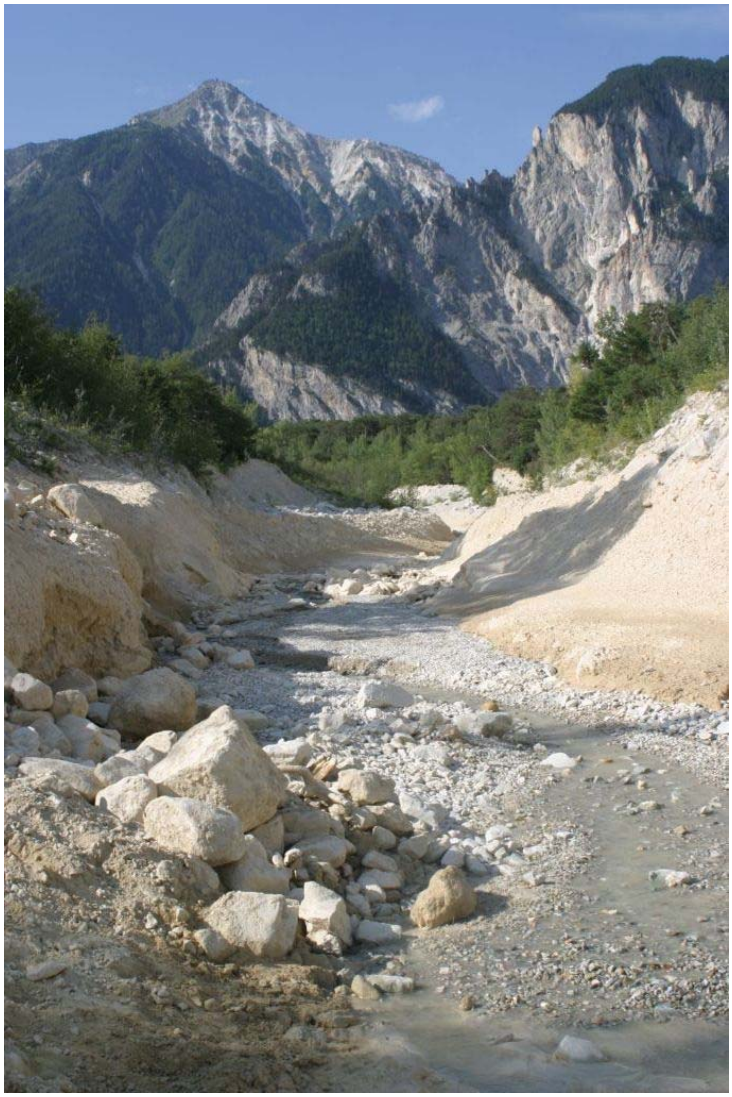

Figure 2-3 The Illgraben catchment from the channel bed on the fan (Corina Gwerder)

Therefore, estimation of sediment delivery on hillslopes, for example the ones from the Illgraben (Figure 2-3), requires not only solid understanding of hillslope and channel processes, it also requires appreciation of the changing patterns of coupling relationships in landscapes, as determined by the connectivity between hillslopes and the valley floor (Kasai, 2005). In general one can differentiate between hillslopes which are coupled or decoupled from the main channel system.

2.3 Erosion

2.3.1 Processes and controls of erosion

Soil erosion is a two-phase process consisting of the detachment of individual soil particles from soil mass and their transport by erosive agents such as running water, wind and gravity. When sufficient energy is no longer available to transport the particles, a third phase, deposition, occurs. Rainsplash is the most important detaching agent (Morgan, 2005). As a result of raindrops striking a bare soil surface, soil particles may be thrown through the air over distances of several centimeters. Running water, wind and freeze and thaw cycles also contribute to the detachment of soil particles. These processes may loosen the soil so that it is easily removable. Transporting agents include those that remove soil approximately uniformly and those that operate in channels. The first group consists of rainsplash, surface runoff (also called overland flow or sheet flow) and wind. The second group includes water in small temporary channels, or rills, or in larger more permanent gullies and rivers as well debris flows (water-solid mixtures, section 2.4) in torrent channels. The severity of erosion depends upon the quantity of material supplied by detachment over time and the capacity of eroding agents to transport it (Morgan, 2005). Erosion is a natural process; human or natural disturbances on the landscape generally increase surface erosion beyond natural levels (Robichaud, 2002).

Rainsplash erosion
Rainsplash can be an important detaching agent where the surface of the slope is not completely covered by vegetation. Erosional reduction and modification of a slope entirely by rainsplash is possible. Water moving over a surface without raindrop impact will initially cause significant erosion, but when the loose surface material has been swept away, erosion due to moving water alone is relatively insignificant. The combination of water on the slope plus raindrop impact energy produces an intermediate value of erosion (Chorley, 1978).

Overland flow erosion
Overland flow occurs on hillslopes during a rainstorm. It can be differentiated between two different types of overland flow. The first type is known as “Hortonian overland flow” and arrives when surface depression storage and the infiltration capacity of the soil are exceeded. The flow is rarely in the form of a sheet of water of uniform depth. The flow is broken up by stones and cobbles and by the vegetation cover, often swirling around tufts of grass and small shrubs (Morgan, 2005). The second type is known as “saturation excess overland flow” and arrives when the top soil layer is saturated with water. Regardless of which of those processes happens, there is also “surface depression storage” happens in holes, slops etc. When those storages are full the water overflows and drains off at the surface.

Rill erosion
Rills initiate at a critical distance downslope where overland flow becomes channelized. In addition to the main flow path downslope, secondary flow paths with a lateral component also develop. The change from overland flow to rill flow passes through four stages: unconcentrated overland flow, overland flow with concentrated flow paths, microchannels without headcuts, and microchannels with headcuts (Merritt, 1984).

Gully erosion
A widely recognized definition used to separate gullies from rills is that gullies have a cross-sectional area greater than $1m^2$ (Poesen, 1994). Gullies are almost always associated with accelerated erosion and therefore with instability in the landscape (Morgan, 2005). They are common features of mountainous or hilly regions with steep slopes (Valentin, 2005). Hillslopes are more prone to gullying when they are disturbed, e.g. deforested or grazed, where eroded soil is readily carried by the flowing water after being dislodged from the ground (Morgan, 2005). Furthermore, they can be generated by a natural dynamic change related to the long-term process of readjustment of the present geomorphologic system to Holocene climate (Avni, 2004).

Wind erosion
The main factor in wind erosion is the velocity of moving air. Because of the roughness imparted by soil, stones, vegetation and other obstacles, wind speeds are lowest near the ground surface. Once in motion, the transport of soil and sand particles by wind takes place in suspension, surface creep and saltation. Suspension describes the movement of fine particles where the downward gravitational forces on the particles are balanced by the upward lift produced by wind. Typically, particles in suspension are transported over long distances. Surface creep is the rolling of coarse grains along the ground surface. Saltation is the process of grain movement in a series of jumps (Morgan, 2005).

2.3.2 Factors influencing erosion

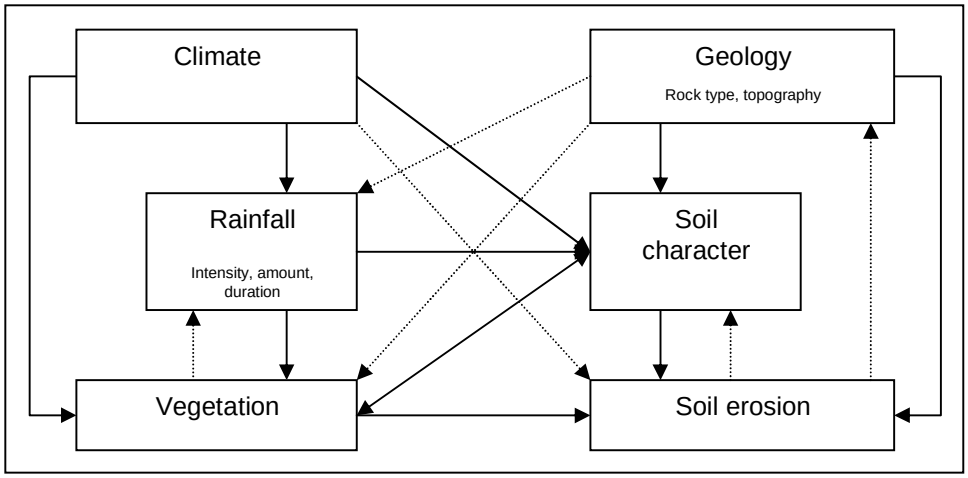

Figure 2-4 Interrelationships between the main factors influencing soil erosion (Selby, 1993)

The factors controlling erosion (Figure 2-4) are the intensity and duration of the eroding agent, the slope of the land and the nature of the plant cover. Climate and geology are the most important influences on erosion with soil character and vegetation being dependent upon them and interrelated with each other. Erosion is therefore reduced by material on or above the soil surface such as naturally occurring vegetation, surface litter, duff, rocks, and synthetic materials such as erosion mats, mulches, and other barriers that reduce the impact of the applied forces (Robichaud, 2002).

The rate of erosion is a function of the power (erosivity) of raindrops, running water, and sliding or flowing earth masses, and the erodibility of the soil. All these factors operate together and their influence can be estimated using the Universal Soil Loss Equation (USLE, equation 1) which is widely used in soil erosion studies in cropland but has not been generally applied to areas with complete grass or tree cover or mass wasting (Wischmeyer and Smith, 1978):

A = RKLSCP (1)

Where: A is the soil loss, R is the rainfall erosivity factor, K is the slope erodibility factor, L is the slope length factor, S is the slope gradient factor, C is the cropping management factor and P is the erosion control practice factor.

Modified versions of the USLE (equation 1) and models applying the USLE have been developed but the focus generally remains on fields or slopes of limited area and are intended to estimate annual sedimentloss, not for geomorphic studies of drainage basin erosion or for sediment yield from individual storms (for example, Forster, 1982; Mitasova et al., 1996; and Finkner et al., 1989).

2.3.3 Measurement of soil erosion

Data on soil erosion and its controlling factors can be collected in the field or under controlled conditions in the laboratory. Whether field or laboratory studies are used depends on the objective. For realistic data on soil loss, field measurements are the most reliable. But because conditions vary in both time and space, it is often difficult to determine the chief cause of erosion or to understand the processes in detail. Field measurements of soil erosion may be classified into two groups: those designed to determine soil loss from relatively small sample areas or erosion plots, often a part of a field experiment, and those designed to assess erosion over a larger area such as a drainage basin. Laboratory experiments are often overly simplified and the results may not be directly comparable with the field, however they are most useful for understanding the exact details of individual processes. The key questions arising with laboratory studies concern the scale of the experiment, the potentially large influence of boundary effects, and the extent to which field conditions are simulated. If possible it is preferable to treat laboratory experiments as representing full-scale field conditions. Even so, many factors cannot be properly simulated and unless the laboratory facilities are very large, neither processes such as rill erosion nor the saltations of soil particles by wind can be properly simulated (Markart, 1995). In recent years the use of rainfall simulators in the field has increased. Rainfall simulators provide the advantages of field conditions for soils, slope and plant cover, all of which are difficult to reproduce in the laboratory, with the benefits of a repeatable storm (Morgan, 2005).

2.3.4 Sediment supply due to erosion

Identification of sediment source areas and estimation of the output of source is central to the sediment yield problem. Landslides are a dominant source of sediment in many mountain river basins and play a key role in the feedback links between hillslopes and channels. However, sediment discharge from landslides to channels can be highly variable in both space and time, making estimation of sediment supply from landsliding and the effect of sediment on the channel difficult to quantify (Schuerch, 2006). Another difficulty is the fact that process relationships developed under present conditions between slope and erosion rate may have only limited relevance to long-term landscape-scale erosion rates in the steep topography of tectonically active mountain ranges (Montgomery, 2003). This is because erosion in mountain regions is influenced by variability in climate (runoff, temperature, amount and type of precipitation), vegetation type, degree of coverage on the surface by vegetation, relief, underlying geology (sediment discharge increases with decreasing erosional resistance of bedrock (Schlunegger, 2002)), recent tectonic activity and landscape character (Dedkov and Moszherin, 1992); (Montgomery, 2003). Soil cover changes between and during rainstorms can for example dramatically affect the incidence and intensity of rill and interrill erosion and therefore both short and long term hillslope erosion response (Bryan, 2000).

2.3.5 Modeling of soil erosion

Some measurement techniques applied in research allow rates of erosion to be determined at different positions in the landscape over various spatial and time scales. However, it is not possible to take measurements at every point in the landscape. Furthermore, it also takes time to set up a sufficient data base to ensure that the measurements are not biased by an extreme event. Long-term measurements are required to study how erosion rates respond to changes in land use and climate or the use of erosion-control measures. In order to overcome these problems, models can be used to predict erosion under a wide range of conditions. The results of the predictions can then be compared with the measurements to ensure their validity. If the predictions are sufficiently accurate, the method may be used to estimate erosion in other areas with similar conditions (Morgan, 2005).

2.4 Debris flow

A debris flow is a channelized landslide in which the individual particles travel separately within a moving mass and where the interaction of the soil material and interstitial water is important. They are potentially a very destructive form of slope movement in mountainous areas, where a sudden flux of water, usually from heavy rain or melting snow, can mobilise debris mantling steep slopes, or material that has accumulated by mechanical weathering, and incorporate it into a debris flow (Hutchinson, 1988). A debris flow consists of a mixture of fine material (sand, silt and clay), coarse material (gravel and boulders), with a variable quantity of water, that forms a muddy slurry which moves downslope, usually in surges induced by gravity and the sudden collapse of bank material. The mixture includes debris ranging from highly fractured rock, clastic debris in a fine matrix or simply fine-grained sediments (Figure 2-5).

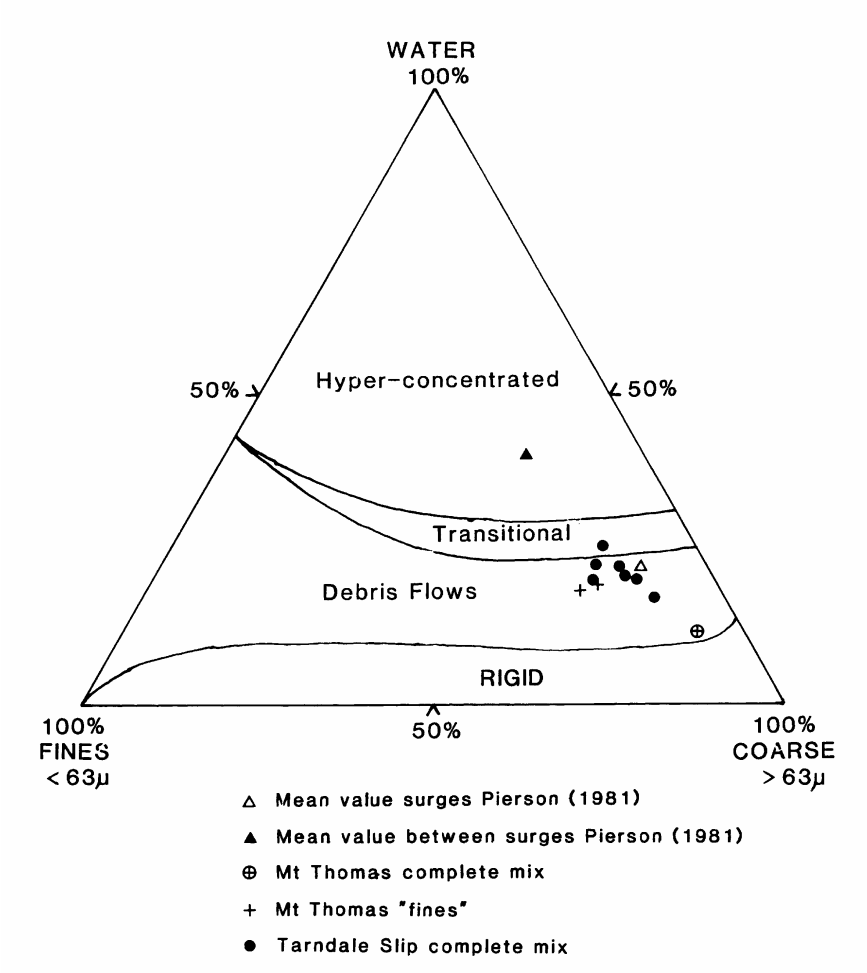

Figure 2-5 Three-phase diagram of debris-flow materials (Phillips and Davies, 1991)

The flow process is physically a continuous, irreversible deformation of a material that occurs in response to applied gravitational stress. Debris flows are characterised by internal differential deformations distributed throughout the mass (Corominas, 1995). Three distinctive elements are distinguishable in a debris flow area: the source area, the main track, and the depositional lobe. Successive surges will construct a debris fan.

Debris flows are present in most climatic environments, from deserts to alpine regions and from arctic to Mediterranean areas.
Limited data are available on the real-time monitoring of debris flows. Many detailed field observations of debris flows have been made in Japan (Suwa, 1989) and in China (Zhang, 1993). More recently, automatic observations on debris flows have been generated in Italy (Arattano et al., 1997; Arattano and Marchi, 2000; Berti et al., 2000; Berti et al., 1999). In recent years, research has focused on laboratory experiments and numerical simulations (Rickenmann and Koch, 1997; Rickenmann and Weber, 2000; Tognacca, 2000). Furthermore, three debris-flow observations stations were installed in Switzerland (Hürlimann et al., 2003).

Figure 2-6 Debris flow event 28.07.06 at the Illgraben: front approaching check dam (Corina Gwerder)

Figure 2-7 Debris flow event 28.07.06 at the Illgraben: the first wave (Corina Gwerder)

Figure 2-8 Debris flow event 28.07.06 at the Illgraben: large boulder flowing over check dam (Corina Gwerder)

Figure 2-9 Debris flow event 28.07.06 at the Illgraben: Boulder Block (Corina Gwerder)

3 Study area

3.1 Setting

The Illgraben catchment (Figure 2-3 and Figure 3-1 to Figure 3-3) is located near the village of Susten, in the Rhone valley between Sion and Brig, in the canton of Valais (southern Switzerland). The watershed has an area of 9.5 km^2 and an exposition to the north.

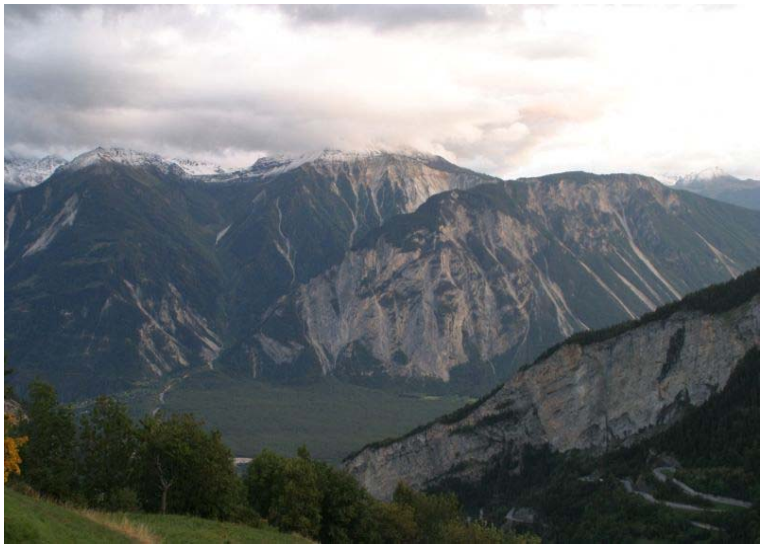

Figure 3-1 Illgraben catchment with the fan; view from Albinen (Corina Gwerder)

Figure 3-2 Bhutan Bridge at the Illgraben catchment (Corina Gwerder)

Figure 3-3 The Illgraben catchment from the south (Corina Gwerder)

The highest point of the basin is the Illhorn with 2717 m a.s.l. and the Illbach flows into the Rhone River at 610 m a.s.l. Adjacent to the Illgraben catchment and located on its fan is a nature reserve, the Pfyn-forest, with a rich biodiversity including rare species (flora and fauna).

3.2 Characteristics and history

As a debris-flow dominated catchment (Figure 2-6 to Figure 2-9), the Illgraben has a very high degree of sediment transport activity and provides a large fraction of the sediment input of the Rhone River into the lake of Geneva. Historical data on debris-flow activity is available from the beginning of the 20th century (A.2) and shows that debris flows have occurred regularly during the last 100 years (Geo7, 2000). A large rockfall event (1961) increased the debris-flow activity in subsequent years. In the1970s, the debris-flow frequency decreased on the fan due to the construction of a large sediment retention dam in the middle reach of the southern torrent. By the early 1980s this ~50 m high dam had filled and is now unable to contain further events. Consequently, debris-flow activity has increased during the last 20 years (Hürlimann et al., 2003).

3.3 Past studies and instrumentation

Due to this high frequency debris-flows activity, the Illgraben was chosen as a debris-flow observation station by the Swiss Federal Research Institute WSL and equipped with instruments in 2000. Instrumentation includes geophones, radar, laser, and ultrasonic depth-measuring devices, video cameras, three rain gauges and a debris-flow force plate. Except for the rain gauges, most of the devices are situated along the channel on the debris fan. The three rain gauges are located in the southern part of the drainage basin, in the primary debris-flow initiation zone. The geophones trigger the measuring devices and the front flow velocity can be calculated from the time lag between the geophone and the radar device signals.

Figure 3-4 The force plate at the Kantonsstrassenbrücke (Corina Gwerder)

Figure 3-5 The force plate at the Kantonsstrassenbrücke (frontal perspective) (Corina Gwerder)

The force plate (Figure 3-4 and Figure 3-5) (McArdell et al., in review) is a 4 m wide, 2 m long (in the flow direction) flat steel structure, installed at a check dam, instrumented with normal force transducer under each corner and two additional shear force sensors on the upslope end. In combination with a laser device mounted overhead, the bulk density and sediment concentration over an entire debris flow wave can be calculated. Moreover, the volume of the flow can be estimated in combination with the velocity data from the reach upstream of the force plate and the cross-sectional area.

3.4 Morphology

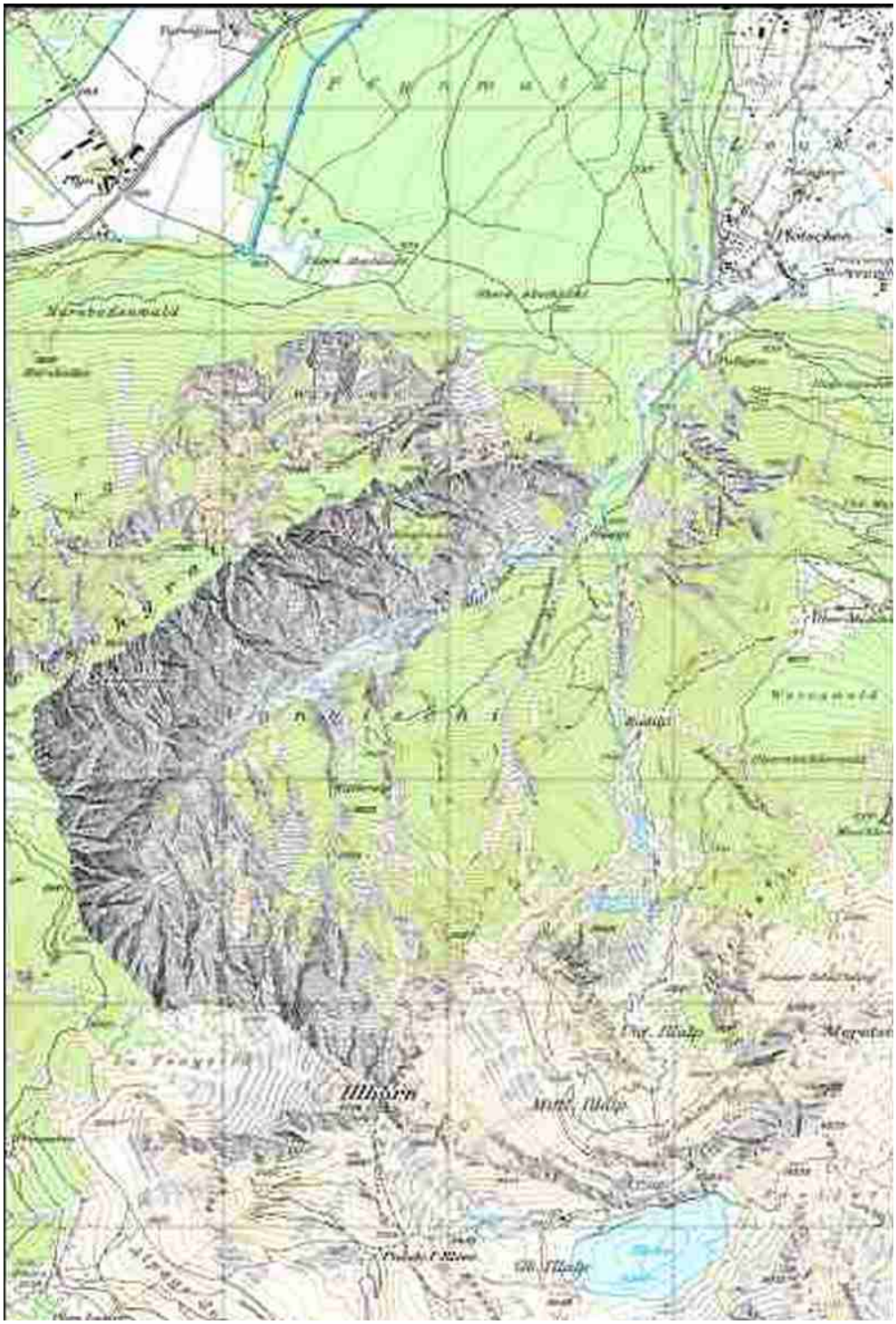

Figure 3-6 Topographical map of the Illgraben catchment (Swisstopo 1:25000, Nr 1287, 1999, copyright Swisstopo 2007)

The Illgraben catchment has an area of 9.5 km^2 and is composed of 44% rocky area, 42% forest area and 14% grassland area (Table 1). A part of the catchment gets drained over the Illbach and the Illsee hydropower reservoir, where no debris flows have been reported, the other part of the catchment get drained through the Illgraben, which is the clear debris flow source area (Figure 3-6). The morphology of the Illgraben catchment can be divided into two zones (Figure 3-7). Erosion has resulted in steep, unstable rock faces that supply the channel with debris (Hürlimann et al., 2003). Another characteristic of the catchment is that the debris fan is unusually large in comparison with similar sized catchments in the region. The fan has a radius about 2 km and a volume of about $500*10^6$ m^3 (Geo7, 2000).

Table 1 Morphology of the Illgraben catchment 2004 survey

Catchment area (km^2)	9.5
Rocky area (%)	44
Forest area (%)	42
Catchment area with grassland (%)	14
Exposure	N

3.5 Geology

The bedrock of the drainage basin is mainly composed of quartzite, calcareous deposits, and dolomites. Erosion strongly affects the southwestern part where quartzites are located. In the northern catchment dolomite and calcite can be found in the steep valley walls (A.3). The dolomite is unusually susceptible to weathering and provides a large amount of silty material. The calcareous deposits and dolomites are strongly jointed and repeatedly cause landslides (Appendix A3). In 1961, a large rockfall occurred in this area of the drainage basin. The loose deposits of the 1961 rockfall and the continuous slope movements further upstream are an abundant supply source for the debris flows which generally consist of a muddy slurry (dolomites) and boulders of quartzite or calcite (Hürlimann et al., 2003).

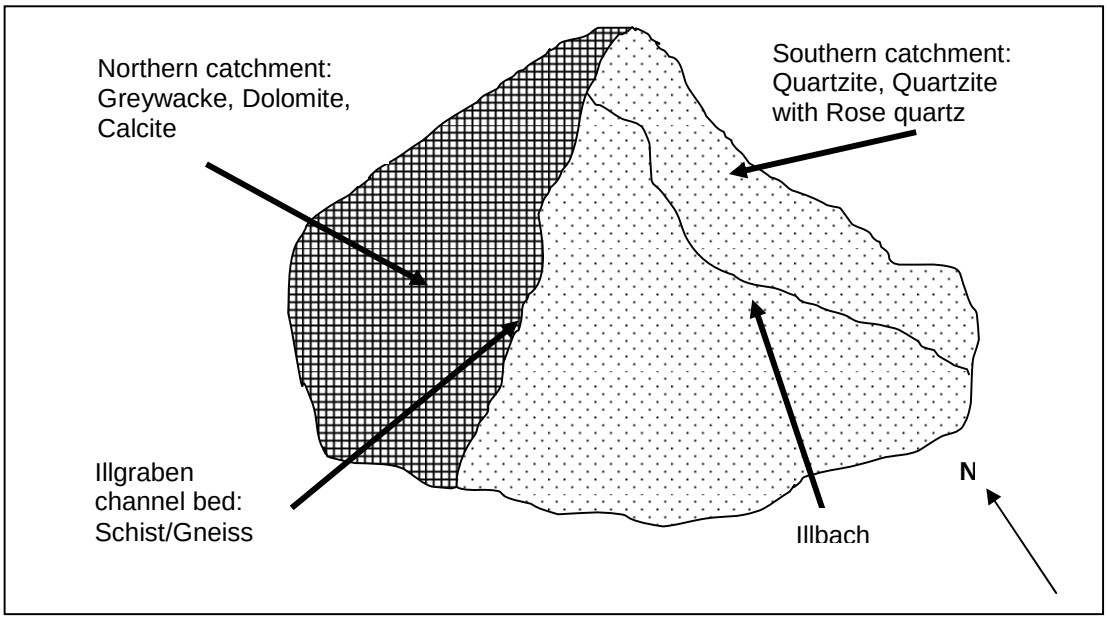

Figure 3-7 Simplified catchment geology

3.6 Vegetation and soil

The soil on the debris fan is dense and has a sparse humus layer as a consequence of the dry climate and the reduced biological activity. The soil is rich in calcium carbonate and has a pH around 7 at a depth of 0.10 m. On the north side of the fan the soil is deeper (1 m) than on the south (0.30-0.40 m). Soils on the debris fan are a mixture of porous stones, gravels and fine materials containing primarily calcareous dolomites and quartzites. The vegetation in the Pfyn-forest area (Figure 3-8 and Figure 3-9) is, because of its large pine-forest, is of national interest. As a pioneer species, the pine profits from the continental climate and the stony soil in the hills and the debris fan. Since the last ice age and the resulted geological shifting, the pine maintained position on the debris fan (Werner, 1985). Further upslope in the catchment, on the southern zone, the pine forest pass over into a typical continental alpine spruce forest. This forest type also contains some larches and rowan berries. The existence of larches points to a strong influence of avalanches, debris-flows and rock fall activity, however, it is damaged by the Bork-beetle, droughts and soil slips.

Figure 3-8 The Illgraben debris fan with the Pfyn-forest (WSL)

Figure 3-9 The Illgraben debris fan with its pioneer forest (WSL)

3.7 Climate

The climate of the Illgraben region is strongly influenced by its location in an alpine valley, which itself has a mild climate and a low annual precipitation (Hürlimann et al., 2003). The mean annual precipitation ranges from 700 mm in the lower part of the drainage basin to 1700 mm at the summit regions (BAFU, 1999). Intense rainstorms occur mainly in summer, and estimated rainfall intensities are between 35 and 57 mm per hour for a 0.5 and 1 hour rainfall duration, respectively, corresponding to a return period of 100 years (BAFU, 1999).

4 Data and Methods

4.1 Data

4.1.1 Debris flow data recorded during the 2006 season, Illgraben

Debris flow data from the force plate from the debris flow season in 2006 are summarized in Table 2. In 2006, six debris flow events were measured at the force plate.

Table 2 Debris flow season 2006

Number	**1**	**2**	**3**	**4**	**5**	**6**
Date	18.05.06	24.06.06	27.06.06	18.07.06	28.07.06	03.10.06
Volume [m^3]	15'000	50'000	70'000	50'000	10'000	50'000

The total volume for the sediment delivery out of the Illgraben catchment through debris flows during the season 2006 amounts to 245'000 m^3. The average mass bulk density, determined from the force plate, was by calculation (Brian McArdell, WSL) 1600 kg/m3. Thus, the total export of sediment by debris flows in 2006 is 245'000 * 1600 = $392*10^6$ kg.

4.1.2 Automatic precipitation data

Three automatic rain gauges are installed within the upper catchment and record precipitation amount and intensity. Pluviometer 1 (Rain gauge 1) is located at 2200 m a.s.l., Pluviometer 2 at 1630 m a. s. l. and Pluviometer 3 at 950 m a. s. l.. Rainfall sums from Pluviometer 1 were always larger than those from Pluviometer 3. Pluviometer 2 was out of order during the summer months due to obstruction by leaves. In this thesis, the precipitation intensity values from Pluviometer 3 were considered for the sediment analysis because it is the one closest to the most important silt fence plots (section 4.2.2) and because of the record is uninterrupted during the investigation period.

4.1.3 Long-term temperature and precipitation data

For the temperature analysis, values in section 5.1.2 from the station Sion (Federal office of Metrology and Climatology MeteoSwiss) were used, for precipitation data were taken from the MeteoSwiss stations Grimentz, Hérémence and Sierre (section 5.1.2).

4.2 Field work

4.2.1 Hillslope erosion measurements: the silt fence technique

Various techniques are available to measure soil erosion, including rainfall simulation, erosion bridges, Gerlach troughs and small watershed techniques. They are often costly and time consuming and are not always in widespread use. Therefore, Dissmeyer (1982) developed a protocol to measure hillslope erosion. A silt fence (Figure 4-1) consists of a synthetic geotextile fabric that is woven to provide structural integrity and small openings that pass water but not coarse sediment. They have low permeability rates, which make them suitable to form temporary detention storage areas allowing sediment to settle and water to pass through slowly. Silt fences can be primarily used to compare erosion rates of naturally occurring erosion. Furthermore, the effect of vegetative or mechanical rehabilitation treatment can be investigated. The application of the silt fence measurement technique for hillslope erosion has, as far as we know, never been used in steep mountain catchments.

Silt fences work best when they are located on uniform slopes with minimal obstruction. The plots are located to collect sediment from a contribution area defined either by natural features or artificial features such as trenches or a PVC plate at the upslope end. They are suitable for use in natural or managed hillslope erosion studies under ephemeral conditions or for continuous water flows from very small first-order streams. The contributing area for a silt fence needs to be designed so it does not overtop the silt fence, with the size of the contributing area selected depending on expected flow and sediment yield (Robichaud, 2002).

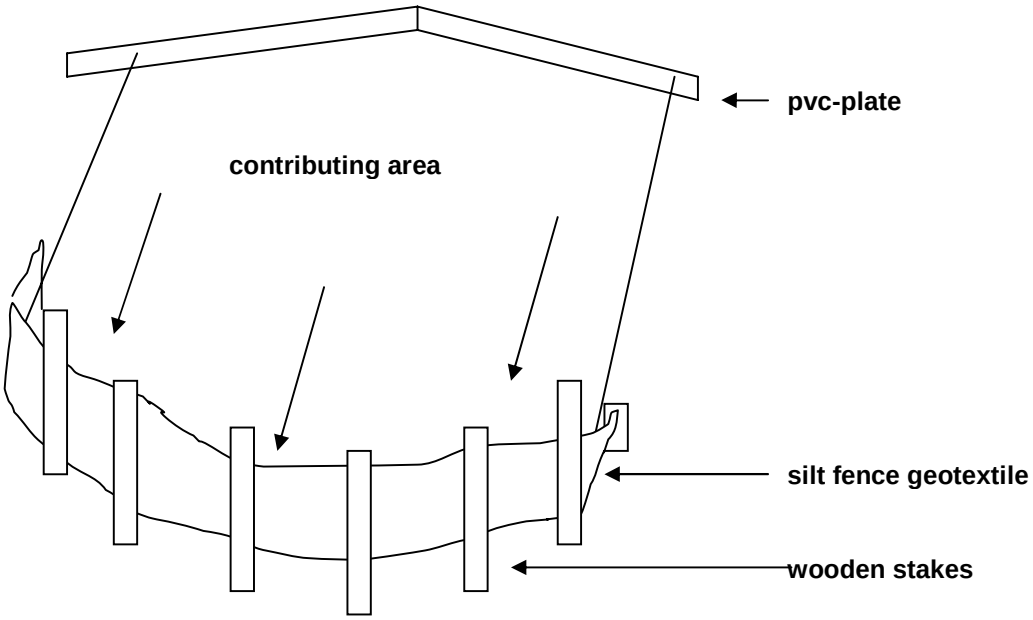

Figure 4-1 Silt fence plot example

4.2.2 Silt fence plots installed at the Illgraben catchment

Hillslope erosion in the Illgraben was measured on 11 silt fence plots (Figure 4-2 and Figure 4-3). Two plots were installed in the forest, two on grassland, four on erosion slopes (slopes free of vegetation) and three on two different scree and avalanche chutes (Figure 4-5). The plots are characterized for their location, exposition, length, width, area, thickness of humus layer, vegetation layer, altitude above sea level, difference of elevation, mean slope inclination and substrate including the grain size distribution of the plot surface layer (0-0.1 m). The eleven silt fence plot sites can be broadly grouped into two areas. One is located at the lower end of the catchment next to the Guetji Alp (plots E, F and G, Figure 4-5) and the other area is on the way to and around the Steinschlag Hut (A1, A2, B1, B2, C1, C2, D1 and D2, Figure 4-5).

Figure 4-2 Silt fences F1 and G1 (Corina Gwerder)

Figure 4-3 Silt fence F1 (Corina Gwerder)

They are labeled (Figure 4-4) A1, A2, B1, B2, C1, C2, D1, D2, E, F, G, where the A-sites correspond to sites situated on an old erosion slope (partially re-vegetated), the B-sites stand on grassland, the C-sites are in the forest, D-sites are on an active erosion slope, E is located in an avalanche chute, F and G are situated on a talus slope. Plots with the lower altitude are labeled with the number 1 and the higher ones with the number 2. The same labeling scheme is used for the rain gauges.

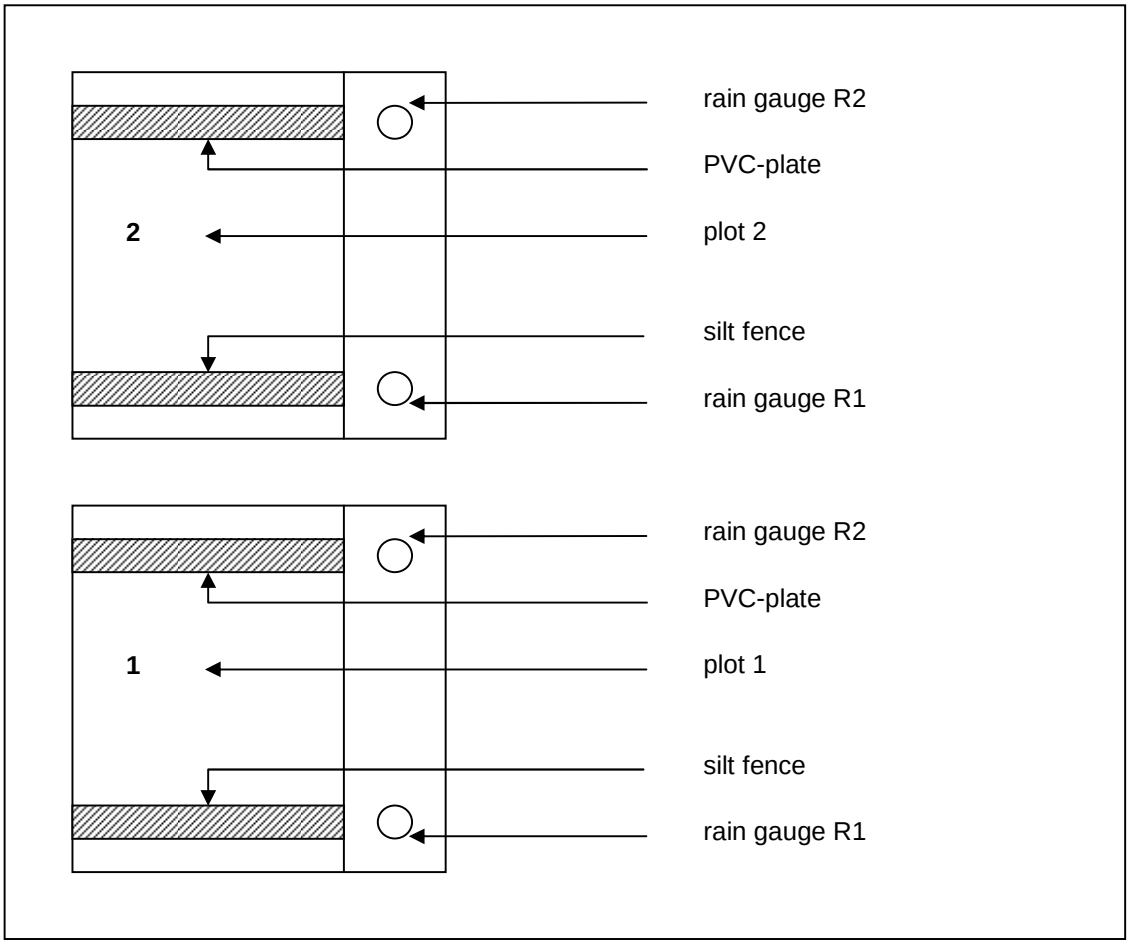

Figure 4-4 Plot site labeling (Corina Gwerder)

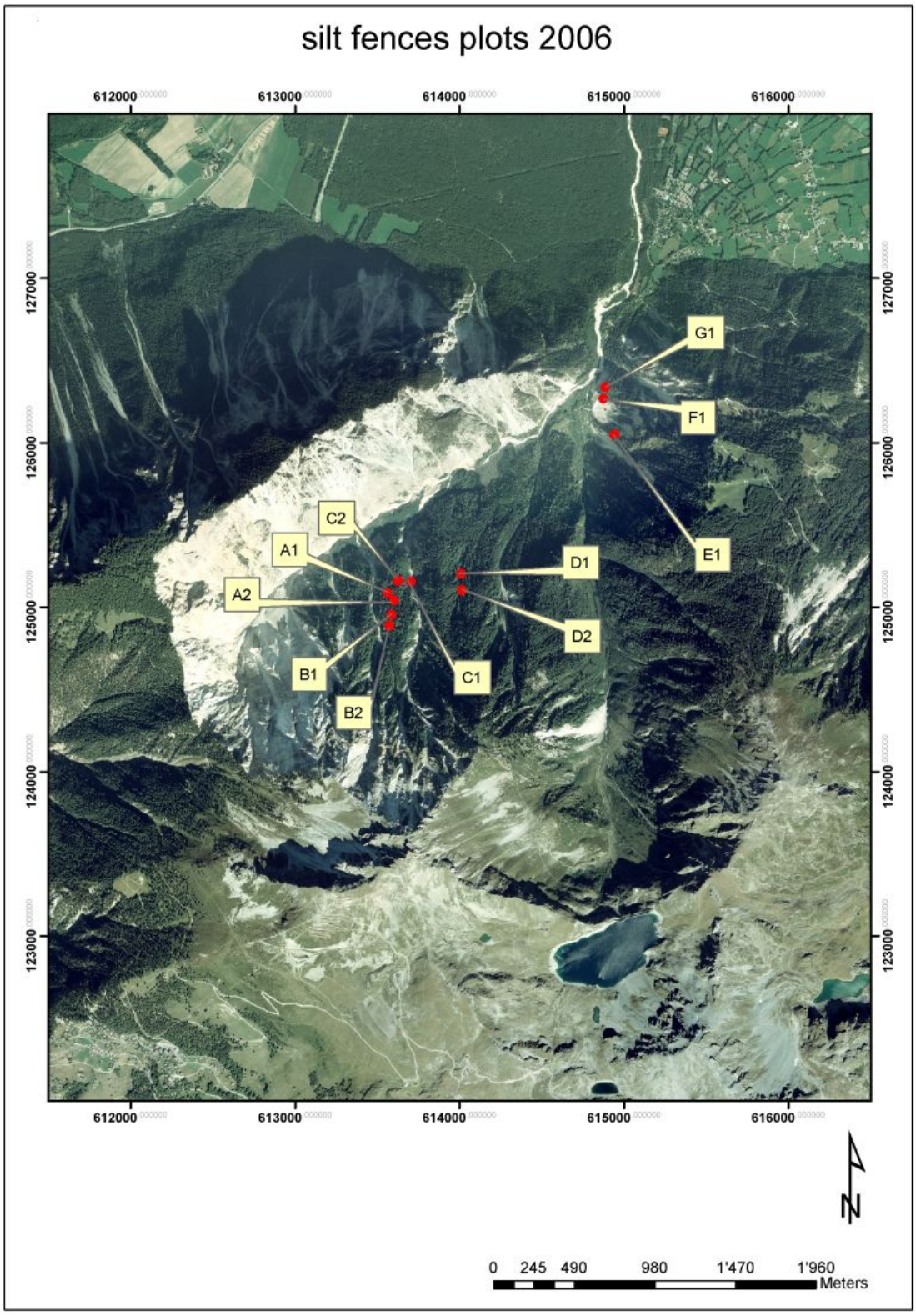

Figure 4-5 Locations of the silt fence plots in the Illgraben catchment 2006 on the orthophoto 2004 (Corina Gwerder)

Silt fence plot A1

Table 3 Plot A1 description

location: erosion slope with sparse vegetation	*altitude silt fence:* 1400 m a. s. l.
exposition: NW	*altitude pvc barrier:* 1412 m a. s. l.
coordinates: 613581/125175	*difference in elevation:* 12 m
accuracy of coordinates: 15 m	*mean slope angle:* 45°
length: 16 m	*altitude rain gauge 1 (R1):* 1400 m a. s. l.
width: 3.6 m	*dominance R1:* 0%
area: 57.6 m^2	*altitude rain gauge 2 (R2):* 1412 m a. s. l.
thickness of humus layer: 0 cm	*dominance R2:* 0%
stock/dominance: 10%	*substrate:* gravel, debris
ground vegetation: meager	*type of plot:* erosion plot

Silt fence plot A2

Table 4 Plot A2 description

location: erosion slope with sparse vegetation	*altitude silt fence:* 1413 m a. s. l.
exposition: NW	*altitude pvc barrier:* 1424 m a. s. l.
coordinates: 613601/125154	*difference in elevation:* 11 m
accuracy of coordinates: 8 m	*mean slope angle:* 40°
length: 12.6 m	*altitude rain gauge 1 (R1):* 1414 m a. s. l.
width: 3.5 m	*dominance R1:* 0%
area: 44.1 m^2	*altitude rain gauge 2 (R2):* 1419 m a. s. l.
thickness of humus layer: 0 cm	*dominance R2:* 0%
stock/dominance: 35 %	*substrate:* gravel, debris
ground vegetation: meager	*plot type:* erosion plot

Plot characteristics
Plots A1 (Figure 4-6 and Figure 4-7) and A2 (Figure 4-8 and Figure 4-9) are located on a steep slope below the Steinschlag Hut which was used as grassland until the mid-1990's. During the period of active use, the land surface became progressively more unstable and erosion occurred, forcing the local farmers to stop using it as a pasture for their sheep. The slope is characterized by a straight erosion scarp (1424 m a. s. l.) at the upslope end and with a local rock outcrop at the lower end.
The vegetation on the slope is meager and contains mostly pioneer vegetation. The ground has no humus layer, shows a large skeletal fraction and is fragile and susceptible to disruption (almost no stabilization, steep, no root penetration).

Figure 4-6 Silt fence plot A1 (Corina Gwerder)

Figure 4-7 Silt fence plot A1 (Corina Gwerder)

Figure 4-8 Silt fence plot A2 (Corina Gwerder).

Figure 4-9 Silt fence plot A2 and rope attached for better accessibility on the right (Corina Gwerder)

Silt fence plot B1

Table 5 Plot B1 description

location: grassland	*altitude silt fence:* 1425 m a. s. l.
exposition: NW	*altitude pvc barrier:* 1430 m a. s. l.
coordinates: 613605/125150	*difference in elevation:* 5 m
accuracy of coordinates: 8 m	*mean slope angle:* 30°
length: 12.6 m	*altitude rain gauge 1 (R1):* 1426 m a. s. l.
width: 3.3 m	*dominance R1:* 0%
area: 30.4 m^2	*altitude rain gauge 2 (R2):* 1430 m a. s. l.
thickness of humus layer: 5 cm	*dominance R2:* 0%
stock/dominance: 40%	*substrate:* gravel, pastures, stinging-nettles
ground vegetation: abundant	*type of plot: grassland*

Silt fence plot B2

Table 6 Plot B2 description

location: grassland	*altitude silt fence:* 1430 m a. s. l.
exposition: NW	*altitude pvc barrier:* 1432 m a. s. l.
coordinates: 613590/125096	*Difference in elevation:* 2m
accuracy of coordinates: 28 m	*mean slope angle:* 25°
length: 9 m	*altitude rain gauge 1 (R1):* 1430 m a. s. l.
width: 3.5 m	*dominance R1:* 0%
area: 31.5 m^2	*altitude rain gauge 2 (R2):* 1431 m a. s. l.
thickness of humus layer: 8 cm	*dominance R2:* 0%
stock/dominance: 5%	*substrate:* gravel, pastures, stinging-nettles
ground vegetation: abundant	*type of plot: grassland*

Plot characteristics
Plots B1 (Figure 4-11) and B2 (Figure 4-10) are located near the Steinschlag hut and were used as grassland until the mid-1990's. The ground is covered by stinging-nettles, grass and birch. The skeletal fraction in the humus layer (8 cm) is large. Because of the presence of the stinging-nettles the floor probably still contains a high amount of nutrients (N, P) from the previous grazing use.

Figure 4-10 Silt fence plot B2, the pvc plate forms the upper barrier (Corina Gwerder)

Figure 4-11 Silt fence plot B1 (Corina Gwerder).

Silt fence plot C1

Table 7 Plot C1 description

location: disturbed forest	*altitude silt fence:* 1360 m a. s. l.
exposition: NE	*altitude pvc barrier:* 1363 m a. s. l.
coordinates: 613713/125202	*difference in elevation:* 3 m
accuracy of coordinates: 17 m	*mean slope angle:* 40°
length: 7.6 m	*altitude rain gauge 1 (R1):* 1360 m a. s. l.
width: 3.3 m	*dominance R1:* 0%
area: 25.1 m^2	*altitude rain gauge 2 (R2):* 1363 m a. s. l.
thickness of humus layer: 10 cm	*dominance R2:* 0%
stock/dominance: 30%	*substrate:* pastures, bushes, gravel
ground vegetation: abundant	*type of plot:* forest

Silt fence plot C2

Table 8 Plot C2 description

location: disturbed forest	*altitude silt fence:* 1390 m a. s. l.
exposition: ENE	*altitude pvc barrier:* 1394 m a. s. l.
coordinates: 613657/125198	*difference in elevation:* 4 m
accuracy of coordinates: 21 m	*mean slope angle:* 40 °
length: 5.1 m	*altitude rain gauge 1 (R1):* 1390 m a. s. l.
width: 3.2 m	*dominance R1:* 30%
area: 16.3 m^2	*altitude rain gauge 2 (R2):* 1394 m a. s. l.
thickness of humus layer: 8 cm	*dominance R2:* 100%
stock/dominance: 40%	*substrate:* needles, branches, gravel
ground vegetation: meager	*type of plot:* forest

Plot characteristics
Plots C1 (Figure 4-12 and Figure 4-13) and C2 (Figure 4-14 and Figure 4-15) are located between the Küferalpgraben and the Steinschlag Hut (Figure 3-6). Plot C1 abuts the Küferalpgraben, which experiences frequent debris flows, avalanches, rock fall and floods. The ground has a humus layer of 8 cm thickness, a large skeletal amount and is covered with pioneer vegetation. The tree composition consists of young birches and rowan trees, without any spruces. Fine herbages form a soft sub layer. Plot C2 lies in a steep old spruce forest marked by slope failure, rock fall and bark-beetle-activity. The ground layer is covered by needles, small branches, a few herbs and a humus layer of 8 cm thickness (acid because of the lignin in the needles).

Figure 4-12 Silt fence plot C1 (Corina Gwerder).

Figure 4-13 Silt fence plot C1 (Corina Gwerder)

Figure 4-14 Silt fence plot C2 (Corina Gwerder).

Figure 4-15 Silt fence plot C2 (Corina Gwerder)

Silt fence plot D1

Table 9 Plot D1 description

location: erosion slope without vegetation	*altitude silt fence:* 1235 m a. s. l.
exposition: N	*altitude pvc barrier:* 1239 m a. s. l.
coordinates: 614184/125458	*difference in elevation:* 4 m
accuracy of coordinates: 5m	*mean slope angle:* 38°
length: 11.7 m	*altitude rain gauge 1 (R1):* 1236 m a. s. l.
width: 3.7 m	*dominance R1:* 0%
area: 43.3 m^2	*altitude rain gauge 2 (R2):* 1240 m a. s. l.
thickness of humus layer: 0 cm	*dominance R2:* 30%
stock/dominance: 25%	*substrate:* gravel, debris
ground vegetation: no	*type of plot:* erosion plot

Silt- Fence Plot D2

Table 10 Plot D2 description

location: erosion slope without vegetation	*altitude silt fence:* 1250 m a. s. l.
exposition: N	*altitude pvc barrier:* 1260 m a. s. l.
coordinates: 614221/125410	*difference in elevation:* 10m
accuracy of coordinates: 6 m	*mean slope angle:* 38°
length: 14.6 m	*altitude rain gauge 1 (R1):* 1251 m a. s. l.
width: 3.5 m	*dominance R1:* 30%
area: 51.1 m^2	*altitude rain gauge 2 (R2):* 1261 m a. s. l.
thickness of humus layer: 0cm	*dominance R2:* 30%
stock/dominance: 5%	*substrate:* gravel, debris
ground vegetation: no	*type of plot:* erosion plot

Plot characteristics
Plots D1 (Figure 4-16 and Figure 4-17) and D2 (Figure 4-18 and Figure 4-19) are located in a steep erosion slope on the path to the Steinschlag Hut. The slope shows evidence of large erosion amounts and frequent rock fall activity. The ground has a large skeletal amount without a humus layer and is fragile to disruption (almost no stabilization, steepness, no root penetration). Abundant wildlife traces (roe deer, chamois, etc.) indicate that the slope is often used as an animal crossing.

Figure 4-16 Silt fence plot D1 (Corina Gwerder)

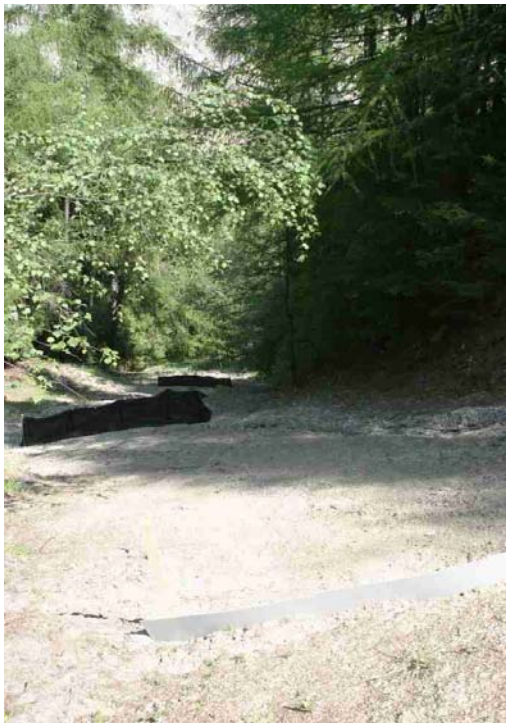

Figure 4-17 Silt fence plots D1 (lower plot) (Corina Gwerder) and D2 (upper plot)

Figure 4-18 Silt fence plot D2 (Corina Gwerder)

Figure 4-19 Silt fence plots D1 (lower plot) (Corina Gwerder) and D2 (upper plot)

Silt- fence plot E1

Table 11 Plot E1 description

location: erosion slope with sparse vegetation	*altitude silt fence:* 1010 m a. s. l.
exposition: WNW	*altitude pvc barrier:* 1021 m a. s. l.
coordinates: 614835/126062	*difference in elevation:* 11 m
accuracy of coordinates: 10 m	*mean slope angle:* 46°
length: 18 m	*altitude rain gauge 1 (R1):* 1010 m a. s. l.
width: 8 m	*dominance R1:* 50%
area: 144 m^2	*altitude rain gauge 2 (R2):* 1021 m a. s. l.
thickness of humus layer: 0 cm	*dominance R2:* 50%
stock/dominance: 40 %	*substrate:* debris, branches, pastures, bushes
ground vegetation: meager	*type of plot:* erosion plot

Plot characteristics
Plot E1 (Figure 4-20 and Figure 4-21) is located in an active avalanche and rock fall channel near the Guetji-Alp at the northern end of the catchment and has compared with the upper plots (A1-D2) a hug area. The channel is characterized by a large square erosion edge with a rock face at the top end. The ground cover is composed of gravel, wood branches, pastures and small bushes without a humus layer. Both sides of the channel abut disturbed forest and pioneer vegetation.

Figure 4-20 Silt fence plot E1 (Corina Gwerder).

Figure 4-21 Silt fence plot E1 (Corina Gwerder)

Silt- Fence Plot F1

Table 12 Plot F1 description

location: erosion slope with sparse vegetation	*altitude silt fence:* 928 m a. s. l.
exposition: NW	*altitude pvc barrier:* 947 m a. s. l.
coordinates: 614871/126269	*difference in elevation:* 19 m
accuracy of coordinates: 39 m	*mean slope angle:* 40°
length: 26 m	*altitude rain gauge 1 (R1):* 928 m a. s. l.
width: 8 m	*dominance R1:* 0%
area: 208 m^2	*altitude rain gauge 2 (R2):* 947 m a. s. l.
thickness of humus layer: 0 cm	*dominance R2:* 0%
stock/dominance: 30%	*substrate:* debris, gravel, pastures, bushes
ground vegetation: meager	*type of plot:* erosion plot

Plot characteristics
Plot F1 (Figure 4-22 and Figure 4-23) is located on a talus slope near the Guetji-Alp at the northern end of the catchment and has compared with the upper plots (A1-D2) a hug area. The ground cover is composed of debris, gravel, herbs and small bushes without a humus layer (pioneer vegetation).

Figure 4-22 Silt fence plot F1, view from below (Corina Gwerder)

Figure 4-23 Silt fence plot F1 (Corina Gwerder)

Silt fence plot G1

Table 13 Plot G1 description

location: erosion slope without vegetation	*altitude silt fence:* 928 m a. s. l.
exposition: NW	*altitude pvc barrier:* 947 m a. s. l.
coordinates: 614869/126273	*difference in elevation:* 19 m
accuracy of coordinates: 24 m	*mean slope angle:* 40°
length: 26 m	*altitude rain gauge 1 (R1):* 928 m a. s. l.
width: 9 m	*dominance R1:* 0%
area: 234 m^2	*altitude rain gauge 2 (R2):* 947 m a. s. l.
thickness of humus layer: 0 cm	*dominance R2:* 0%
stock/dominance: 0%	*substrate:* debris, gravel, sand
ground vegetation: no	*type of plot:* erosion plot

Plot characteristics
Plot G1 (Figure 4-24 and Figure 4-25) is located on a talus slope near the Guetji-Alp at the northern end of the catchment and has compared with the upper plots (A1-D2) a hug area. The debris field is characterized with a hug square erosion edge with a rock face at the top end and abuts to a birch forest on the left side. The ground cover is composed of gravel and sand without any vegetation.

Figure 4-24 Silt fence plot G1 (Corina Gwerder)

Figure 4-25 Silt fence plot G1 (Corina Gwerder)

4.2.3 General measurement and maintenance information

Periodic emptying of the silt fences is required to obtain reliable measurements of erosion. Depending on the need for accuracy, one can clean them after each storm, monthly, or twice a year. For this thesis, the fences were cleaned once to twice a week from July to mid October, except for a few plots which were inaccessible for a few periods, as described later. The total weight of accumulated sediment was measured in the field with a hanging scale with a maximum capacity of 10 kg. Generally, the water content of the sediment needs to be subtracted from the field collected soil material weight to obtain the correct dry weight. Because the collected sediment in the Illgraben silt fences consisted mostly of gravel with a minor amount of soil material, the water content was negligible. Additionally, the water in the fines or in the gravel most likely evaporated before being collected due to the large solar radiation, wind and the mild climate. Four samples from the accumulated sediment and one from the undisturbed plot surface, at a depth of 0 to 0.1 m, were collected for grain size analysis. Two simple collecting rain gauges (Figure 4-26) were installed on each plot, one near the upslope PVC-plate and the other next to the silt fence. They recorded the precipitation amount for each plot during a measurement interval. To reduce evaporation, a small amount oil was added to the gauge after each measurement.

Figure 4-26 Rain gauge for the measurement of the plot site precipitation

Measurement period 2006

Site selection and preparation
The silt fence measurement technique was chosen in the Illgraben to provide a better understanding of the processes in the catchment area. Previous research activities and measurements at the Illgraben catchment make this an ideal site to investigate geomorphic connectivity and sediment delivery. Plots (A1, A2, B1, B2, C1, C2, D1 and D2) locations were selected during a field trip on the 8 June with members of the debris flow group from WSL. Locations for the remaining plots (E, F and G) were selected on 26 July by François Dufour (WSL) and me. The preparation for the installations included the organization of materials, transport and coordination of assistants:

- Materials: The publication "Silt Fences: An Economical Technique for measuring hillslope erosion" (Robichaud, 2002) provides a detailed equipment list. The silt fence installation tools (shovels, Pulaski, hand trowels, hammer, heavy-duty stapler and measuring tape) could all be organized at the WSL, where most of the installation supplies (wooden stakes, tape and strips) were bought at garden center stores. The rain gauges could be purchased locally, and the silt fence textile was purchased at a local company that specialized in geotextiles (Schöllkopf AG).

- Transport: Because of the large distance to the investigation area and the steepness and low quality of the trail the material transport to the Steinschlag hut was done by helicopter (Air Zermatt). On the first day of installation the geotextile, PVC-plates, shovels and most of the other required tools were transported from the Bhutan Bridge to the Steinschlag Hut.

Installation and put into operation
For installation we generally followed the instructions by Robichaud and Brown (2002) in the publication:

1. A trench 0.2 m deep was dug along the contour with the ends of the trough gently curving uphill to prevent runoff from circumventing the silt fence. The excavated material was placed on the downhill side of the trench for later use in backfilling.
2. The silt fence was laid out along the trench covering the bottom and uphill side of the trench. The excavated soil was then used to backfill the trench.
3. Wooden stakes were installed such that 0.5m of the silt fence would be against the upright stake and it could be fastened securely.
4. The silt fence was attached to the stake with strong staples and cable retainer.
5. For additional stability we fixed a garden hedge barrier (green, for use with ornamental plants with 0.8 m height) behind the silt fence.

The installations were carried out in June and July 2000 (Figure 4-27 to Figure 4-32) where we can differentiate between two installation phases (Table 14): The first installation phase started 25 June and ended 4 July. In this Phase plots A1, A2, B1, B2, C1, C2, D1 and D2 were constructed and put into operation. The second installation phase started 28 July and ended 2 August. In this phase plots E, F and G were constructed and put into operation (A.6.1).

Table 14 Start and end of operation of the silt fence plots and the corresponding total measurement intervals

	A1	**A2**	**B1**	**B2**	**C1**	**C2**	**D1**	**D2**	**E**	**F**	**G**
start	26.06	26.06	26.06	26.06	26.06	26.06	26.06	26.06	28.07	02.08	02.08
end	11.10	11.10	11.10	11.10	11.10	11.10	11.10	11.10	11.10	11.10	11.10
days	107	107	107	107	107	107	107	107	75	69	69

Figure 4-27 Installation work 1, (Corina Gwerder)

Figure 4-28 Installation work 2 (Corina Gwerder)

Figure 4-29 Installation work 3 (Corina Gwerder)

Figure 4-30 Installation work 4 (Corina Gwerder)

Figure 4-31 Installation work 5 (Corina Gwerder)

Figure 4-32 Installation work 6 (Corina Gwerder)

Measurements

During the total investigation period I took 10 to 14 measurements per plot, so I collected sediment over at least 10 intervals per plot (Table 15). Measuring the sediment in the silt fences (Figure 4-33 and Figure 4-34)involved a long field day with a total of 7 hours of train travel, up to 4 to 5 hours of walking with up to 1000 meters ascent from the train station to reach the uppermost plots. For safety reasons, there was always an assistant accompanying me and a radio in my rucksack. To clean out the fences I used a hanging scale with a capacity of 10 kg, a shovel, bucket, a hand trowel and plastic bags which were filled and returned to the laboratory for grain size determination.

Figure 4-33 Silt fence sediment content example at plot A2 (Corina Gwerder)

Figure 4-34 GPS surveying work with Pat and Christian at Plot G1 (Corina Gwerder)

Table 15 Measurements on plots (x = measurement taken)

Date	A1	A2	B1	B2	C1	C2	D1	D2	E	F	G
11.07	x	x	x	x	x	x	x	x			
13.07	x	x	x	x	x	x	x	x			
20.07							x	x			
26.07	x	x	x	x	x	x	x	x			
02.08									x		
06.08							x	x	x	x	x
11.08	x	x	x	x	x	x	x	x	x	x	x
16.08							x	x	x	x	x
23.08	x	x	x	x	x	x	x	x	x	x	x
30.08	x	x	x	x	x	x	x	x	x	x	x
07.09	x	x	x	x	x	x	x	x	x	x	x
20.09	x	x	x	x	x	x	x	x	x	x	x
27.09	x	x	x	x	x	x	x	x	x	x	x
04.10							x	x	x	x	x
11.10	x	x	x	x	x	x	x	x	x	x	x

Problems encountered during the investigation period

During the measurement period I had, except for crossing the Küferalpgraben (Figure 4-35 and Figure 4-36), no difficulties. However there were some points I had to keep in mind. The weather and its change during the measurement day posed a hazard. Due to the steep walls the view out of the catchment is quite restricted. Storms coming from the south arrive therefore unanticipated and fast. Because storms from that direction often bring strong precipitation to the Illgraben which can give rise to debris flows, it was safer to do the measurements on a clear day or to immediately leave the catchment if there was a storm approaching. When the weather was uncertain I often informed a person to observe the weather radar at home and give alarm through mobile telephone when the weather was deteriorating. In addition to the debris flow danger, wet weather reduced the ground stability and made walking on the steep slopes difficult.

Figure 4-35 Küferalpgraben – crossing in July, 2006 (Corina Gwerder)

Figure 4-36 Küferalpgraben – Crossing in August, 2006 (Corina Gwerder)

The crossing of the Küferalpgraben, which is necessary to arrive to the Steinschlag Hut and the surrounding plots, was a particularly serious hazard. During our site selection in June 2006 we did not recognize the Küferalpgraben as an almost impassable gully because at that time its trench was filled with avalanche snow and mud and was therefore easy to cross. On our first installation day a small debris flow passed through the gully after our crossing and sensitized us to the processes and hazards. The Küferalpgraben changed continuously due to warming and snow melt, erosion, debris flows, rock fall, and caused each crossing to be unique and potentially hazardous. Although the installation of a fixed rope and abseiling down to the gully floor ground with mountaineering gear made the crossing possible, it could not be safely done every time due to uncertainty in the weather forecast. Due to this circumstance the numbers of measurement and intervals vary from plot to plot (Table 15). To ensure sufficient data, three more silt fence plots (E, F and G) were built in a second installation phase.

4.3 Aerial photographs

4.3.1 Available aerial photographs of the study area

Many aerial photographs are available from the Illgraben and its surrounding areas. Mostly the pictures are focused on the debris fan and the Pfyn-forest, only a few contain the entire catchment (Table 16).

Table 16 Available aerial photographs of the study area

Date	Location	Number	color
1959	Department of Geology Uni Bern	-	Black and white
1963	Swisstopo	548-549	Black and white
1967	Swisstopo	2203-2208, 2048-2051	Black and white
1969	Swisstopo	7252-7255	Black and white
1974	Swisstopo	3263-3267	Black and white
1980	Swisstopo	3072-3079, 3961-3962	Black and white
1986	Swisstopo	7757-7759	Black and white
1992	Swisstopo	-	Black and white
1999	Swisstopo	-	Color
2000	Swisstopo	-	Color
2004	Swisstopo	-	Color

The aerial photograph-based catchment analyses were carried out with the 1959, 1999 and 2004 images. This choice was constrained by image availability and the interval between images. On the basis of this selection comparisons between changes during a longer period (1959-1999) and a shorter period (1999-2004) could be made.

4.3.2 Orthophotos

For the image analyses, the selected aerial photographs were transformed into orthophotos. This work was done together with David Schnydrig (University of Berne) using ERDAS (photogrametry software). For the images of 1959 and 2004, all the necessary reference points were measured by students from the University of Berne in a field course that I also attended. The 1999 image was already georeferenced by Swisstopo and as a complete orthophoto available for order via ETH Zurich. The generation of the orthophotos from the 2004 and 1999 images took, due to the complexity of the ERDAS software, more time then estimated.

4.3.3 Catchments area and slope distribution

The Illgraben catchment consists of forest, grassland and erosion areas. The distribution of those different subsystems has been digitalized with ArcGis for 2004 and out of those files size of the areas belonging to the different subsystems could be calculated. Applying the DEM25 by Swisstopo together with the Orthophoto 2004 and the related files, the distribution of slope angles in the subsystems and the entire catchment could be generated.

Due to the high degree of geomorphologic activity observed in the Illgraben catchment the two other established orthophotos were analyzed for the calculation of the subsystem (land cover) area distribution. The years in between the orthophotos form a time period were significant changes could occur and be detected. For the analyses a long time period (1959 to 1999) and a short time period (1999 to 2004) were chosen (Figure 4-37).

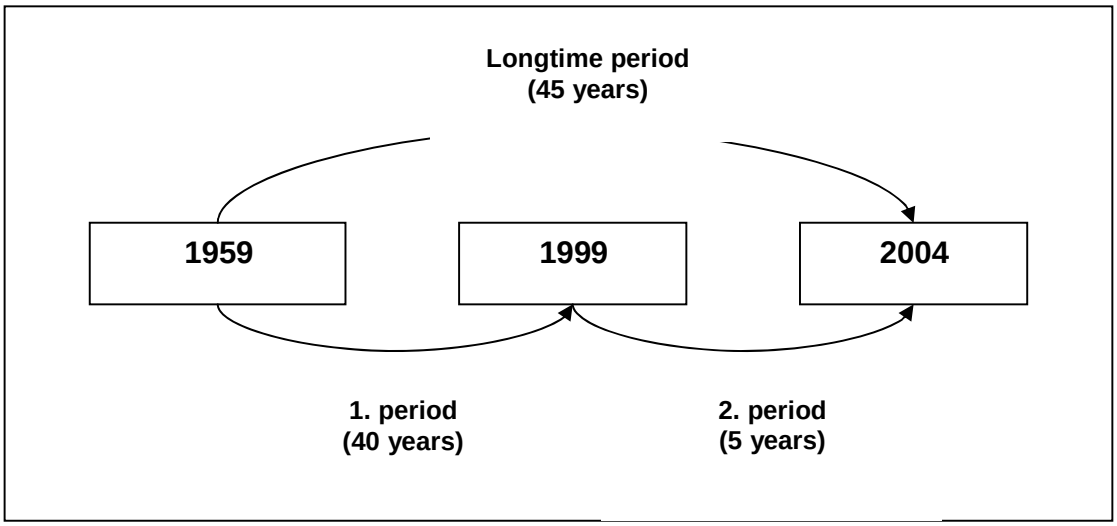

Figure 4-37 Catchment changes observation periods (Corina Gwerder)

4.3.4 Coupling relationship

The coupling relationship within the investigated catchment was determined for all three years (1959, 1999 and 1999) by digitalizing the areas that are directly connected with the channel (coupled system), and the areas decoupled from the channel network (decoupled system). The decoupled system is further divided into subsystems: forest areas, grassland areas and erosion areas (decoupled erosion). The coupled system consists only of erosion areas that are connected to the channel network. Coupled and decoupled erosion areas belong in this regard to different systems (coupled- and decoupled systems) (Figure 4-38).

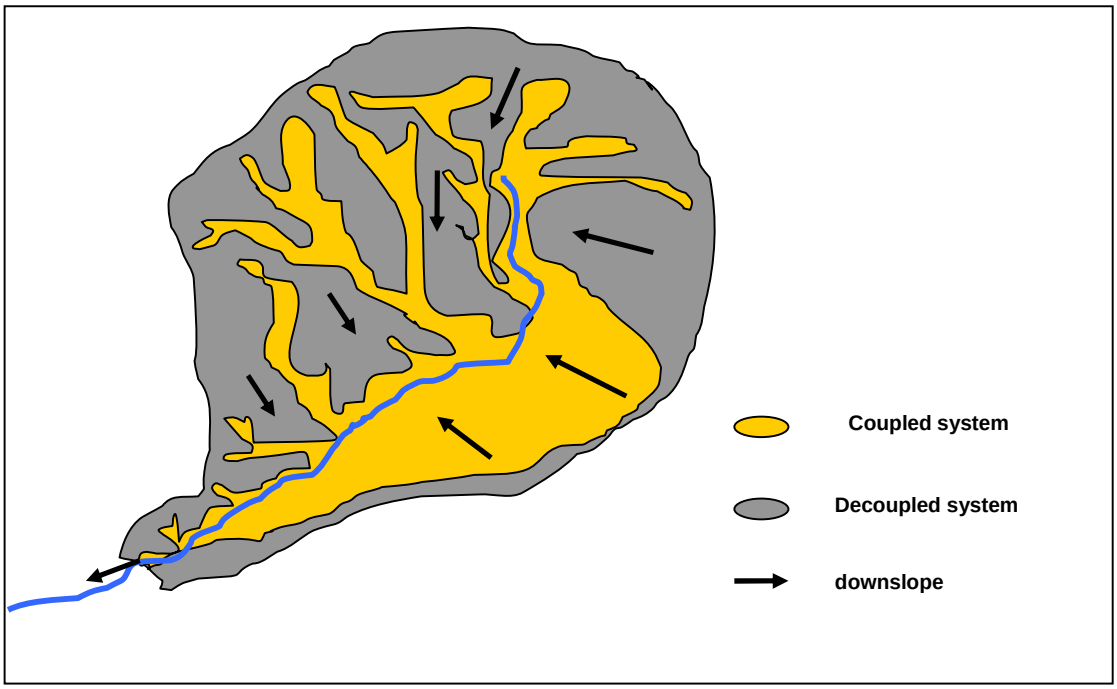

Figure 4-38 Example of a catchment with a coupled- and decoupled system (Corina Gwerder)

4.4 Process rates and Sediment budget

Using the field data from the silt fence plots and data from the WSL force plate, process rates could be determined for the two systems and their subsystems. The sediment and erosion rate is given in [g / (m^2*day)]. For the decoupled system it was calculated using measured silt fence sediment amounts in relation to the corresponding plot size and length of measurement interval. That means the process rates in the decoupled system consist of the measured silt fence sediment amounts, the silt fence plot size and the measurement interval. For the individual silt fence plot sites the process rates were averaged over the measurement period so that the different plot sites can be compared with each other. The process rate for the subsystems and the entire decoupled system were composed of the process rates on the individual silt fences weighted by catchment area. Thought has been given also to the maximum process rates on the individual silt fence plots, but they haven't been considered for the calculations in this thesis due to time constraints. The process rate for the coupled system was determined using debris flow data measured at the force plate. This total sediment output out of the coupled system was averaged over the time between the first and last debris flow occurrence in 2006 (138 days) and over the size of the coupled area.

Based on these process rate data, comparisons between the different systems could be done and a sediment budget could be constructed. The sediment budget considers the different areas with their process rates based on the data from the silt fences. For the decoupled subsystems and decoupled system, the process rates were extrapolated to a year (365 days) for the sediment budget calculations. Because the process rate of the coupled system is based on debris flow data, the calculation for this system hasn't been done over the entire year but only over the period during which debris flows and intensive precipitation events occurred. In the measurement year 2006 there where 138 days between the first (in spring) and last (in autumn) debris flow event. On the remaining days intense precipitation events are normally rare and the precipitation falls in the form of snow.

4.5 Distributions and compositions

4.5.1 Grain size distribution

The grain size distribution was measured twice for the collected silt fence volumes and ground layers of each plot. Twice I measured the silt fence volumes in the field by means of a gravel raster (the small fraction was determined in the laboratory). In the laboratory three more samples per plot were measured to determine the grain size distribution of the fine sediments. The laboratory work was carried out with the dry sieving method. Out of the grain size distribution the D50 and D90 were calculated. The following sieves were used: 45, 32, 22, 20, 10, 4, 2, 1, 0.5, 0.355 and 0.1 mm.

4.5.2 Petrography composition

The petrographic composition determined by David Schnydrig (UniBe) (Table 17) was used to detect the sediment sources and proportions of the coupled sediment output. Due to the fact that the southern Illgraben catchment is composed of quartzite deposits and the northern zone of dolomite and calcareous deposits, the petrographic composition can indicate the origin of the sediment, indicating which areas are active in delivering sediment. Although not investigated herein, such information could potentially be used to design hazard mitigation concepts in heterogeneous catchments.

Table 17 Petrography composition (David Schnydrig, UniBe)

Quartzite	Quartzite with Rose quartz	Greywacke	Dolomite	Calcite	Schist and Gneiss
Southern-catchment	Southern-catchment	Northern-catchment	Northern-catchment	Northern-catchment	Channel bed
43.7%	16.8%	1.9%	3.0%	20.5%	14.1%

4.5.3 Temperature and precipitation distribution

Because observed climate change could influence the erosion rate and behavior, the temperatures and precipitation events for recent years were analyzed. As it was not the aim of this study to confirm global warming by data and analysis, the carried out investigations were not based on statistical tests. The temperature and precipitation distribution should however provide a better background and support the discussion of the results. For the temperature distribution, values from the MeteoSwiss station Sion were used. Of note were the mean temperatures of the months January and July for the years 1864 to 2005 as well as the number of days with a mean temperature higher than 0° for the years 1954 to 2005. In contrast to temperature values, long-term precipitation data from in the Illgraben region are rare. Only four stations near the Illgraben provide values from 1961 to 2006: Grimentz, Sierre, Hérémence and Leukerbad. The last one, although close situated to the Illgraben, could not be used because the climate there is northern Alpine. For Grimentz, Sierre and Hérémence daily values were used for the analysis. Two different periods, based on measurement intervals for the aerial photography used herein, were evaluated in an attempt to identify a trend to more intense rainfall due to climate warming: 1961-1999 and 2000-2004. Unfortunately, no data are available before 1961. Nevertheless, the rainfall distribution for the two periods may be compared and a possible accumulation of intense precipitation events or a local change in precipitation amount could possibility be shown.

5 Results and discussion

5.1 Climate

5.1.1 Automatic precipitation measurements at the Illgraben

For this thesis, the measurements from the automatic precipitation pluviometer 3 (Table 18) were considered for the silt fence plot analysis and pluviometer 1 (Table 19 and Table 20) for the debris flow analysis. This choice has been made due to the proximity of the rain gauges to the plot sites and the debris flow initiation zone respectively, and the fact that Pluviometer 2 was out of order during the 2006 summer months.

Table 18 Automatically precipitation values pluviometer 3, Illgraben

#	dates	P3 sum [mm]	P3 max. intensity [mm/h]	# P3 h with precipitation	# P3 10min intensity >2mm	# P3 10min intensity >1mm	# P3 60min intensity >4mm
1	26.06.-11.07.06	39.6	9.2	31	2	3	1
2	11.07.-13.07.06	0	0	0			
3	13.07.-20.07.06	4.2	2	3			
4	13.07.-26.07.06	6	2	6			
5	20.07.-26.07.06	1.8	0.8	3			
6	26.07.-06.08.06	43.2	5.8	38	1		
7	28.07.-02.08.06	9.2	1.2	7			
8	02. 08.-06.08.06	9.2	3.2	30		3	
9	26.07.-11.08.06	44.4	5.8	40	1		
10	06.08.-11.08.06	1.2	0.6	2			
11	11.08.-16.08.06	17.6	1.8	23			
12	11.08.-23.08.06	25.2	2.4	35	1	1	
13	16.08.-23.08.06	7.6	2.4	12	1	1	
14	23.08.-30.08.06	40	6	33		4	1
15	30.08.-07.09.06	0.8	0.4	3			
16	07.09.-20.09.06	13.8	1.6	27			
17	20.09.-27.09.06	5.8	0.8	16			
18	27.09.-04.10.06	22.4	7.2	18	1	6	1
19	27.09.-11.10.06	28.2	7.2	22	1	6	1
20	04.10.-11.10.06	5.8	4	4			1

During the measurement interval, precipitation in the Illgraben catchment was low. This was due to the dry and hot climate conditions during the summer 2006 and the location in an inneralpine valley, which is already characterized by a mild climate and a low annual precipitation. Between the 26th of June and the 11th of October we had 329 hours with rain, of which the maximum precipitation intensity during one hour was 9.6 mm (pluviometer 1). On 5 days we could measure a precipitation rate higher than 2 mm per 10 minutes (pluviometer 1, Table 19) and on four days a precipitation rate higher than 4 mm per hour (pluviometer 1, Table 19). Every precipitation rate higher than 2 mm per 10 minutes at pluviometer 1 was correlated with one of the five debris flows during the silt fence plot measurement period. Values from pluviometer 1 correlated better with debris flow occurrence than pluviometer 3 values. Even though the values at pluviometer 3 were much smaller, they showed (as the ones at pluviometer 1) the highest intensity rates during days where a debris flow occurred.
This shows clearly that the coupled system output which has been quantified by the debris flow outputs is related to precipitation conditions. From the precipitation data it becomes apparent that debris flows out of the Illgraben catchment were not correlated with precipitation amount but by precipitation intensity. In an other study by Selby (1993) three potential sources of excess water were identified: intense rainfall, rapid snowmelt, and more rarely, glacier or lake overflows which mobilizes unconsolidated materials in their path. Due to the fact that all debris flows in 2006 correlated with an intensive rainfall event, snowmelt only could have been a supporting force for the first three debris flows.

Table 19 Debris flow events and precipitation intensities from pluviometer 1

Debris flow events	Max.10 min intensity [mm/10min]	Max. 30 min intensity [mm/30min]	Max. 60 min intensity [mm/60min]
24.06.06	8.4	19.2	24.2
27.06.06	4.2	11.2	13.4
18.07.06	9.6	21	27.4
28.07.06	5	8.6	13
03.10.06	3.8	8.6	14

Table 20 Debris flow events and maximum precipitation intensities for a 10 minutes interval from pluviometer 3

Debris flow events	Max.10 min intensity [mm/10min]
18.05.06	1.8
24.06.06	3.6
27.06.06	3.6
18.07.06	1.6
28.07.06	2.6
03.10.06	2.2

5.1.2 Long-term temperature and precipitation distribution

Future global warming has a number of implications for fluvial geomorphology because of changes in phenomena such as rates of evaporation, precipitation characteristics, plant distribution, evapotranspiration, sea level, glacier and permafrost melting, and human response (Goudie, 2006). Many climatologically, hydrological and vegetation scenarios have not been considered for the most part by the development and scenarios of future geomorphological change in fluvial systems. By itself, increases in temperature, estimated by the Intergovernmental Panel of Climate Change (IPCC, 2001) to be between 1.5 and 6°C on a global basis by 2100, will tend to melt snow and ice and promote greater loss of soil moisture through increased evaporation. In addition, changes will occur in the amount intensity, duration, type and timing of precipitation, which will affect river flow and groundwater recharge. (Goudie, 2006). There is evidence from a number of European data analyses that the wintertime changes are associated with an increase intensity and frequency of rainfall (Klein Tank and Können, 2003). For Switzerland, statistical significant frequency increases for intense events in winter and autumn for a large number of stations in the Alpine regions were found (Frei and Schär, 2000; Frei, 1998). More frequent heavy precipitation events in the Alpine region may significantly increases the risk of damage from flooding, erosion, debris flow or landslides (Fuhrer, 2006). Furthermore, where vegetation cover will respond to temperature and precipitation changes, with concomitant changes in sediment yield and the operation of erosional processes are expected. Bogaart (2003) pointed out that landscape response to climate change is highly non-linear, and characterized by numerous feedbacks between different variables and by lead-lag phenomena. Modeling studies from a range of different environments suggested that the increases in rates of erosion could be on the order of 25-30 % (Goudie, 2006). Climate (precipitation and temperature) influences erosion rates also through its variability, which for example changes chemical erosion rates worldwide (Riebe, 1991). An example how a system may responds to climate change has been investigated with a study on gully-erosion formation (Valentin, 2005). Where under cold conditions global warming was expected to increase the frequency of freeze-thaw cycles and therefore exacerbate the risk of gullying.

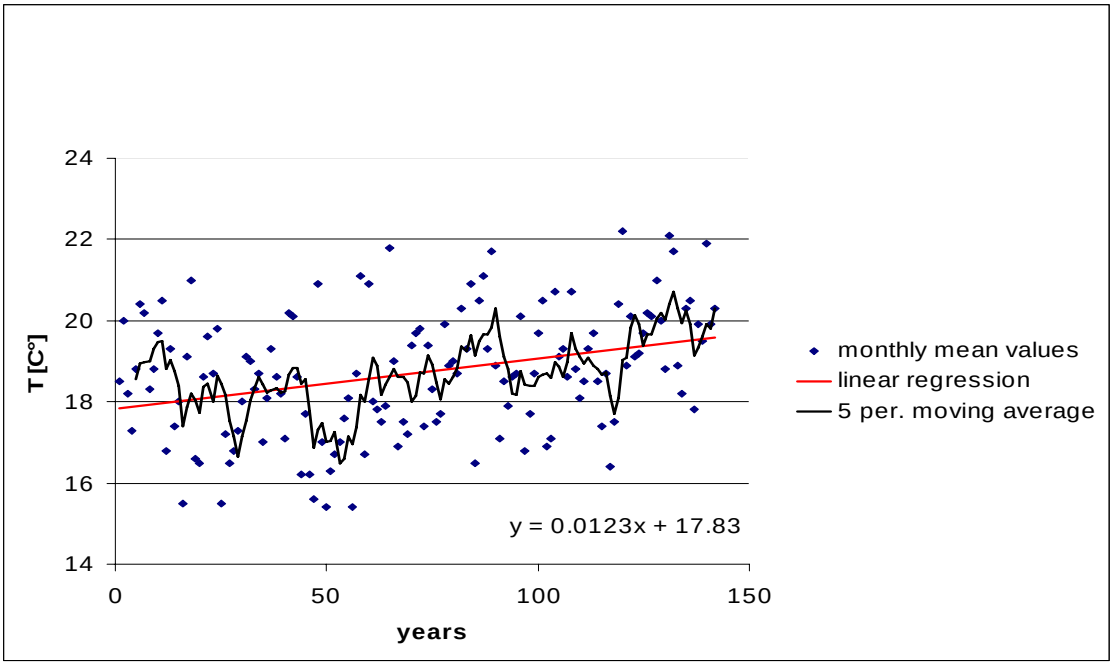

Figure 5-1 Mean monthly July temperature for the years 1864-2005 (data: MeteoSwiss)

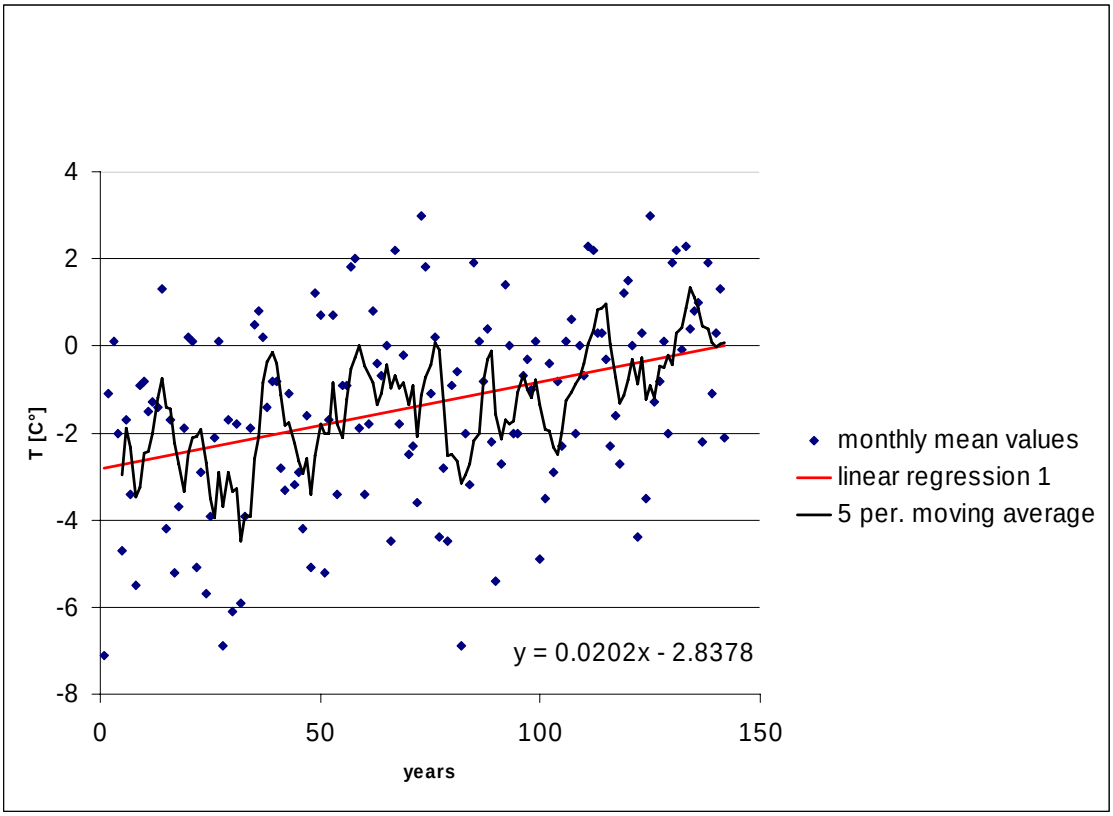

Figure 5-2 Mean monthly January temperature for the years 1864-2005 (data: MeteoSwiss)

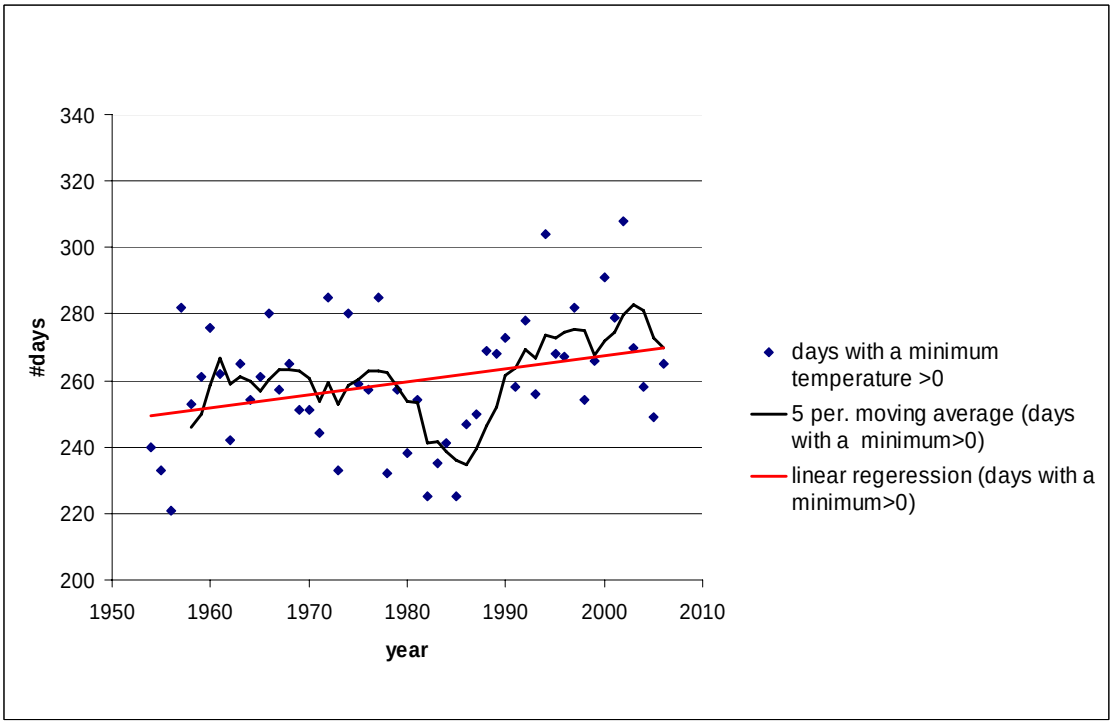

Figure 5-3 Numbers of days with a temperature higher than 0° C for the years 1954-2005 in (data: MeteoSwiss)

The temperature distributions for the station Sion showed an increase for recent years (Figure 5-1 to Figure 5-3). The temperature increase was higher in the winter (January) than in the summer (July). On the average there are more days with a mean temperature over 0°C from 1990 until 2006 than from 1954 until 1990. Even if those conclusions weren't statistically tested herein, they show a trend towards a climate warming and correlate with the scenarios by the Intergovernmental Panel of Climate Change (IPCC, 2001) and related studies. Out of the precipitation amount distribution at the stations Grimentz (Figure 5-4), Sierre (Figure 5-5) and Hérémence (Figure 5-6) there was no obvious trend towards more intense rainfall events. The distribution of the period 1959 to 1999 was almost identical to the period 2000 to 2004. This showed that there was no large change in precipitation intensity distribution during the last 45 years. However, these precipitation amount distributions are, due to the fact that they are daily sums and not hourly (or shorter) values, must be cautiously interpreted. On the basis of the frequency increase for intense events in winter and autumn in the alpine region of Switzerland, a trend towards more short and intense rainfalls can not be excluded at the stations considered herein. One consequence of a frequency increase for intense rainfalls in winter and autumn is the change to a longer debris flow period and therefore an increase or a seasonal shift in the debris flow occurrence for the future.

Even if the temperature increase wasn't statistically tested and an increase in precipitation intensity couldn't be demonstrated using daily precipitation amount, climate warming probably has most likely an effect on the Illgraben geomorphology, at least with the degration of probable permafrost on the north face of the Illhorn. How important this effect is for an alpine catchment, is a major research priority for geomorphologists (Goudie, 2006).

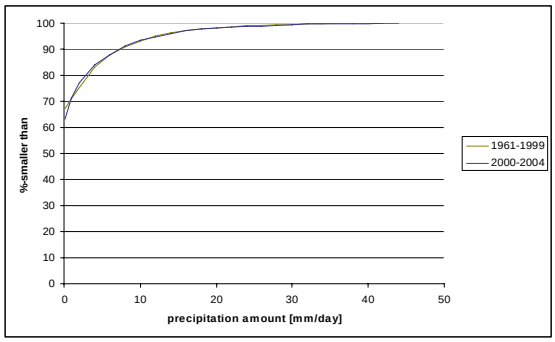

Figure 5-4 Long-term precipitation distribution Grimentz

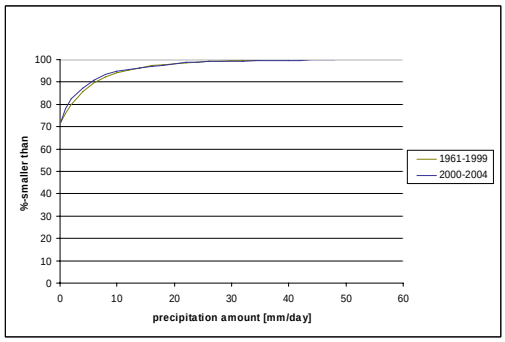

Figure 5-5 Long-term precipitation distribution Sierre

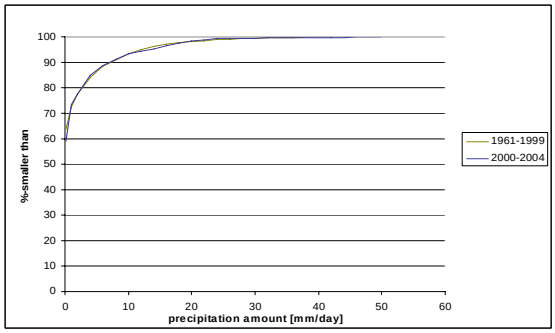

Figure 5-6 Long-term precipitation distribution Hérémence

5.2 Silt fence sediment measurements

5.2.1 Effect of variables

The rainfall variables (Table 42 and A.4) were compared with total sediment amount (Table 44, A.4). The sediment transport rate consists of the sediment amount divided by the measurement interval. This rate was calculated to get a better basis for comparison between the different plot sites that showed less measurement intervals due to the inaccessibility. In the results, the variable “sediment rate” had a better correlation with “precipitation amount” than “sediment amount” and distinguished the differences between the upper- and lower plot sites. The variables can be split into two groups:

Precipitation: The variables “precipitation amount” (Table 42, Figure 5-7, and Figure 5-8) and “precipitation rate” (Table 43, Figure 5-9 and Figure 5-10) belong to the precipitation group. The variable “precipitation amount” represents the total precipitation during one measurement interval, whereas the “precipitation rate” describes the average amount of rain during the number of precipitation hours in one measurement interval from pluviometer 3. The sediment data showed interestingly a better correlation for the variable “precipitation amount” than for “precipitation rate” (Table 21, Table 22). This may be due to the high number of hours with precipitation that had only a very small amount. There were so few events with intensive rainfall during one hour that for the analysis, the “precipitation rate” was rather misleading than useful and will therefore not be used for further discussions. The absence of a correlation with “precipitation rate” measurements on the plot sites created an unanticipated problem. It is usually reported that soil erodibility increases with rainfall duration (Bryan, 2000), strong intensities and high that kinetic energy values of rainfall are considered the main variables explaining erosion (Descroix and Mathys, 2003). In the Black Marls of the French Alps, observations and measurements similar to those carried out in the Illgraben were performed at the plot scale with simulated rainfall and natural rainfall (Mathys, 2005). They had almost no erosion under low-intensity rainfall simulations, where the low sediment yield was due to both to the low erosivity of the raindrops and low runoff available for sediment transport. In high-intensity rain, erosion was notable and the two plots that represented the highest runoff also showed the highest sediment yield. With very high-intensity of short duration, the total amount of sediment increased considerably. As a result of missing high-intensity rainfall events during the 2006 measurement period and the prevailing soil conditions in the Illgraben (for example the very large infiltration rate for the lower erosion slopes), surface runoff was never observed.

Measurement interval: The variable “measurement interval” (Figure 5-11) represents the time period between the measurements at the silt fence plots. It corresponds to the time where erosion processes can occur. This variable showed a better correlation with “sediment amount” and “sediment rate” than the precipitation variable. In section 5.2.3 some statements are made to explain this finding. Important processes could have been the natural gravity (dry ravel), weathering, particle dislodgement due to animal activity at animal crossings. The weighting for those different processes and appearances are not yet known.

Sediment amount versus plot precipitation

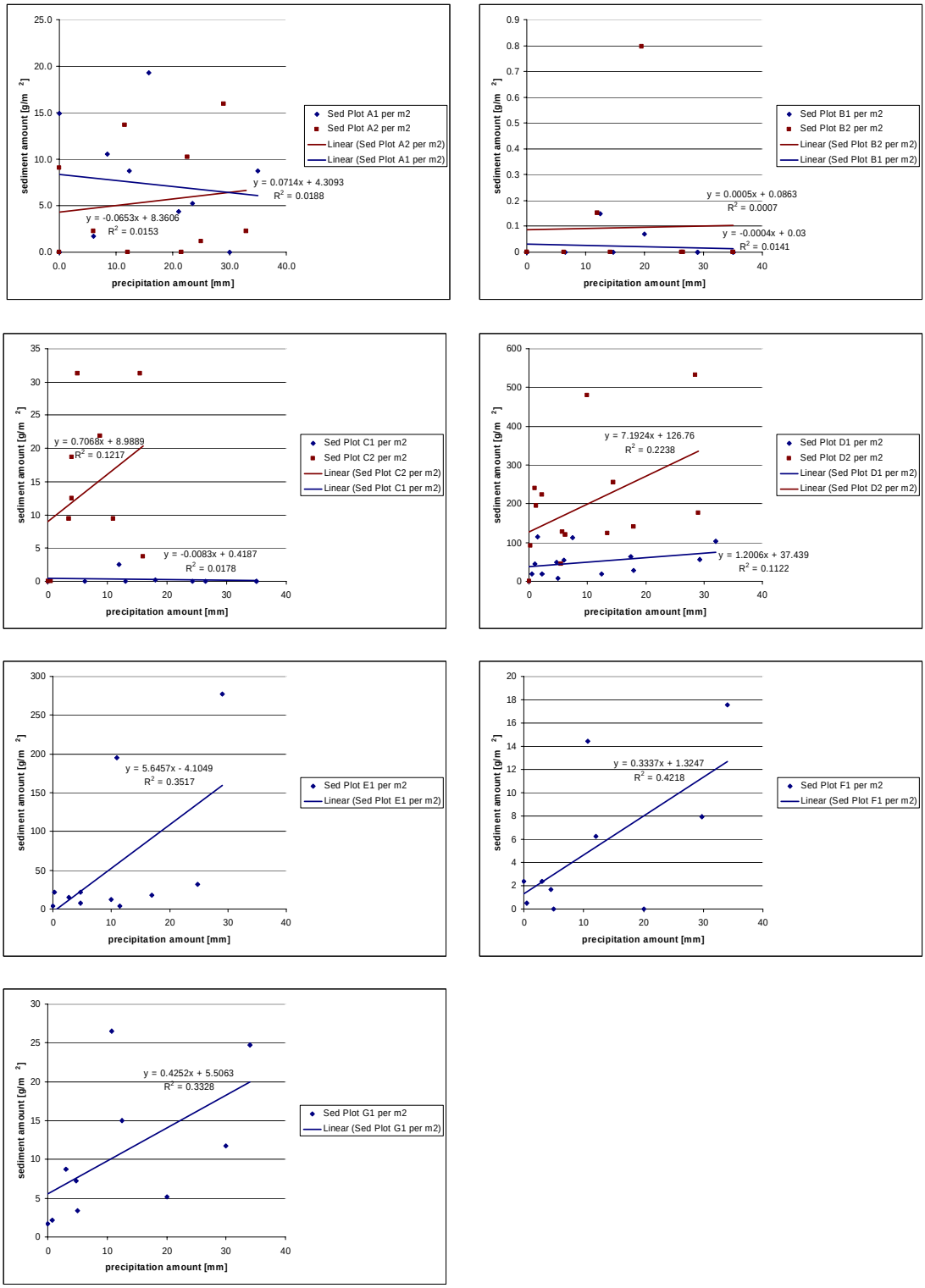

Figure 5-7 Sediment amount versus precipitation amount on the individual silt fence plots.

Sediment amount versus plot precipitation rate

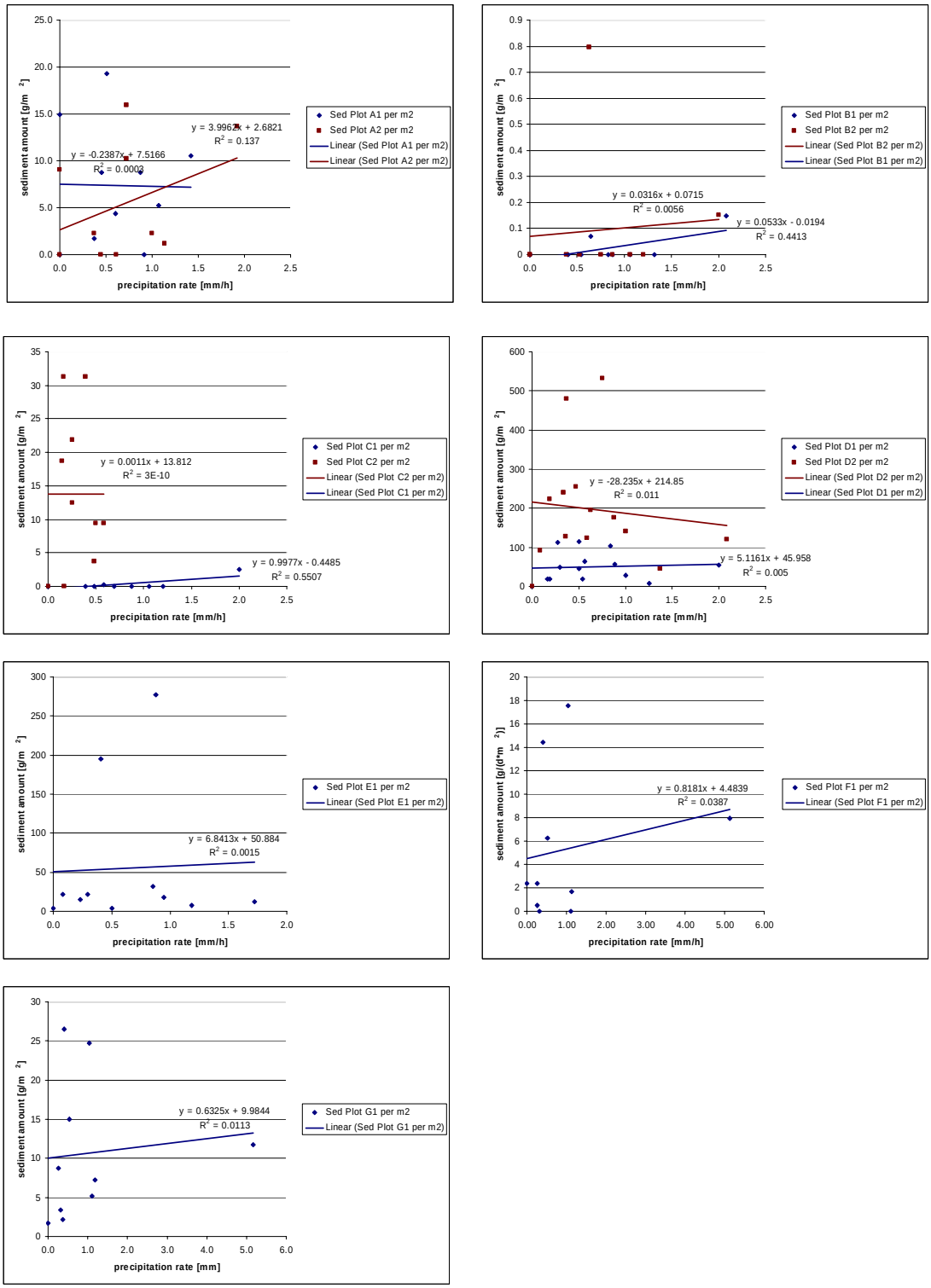

Figure 5-8 Sediment amount versus precipitation rate on the individual silt fence plot sites

Sediment rate versus plot precipitation amount

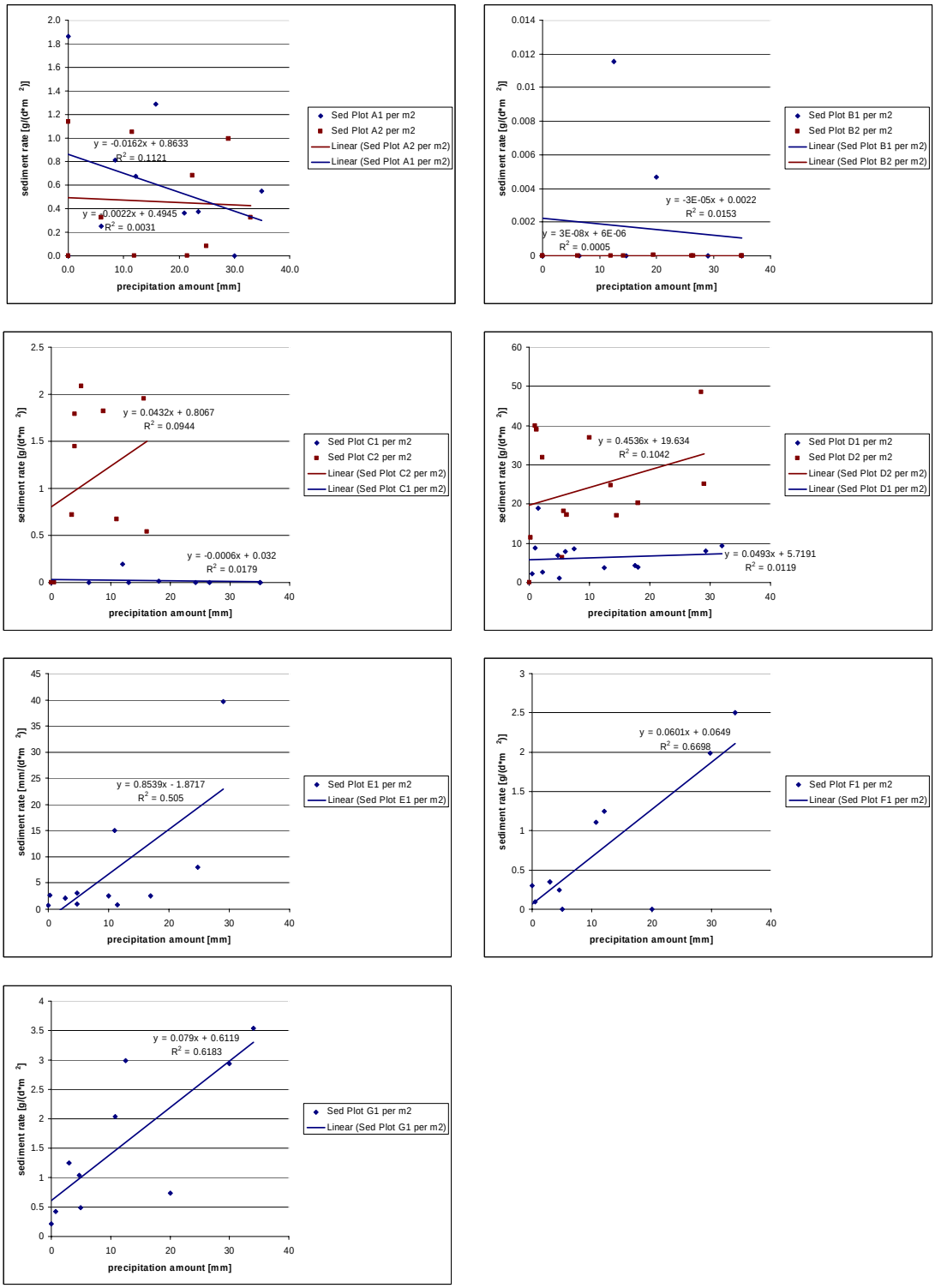

Figure 5-9 Sediment rate versus precipitation amount on the individual Silt fence Plot sites

Sediment rate versus plot precipitation rate

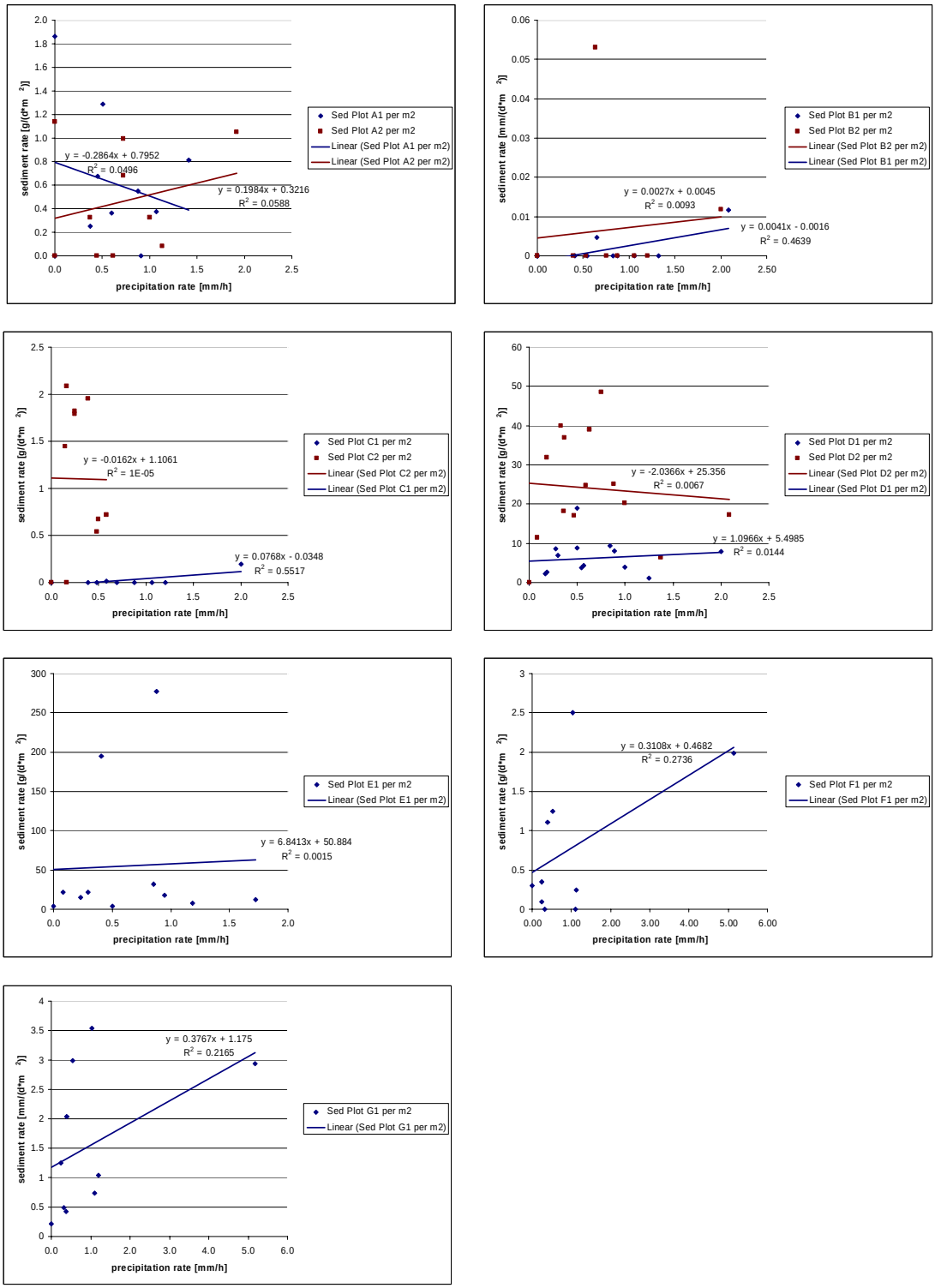

Figure 5-10 Sediment rate versus precipitation rate on the individual Silt fence sites

Sediment amount versus measurement interval duration

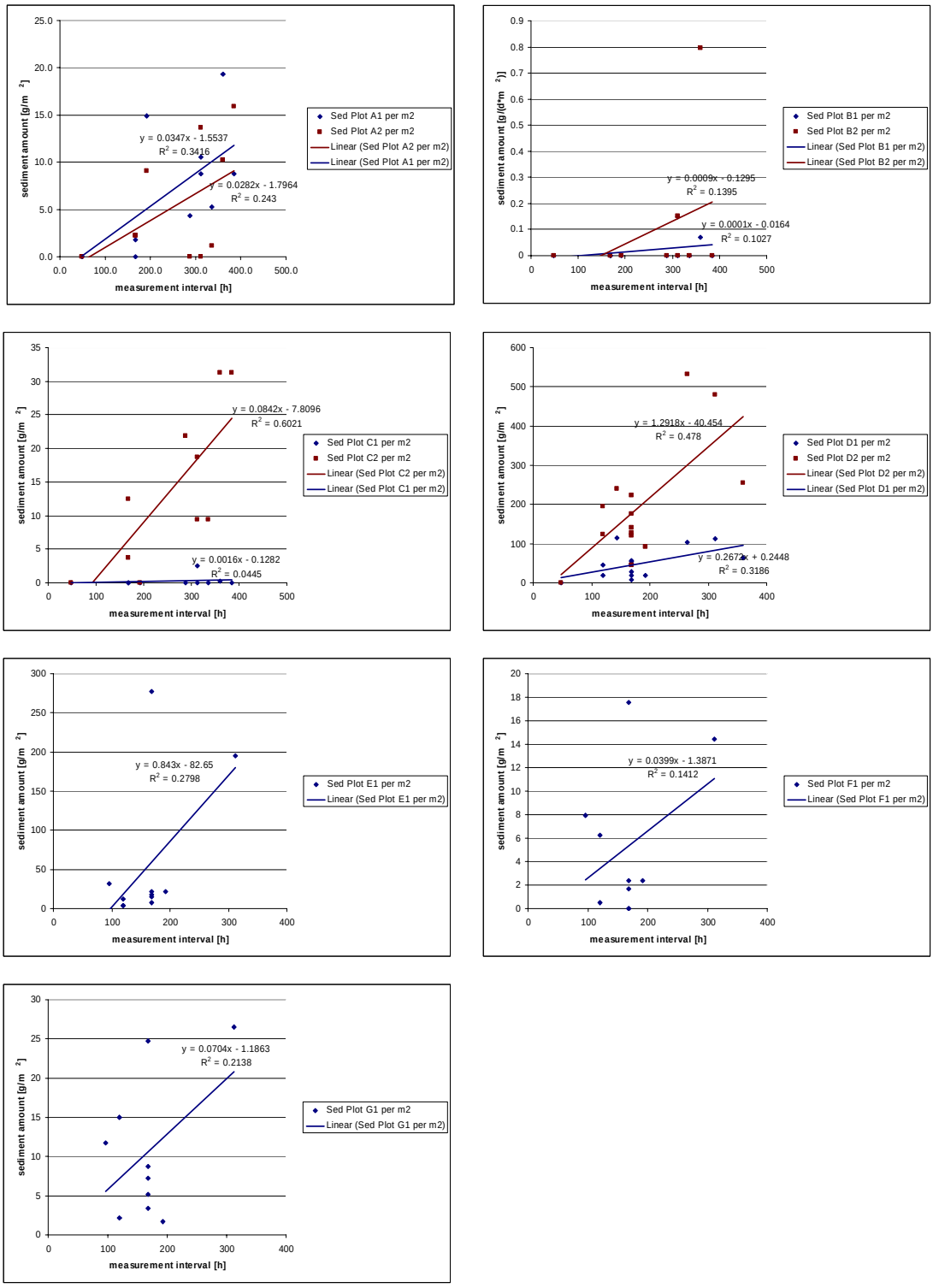

Figure 5-11 Sediment amount versus duration of measurement interval on the individual silt fence sites

5.2.2 Correlation on the basis of the R2-coefficient

These correlations correspond to the figures Figure 5-7 to Figure 5-11 and are not based on statistical tests. The tables should help for a better understanding of the different relations and perform an overview for the reader.

0 = no correlation (0 <= R^2 0.1)
\+ = small positive correlation (0.1 <= R^2 < 0.3)
++ = medium positive correlation (0 .3<= R^2 < 0.6)
+++ = strong positive correlation (0.6 <= R^2 < 0.8)
++++ = very strong positive correlation (0.8 <= R^2 < 1.0)

Table 21 Plot sediment amounts [g / m] versus different variables

Plots Sediment amounts	Precipitation amount [mm]	Precipitation rate [mm/h]	Measurement interval [h]
A1	0	0	++
A2	0	+	+
B1	0	++	+
B2	0	0	+
C1	0	0	0
C2	+	++	+++
D1	+	0	++
D2	+	0	++
E1	++	0	+
F1	++	0	+
G1	++	0	+

Table 22 Plot sediment rates [g / (m*d)] versus different variables

Plots Sediment rates	Precipitation amount [mm]	Precipitation rate [mm/h]
A1	+	0
A2	0	0
B1	0	++
B2	0	0
C1	0	++
C2	0	0
D1	+	0
D2	0	0
E1	++	0
F1	+++	+
G1	+++	+

The erosion slope next to the Steinschlag hut (A1, A2) shows the best correlation between the sediment amount and the measurement interval. The same applied with a few exceptions for the grassland (B1 and B2), the forest (C1 and C2) and the erosion slope on the way up to the Steinschlag hut (D1 and D2). The exceptions were the correlation of B1 between the sediment amount and the precipitation rate (R^2 = 0.44) and between the sediment rate and the precipitation rate (R^2 = 0.46) as well as the only correlation of C1 between the sediment rate and the precipitation rate (R^2 = 0.55).

5.2.3 Behavior in and between the different subsystems

As described previously the silt fences plots were built in the decoupled system on three subsystems: forest, grassland and decoupled erosion. Two fences (C1, C2) belonged to the forest-, two others to the grassland- (B1, B2) and the remaining ones to the decoupled erosion subsystems (A1, A2, D1, D2, E1, F1 and G1). First, we discuss the individual subsystems separately, and second we focus on the relations among those subsystems:

Forest: Plot C1 and C2 differed strongly in their response to the variables. The sediment amount in C2 was strongly correlated with the "measurement interval" and further by the "precipitation amount". In contrast, Plot C1 showed no correlation to those individual variables. Opposite behaviors between those plot sites were based on different ground cover and vegetation. C1 was located in a pioneer forest with a tree composition of young birches and rowan trees. The ground layer consisted of fine pastures that formed a soft layer. The precipitation, even the strongest events in summer 2006, did not cause erosion. Therefore C2 had, except for organic material (which was not measured), no sediment in its silt fence. The pastures and the pioneer trees must have protected this ground with their roots and cover from rain and protect the ground from surface runoff and erosion processes. Plot C2 had was located in a steep old spruce forest marked by slope failure, rock fall and bark-beetle activity - entirely different processes. Bratton (1979) found a relation between erosivity and vegetation, where the spruce forest was the most erosion sensitive plant communities. The high erosion sensitivity of spruce forest is due to a missing ground layer, finer grain sizes and the hydrophobic needles, that reduce the ground infiltration and therefore maximize surface runoff and slope erosion. If there were more intense rainfalls than during summer 2006 the erosion rates between C1 and C2 would differ perhaps even more strongly than now.

Grassland: Plots B1 and B2 were located close to each other on the same grassland and their similar behavior is to be expected. During the measurement season 2006, there was a negligible amount of sediment in their silt fences and they showed only a small correlation with the variable "measurement interval". The correlation between "sediment amount" and "measurement time" could have been a statistical error, due to the fact that the amounts were infrequently measured and small. The vegetation and deeper ground layer than on the other plot sites protected the ground from erosion processes (through roots, a high water infiltration, etc.). Those negligible sediment amounts correspond to other studies, where erosion in bare outcrops was more than 1000 times higher than in grassland (Descroix and Mathys, 2003).

Decoupled erosion: Because seven plots belonged to the subsystem "decoupled erosion" the variability between the individual plots was higher and more processes played a role than in the other subsystems. Plots A1 and A2 responded similarly and showed interestingly only correlations with the variable "measurement interval". The reason could have been a high ground stability (the ground could already have been saturated), too little precipitation for ground saturation or the fact that no stones could have jumped from uphill of the PVC plate into the plot sites (the silt fence were located on the top of the erosion slope). Plots D1 and D2 showed related behaviors as A1 and A2. They had a slightly higher correlation to the variable "measurement interval" and in addition a small correlation with the "precipitation amount". The higher correlation over "measurement interval" could have resulted from stones coming from locations uphill of the PVC plates that jumped over them and stopped in the silt fence. The detachment of those stones could have been through natural gravity processes (slope angles around 45°) and nimal-induced dislodgement of particles at animal crossings. How much those animals crossing influenced the results is not known, but the presence of animal trails confirmed their existence. Plots E1, F1 and G1 all showed a correlation with "precipitation amount" and a smaller extent with "measurement interval", where they acted similarly. The possibility of stones coming from areas uphill of the PVC plate into the plot sites and silt fences was pervasive but not as high as it was on D1 and D2. Why the lower plots correlated much better with "precipitation amount" than the upper ones (A1,

A2, D1 and D2) is of interest. Due to the location of the silt fences E1, F1 and G1 in the lower end of the long erosion slopes, processes originating from upper sites into the plot sites could have been more frequently measured downslope than in the upper plots (Figure 5-122).

Figure 5-12 Difference in location of the plot sites between the upper- and lower ones

Explanations for those processes on the plots E1, F1 and G1 were based on three assumptions:

1. **Reduction of resistance**: Water could have reduced the resistance and produced therefore movements in the steeper parts (the angle of repose decreased). This was the only hypothetical explanation for the plots E1, F1 and G1 that assuming that the PVC plate is impassable (assumes that rocks could not have jumped over the upper barrier).

2. **Reduction of resistance and surface runoff**: Besides the reduction of resistance through water, surface runoff mobilized small particles and stones. When the resistance decreased, the natural angle of repose decreased and therefore material with a reduced resistance could have been moved easily by surface runoff. This assumption is based on a permeable upper boundary, where the surface runoff could have gone across and stones could have been jumped over.

3. **Rockfall triggering through precipitation**: The last assumption (Figure 5-13) is based on rockfall triggered by precipitation, also known as a dry ravel process. At the upper end, the erosion slope passes into steep rock walls where rainfall could have initiated small rockfalls. The stones could have fallen down the wall to the upper end of the erosion slopes. During their deceleration they could have passed their energy to proximate stones on the erosion slope what could have released a chain which initiated individual stone movements or a small rock avalanche.

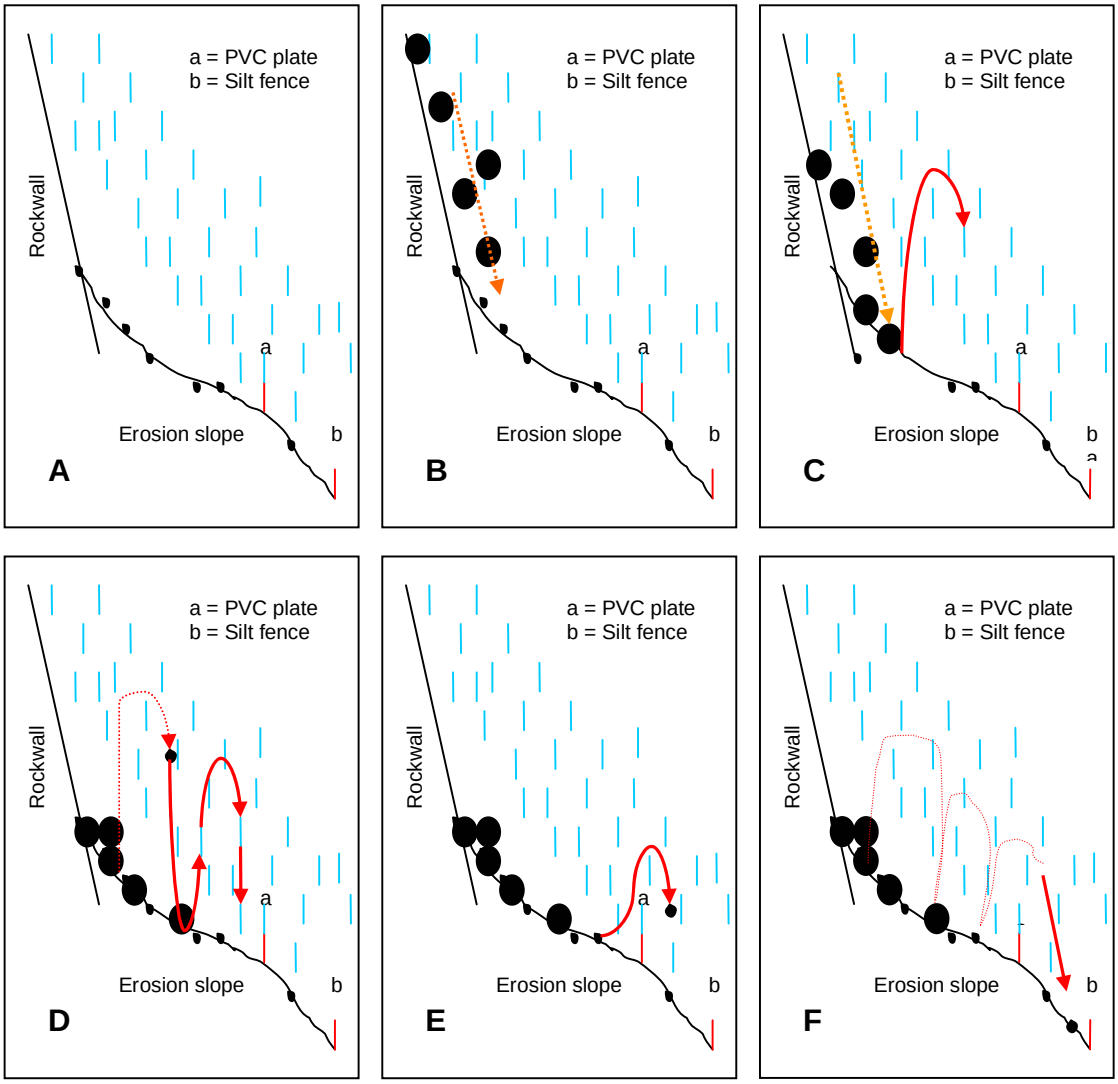

Figure 5-13 Assumption 3: Rockfall triggered by rainfall and dry ravel. Intense precipitation (A) initiates rockfall in a steep wall (B). The disturbed stones fall down to the upper end of the erosion slope, where they decelerate. During the deceleration process the stones pass on their energy (due to the fall) to neighboring stones on the slope. Through this input energy a stone is dislodged and moves downwards (C). With every landing it will decelerate and pass the energy to another stone (D). Through the received energy it is possible that the stones jump higher than the upper plot site border (E) and arrive therefore in the plot site and get caught in the silt fence.

Behavior between subsystems and plots
All plots and therefore all subsystems showed a correlation to the variable “measurement interval”. The longer a measurement interval the higher the sediment amount in the silt fence. That pointed to processes such as: gravity, animals, natural sedimentation and decomposition etc. The influence of precipitation on the upper plots (A1, A2, B1, B2, C1, C2, D1 and D2) was small to negligible compared to the lower ones (E1, F1 and G1). Reasons for this disagreement could have been because of different soil water conditions and “erosion slope length” because the lower plots were located on much longer slopes that passed into steeper rock walls than the upper slopes. The assumptions made further for E1, F1 and G1 didn’t hold for the upper plots, because of missing upper rockwalls (assumption 3) and except for D2 the impossibility of stones that have jumped over the PVC plate (slope too short; assumption 2). On the upper plot sites D2 had a long erosion slope above the PVC plate and could have acted as described in assumption 2. Due to the assumed animal crossing, the possible influences from processes such as assumption 2 could have been muted. On all accounts there was no correlation visible out of the values for that assumption. The gravel cover on the plot sites will have also played an important role for the individual behaviors. Only certain plot sites, with particular soil types, can be saturated by specific rainfall events because of their physical properties (Crosta, 1998). Those physical properties also control runoff and erosion processes for the individual sites, where under low-intensity conditions, infiltration is increased, but with high-intensity rainfall, the runoff is increased (Mathys, 2005). The resulting soil water retention characteristics influence besides the rainfall patterns the soil water regime that could have had in addition influence on the groundwater condition. Variations in soil water strongly affected further soil conditions, and contributed to temporal changes in erodibility (Bryan, 2000). Due to the fact that physical properties for the individual plot site weren’t measured, there was no knowledge about soil water content, saturation conditions, infiltration, or runoff, which made explanations for the different reactions impossible. During the measurement period in 2006 surface runoff was never observed in the decoupled system. This could have been due to a lack of intense rainfall events, to small precipitation amounts, or soil conditions. For example, Plot G1 was located in an erosion slope that consisted of a large amount of gravel. Due to absent humus layer, the holes between the gravel stones were not filled and offered room and discharge flow-through for water. With no high-intensity rainfalls, runoff could not have occurred due the high infiltration capacity. If there really was no rainfall, assumption 2 would be false, which would have made the different soil water conditions more relevant.

5.2.4 Behavior on individual plots

For an analysis on individual behavior on the plot sites, plots E1, F1 and G1 were chosen (Figure 5-14 to 5-19). This choice was due to the better correlation with precipitation on the lower than the upper plots. Because the sediment wasn’t collected after each rainfall event, it was not possible to make statements about the behaviors on individual events (A.5). However, the correlation between the sediment rate [mm/ (d*m^2)] and precipitation was much better for all three plots (R^2 between 0.51 and 0.67) than the correlation between the sediment rate [mm/ (d*m^2)] and the maximum measured value at P3 during one hour [mm/h] (R^2 between 0.09 and 0.20). Plot E1 with the lowest correlation with precipitation amount showed the best correlation with the intensity between those three plots. In general the sediment rate was better correlated with precipitation amount than intensity. This could be due to unrepresentative values from pluviometer 3 for the three plot sites (even if this rainfall measurement station was very close to the plot sites), missing heavy rainfall events during the measurement times (from the precipitation history in the appendix we can see that the measurement time was more characterized through long and low-intensity rainfall events) or a physical soil process, that was more active during long, low-intensity rainfall than during short, intensive rainfall events.

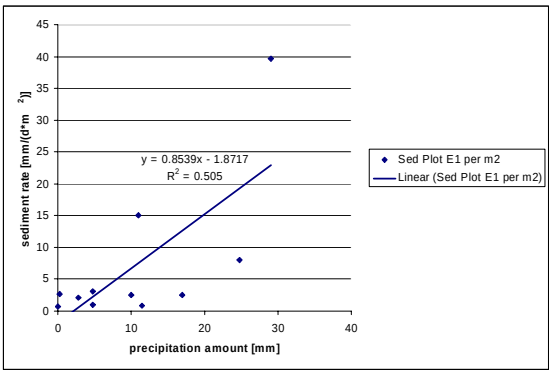

Figure 5-14 Sediment rate versus precipitation intensity F1

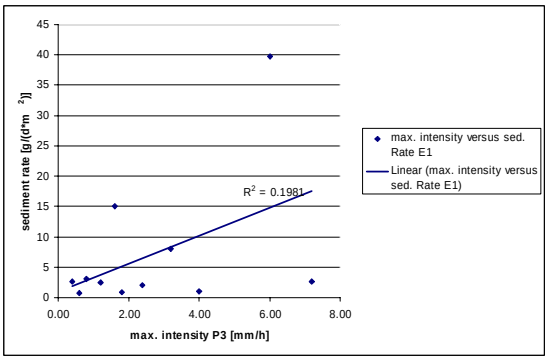

Figure 5-15 Sediment rate versus precipitation intensity on E1

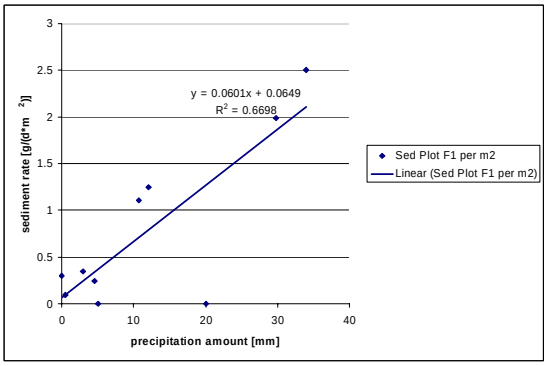

Figure 5-16 Sediment rate versus precipitation F1

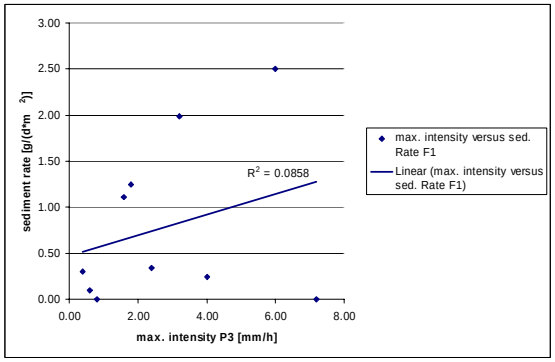

Figure 5-17 Sediment rate versus precipitation intensity on F1

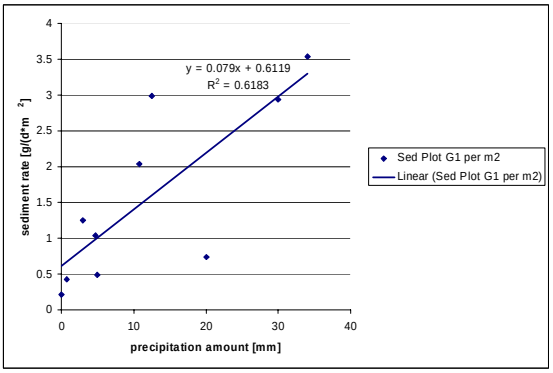

Figure 5-18 Sediment rate versus precipitation G1

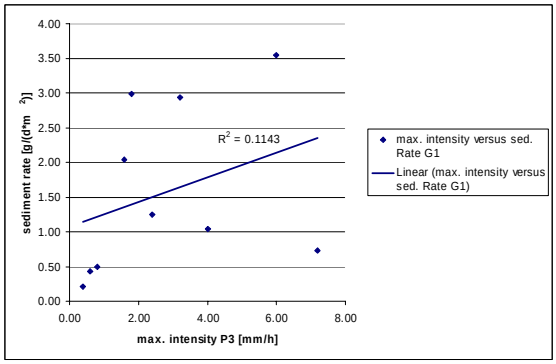

Figure 5-19 Sediment rate versus precipitation intensity on G1

5.2.5 Grain size distribution silt fences sediment and plots

The grain size analyses provided the distribution of soil types according to the different systems and subsystems in the Illgraben catchment. The grain size distribution (Figure 5-20 and Figure 5-21 as well Table 23 and Table 24) for the transported sediment caught in the silt fences varied for the different subsystems: grassland (B1, B2), forest (C1, C2) and erosion slopes (A1, A2, D1, D2, E1, F1 and G1). On decoupled areas a much larger average was measured on the erosion slopes (23.7 mm) than on the forest (9.65 mm) or grassland (1 mm). In contrast, the mean values of the grain size distribution for the silt fence plot substrates were much more similar to each other: erosion slopes 4.2 mm, forest 4.3 mm and grassland 1.2 mm. The grain size distribution varied, except for B1 and B2 (grassland), strongly between the silt fence transport samples and the plot substrates. How transport and substrate were linked with the different erosion rates will be further analyzed in section 5.2.1.

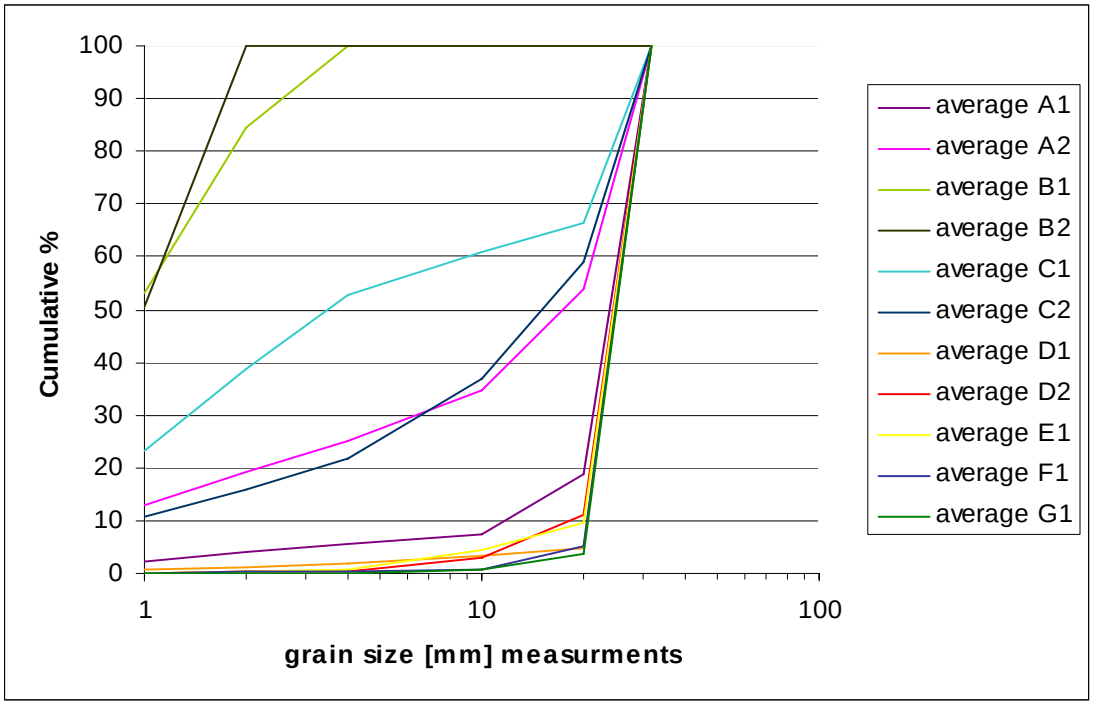

Figure 5-20 Grain size distribution of silt fences contents

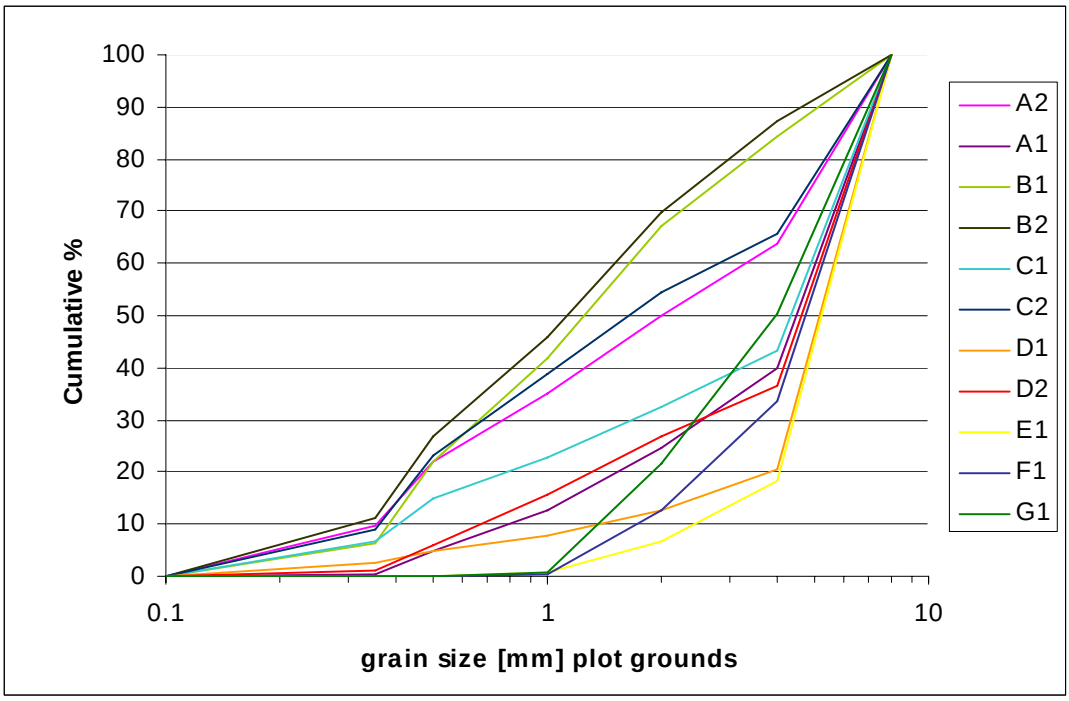

Figure 5-21 Grain size distribution of the substrate in the silt fence plots

Table 23 Grain size distribution of sediment trapped in the silt fences

	D50 amount	D50 interval	D90 amount	D90 interval
A1	24	22-32	30	22-32
A2	17	10-20	28	22-32
B1	1	1-2	2.7	2-4
B2	1	1-2	1.8	1-2
C1	3.3	2-4	28	22-32
C2	16	10-20	28	22-32
D1	25	22-32	30	22-32
D2	25	22-32	30	22-32
E1	25	22-32	30	22-32
F1	25	22-32	30	22-32
G1	25	22-32	30	22-32

Table 24 Grain size distribution of substrate sediment in the plot area.

	D50 amount	D50 interval	D90 amount	D90 interval
A1	4.5	4-10	7.5	4-10
A2	1.9	1-2	6.5	4-10
B1	1.3	1-2	4.6	4-10
B2	1.1	1-2	4.7	4-10
C1	4.1	4-10	7.5	4-10
C2	4.5	4-10	7.5	4-10
D1	5	4-10	7	4-10
D2	4.7	4-10	7	4-10
E1	5	4-10	7	4-10
F1	4.5	4-10	7	4-10
G1	4	4-10	7	4-10

5.2.6 Description of silt fence plot content

The silt fence transported sediments consisted mostly of pebbles, debris and a small fraction of sand. The material dried very quickly and was always processed on-site. This was due to the absence of clay- and silt-sized particles. The organic content varied from plot to plot and by season and was often the only silt fence content. For the measurements all the organic contents have been separated and were not used. For a reasonable explanation of the difference between the plot substrate samples and silt fence content samples, grain size and other factors (like slope angle, rainfall intensity, possible erosion mechanisms etc.) had to be considered, which was discussed in section 5.2.4.

5.3 Aerial photography

5.3.1 Catchment area distribution in 2004, 1999 and 1959

The catchment area was divided in different systems and subsystems: forest, grassland, entire erosion, decoupled erosion, coupled erosion and the entire catchment (Figure 5-22, as well as A.1). The coupled system together with the decoupled erosion comprises the entire erosion (Table 25, Table 26, Table 27 and A.1).

Table 25 Catchment area distribution in 2004, 1999 and 1959

	2004 [km^2]	**1999 [km^2]**	**1959 [km^2]**
Entire catchment	9.5	9.5	9.5
Decoupled erosion	1.4	1.1	0.7
Coupled erosion	2.8	2.8	3.1
Forest	4.0	4.3	3.3
Grassland	1.3	1.4	2.5
Entire erosion	4.2	3.9	3.7

Table 26 Catchment area distribution in 2004, 1999 and 1959

	2004 [%]	**1999 [%]**	**1959 [%]**
Entire catchment	100	100	100
Decoupled erosion	15	12	7
Coupled erosion	29	29	32
Forest	42	45	35
Grassland	14	14	26
Entire erosion	44	41	39

Table 27 Catchments areas changes between 1959-2004, 1999-2004 and 1959-2004

	1959-2004[%]	**1999-2004 [%]**	**1959-1999 [%]**	**1959 [%]**
Entire catchment	0	0	0	100
Decoupled erosion	7.7	2.9	4.8	7
Coupled erosion	-2.9	0.1	-3.0	32
Forest	7.4	-2.6	10	35
Grassland	-12.3	-0.4	-11.9	26
Entire erosion	7.7	3	1.8	39

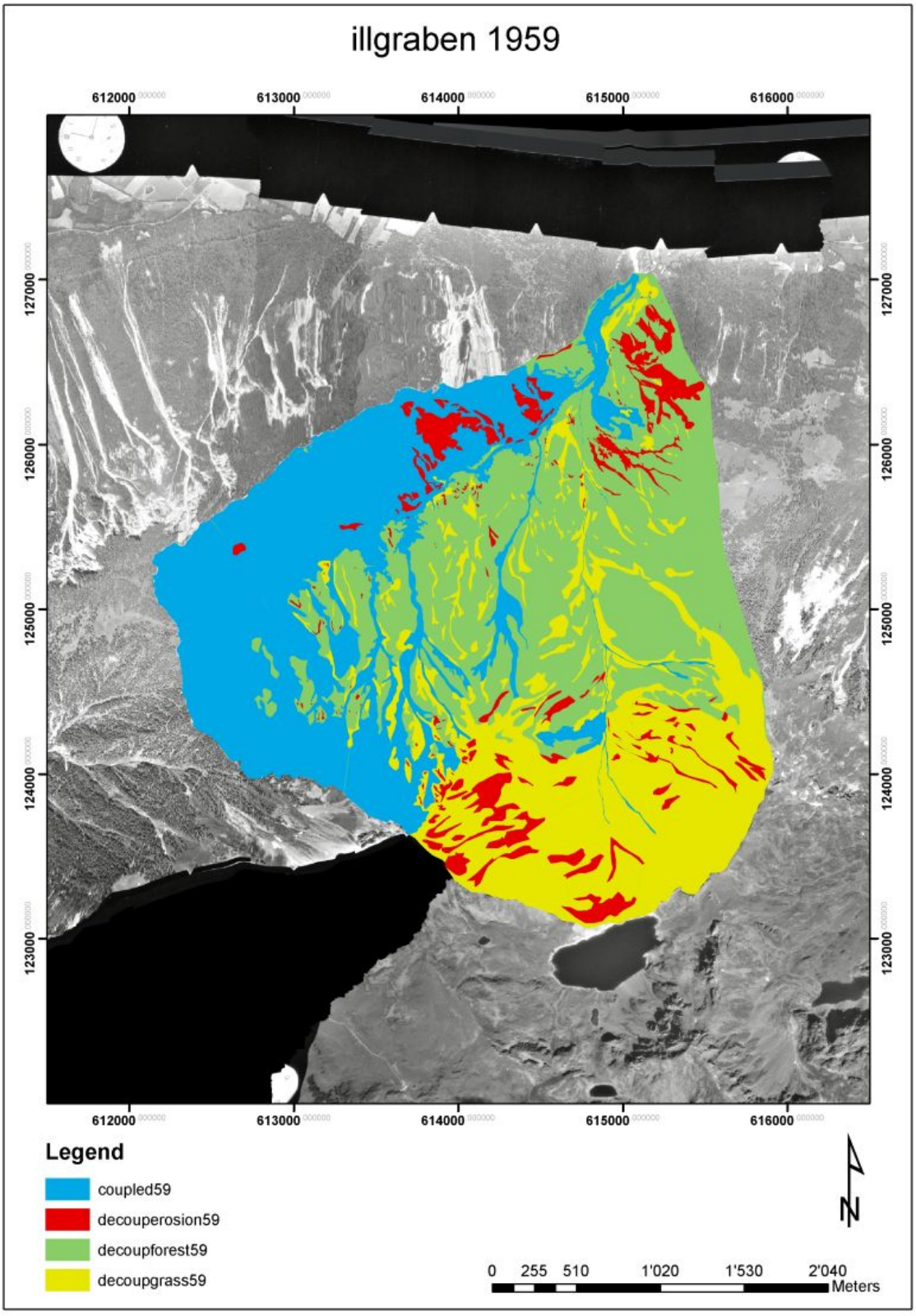

Figure 5-22 Illgraben catchment 1959

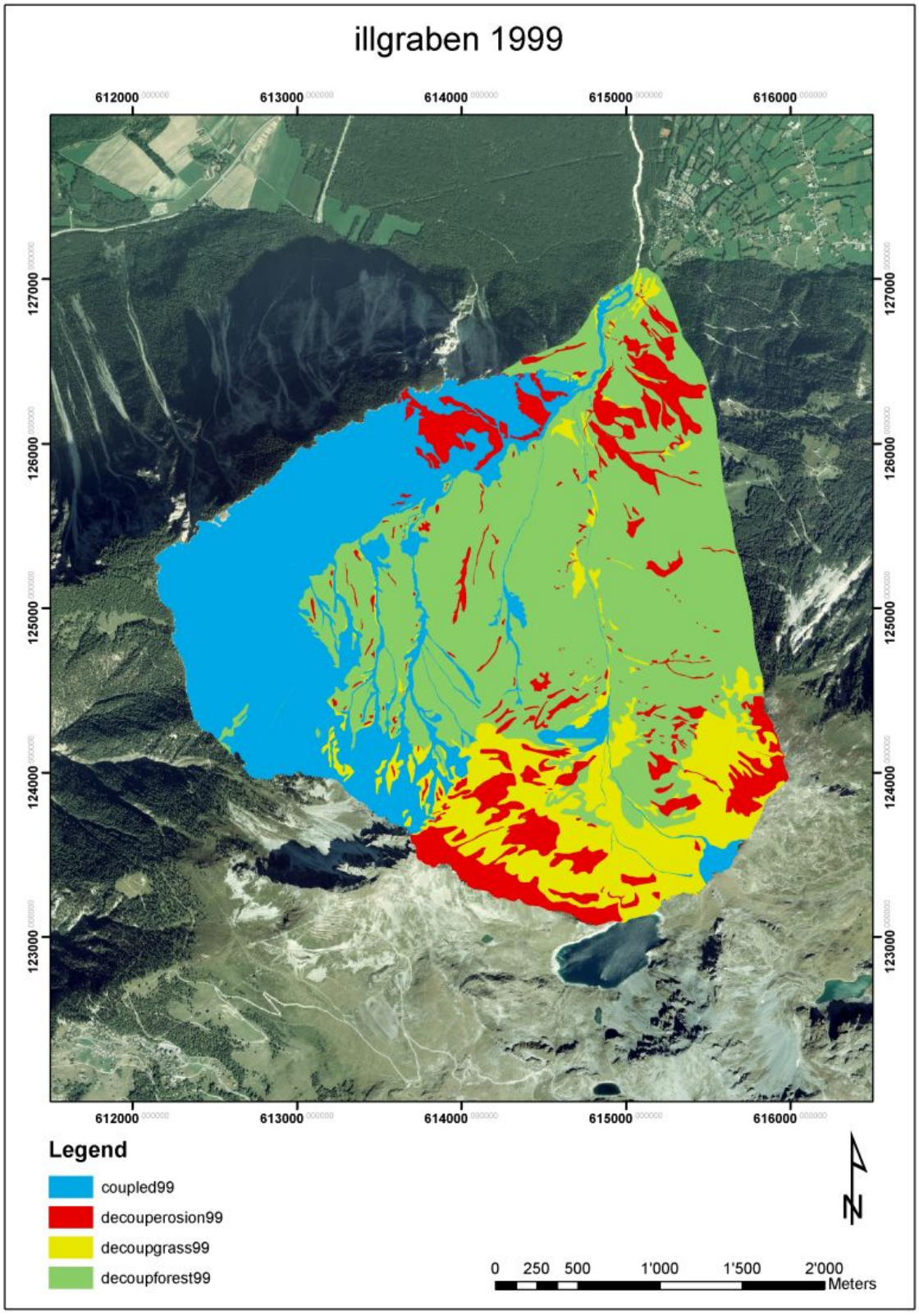

Figure 5-23 Illgraben catchment 1999

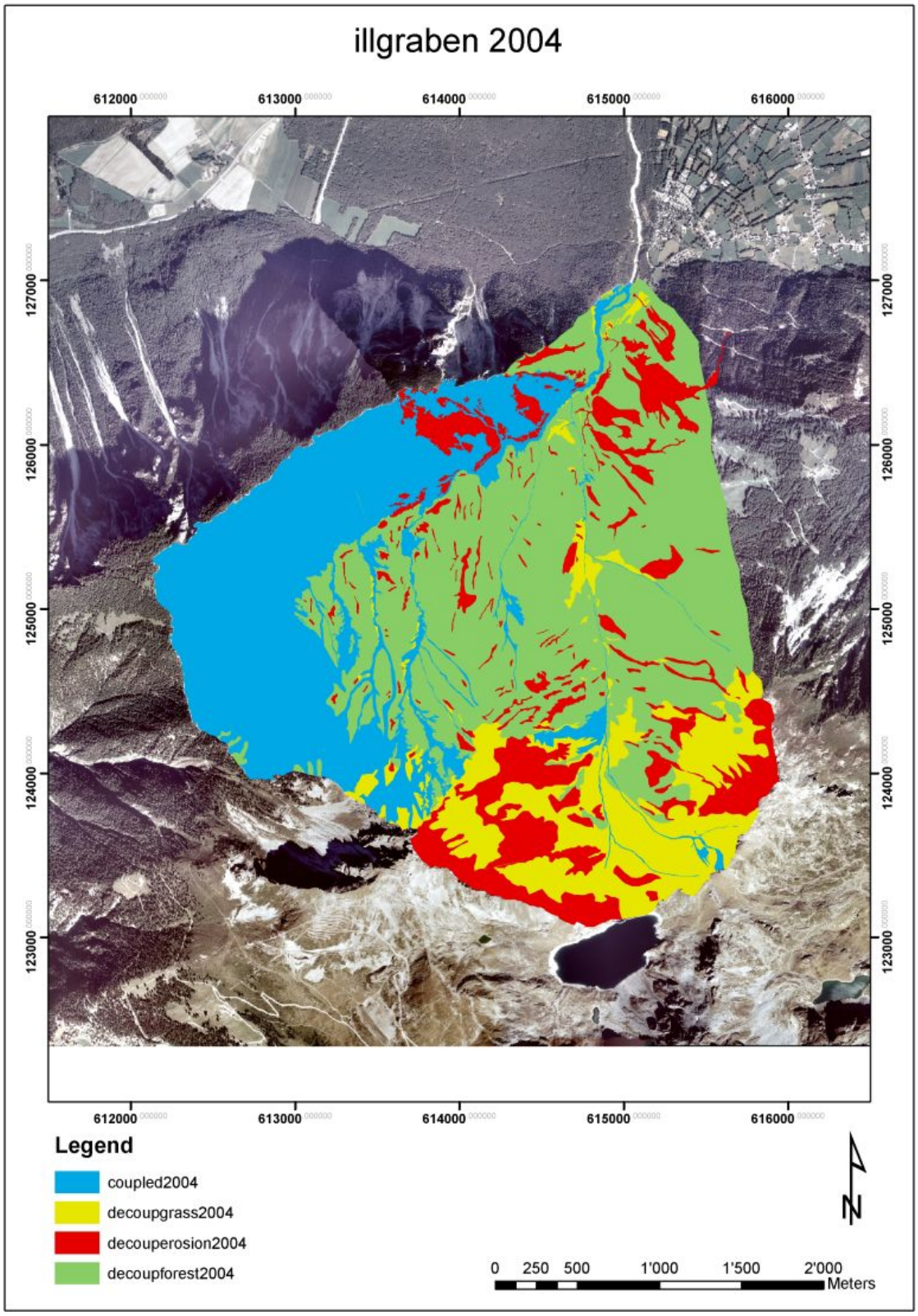

Figure 5-24 Illgraben catchment 2004

The largest change between the different subsystems between 1959 (Figure 5-22) and 2004 (Figure 5-24) was the reduction of grassland and the increase of forest and decoupled erosion. The grassland area changed from 26% in 1959 to 14% in 2004, which means a reduction of over 46% of the area covered by grassland. In contrast, the forest area had grown over 17% during the last 45 years and in 2004 covered 42% of the entire catchment area; whereas the decoupled erosion subsystem doubled in area during the last 45 years. Between 1959 and 1999 (Figure 5-23), the increase in the decoupled erosion was 0.12% per year of the entire catchment area (which corresponded with a gain of 0.01 km2 decoupled erosion per year) and between 1999 and 2004 was 0.58% per year of the entire catchment area (which corresponded with a gain of 0.06 km^2 decoupled erosion per year). Those two annual increments have a high error probability due to long periods without information during the intervals 1959-1999 and 1999-2004. Particularly during the observation interval 1959 to 1999, the formation of decoupled erosion areas and subsequent vegetation regrowth was not investigated.

The increase of forest and decrease of grassland corresponds with results of other studies conducted in the Swiss Alps (Kaufmann-Havoy, 2005). A statistically significant relationship between the increase in forest areas and variables of structural change in agriculture and a north-south distribution was found, where the southern part of Switzerland showed a higher natural regrowth rate. The natural regrowth of forest tended to occur more frequently where the costs of cultivation exceed yields (high, steep, poor accessibility etc). This is consistent with the observation that about two thirds of the abandoned areas were alpine pastures. Other influences for a natural regrowth of forest were the distance to forest edges, the rate of change of population, the soil stoniness and the slope, the proportion of employed persons in the primary sector, the distance to road and the proportions of full-time farms. In 1959 farmers used parts of the Illgraben catchment for agricultural purposes; this area is much smaller today. This decrease is also almost certainly related also to the high degree of exposure to natural hazards (avalanches, debris flow, rock fall and storms) in the Illgraben catchment. For example, in 1959 the Steinschlag hut was used as an alp for cows and goats, whereas in 2006 the access to the Steinschlag hut (where 6 silt fences plots were located) posed a challenge which could only be overcome with mountaineering equipment.

Whether or not the decrease of grassland is related to the increase of decoupled erosion areas is disputed, and topic of current research programs. In European mountain regions during recent decades, grassland changes in agriculture led to reduced management or abandonment of subalpine and alpine grasslands (Bätzing, 1996), which could affect the vegetation composition, soil structure, water balance, productivity, microclimate and therefore potential erosion level. To determine the decisive factors for a change in erosion potential, researchers at the European Academy Bozen and the University of Innsbruck investigated 42 factors, where out of this three factors (exposition, slope inclination and soil depth) did not depend on land use and another nine (vegetation and snow gliding, vegetation and rooting and pasturing) influenced by land use were found to be decisive (Tasser, 2003). The type and intensity of land use also had a decisive influence on the occurrence of erosion: mowing and grazing caused a decreased erosion potential, while abandoned grasslands carried a higher erosion risk. Explanations include:

- Land use affected the vegetation in the study areas (different types of land use and intensity could be assigned to specific plant communities and vegetation structures). They, in turn, caused a change in soil roughness, which had again an effect on snow gliding. Snow gliding itself doesn't cause surface erosion, rather is indirect through abrasion due to the transport of stones and drag force on plant parts (Tasser, 2003).
- In terms of total root length and of root density the erodible areas showed lower values than non-erodible ones. The reduction of root density was thus related to a decrease in soil stability (Nilaweera, 1999). Tasser et al. (2001) found that root density decreased in his study sites with time of abandonment (root density is mainly controlled by vegetation and therefore by land use).
- Grazing and trampling by animals had both positive and negative effects on slope stability. In managed grasslands with a large number of animal trails, the trails reduced snow gliding and snow abrasion, because the small terraces increased surface roughness. However, irregular grazing on large, lightly stocked grasslands and increasing weight of the pasturing animals could have had negative effect on slope stability (Tasser, 2003).

How the increase in decoupled erosion in the Illgraben is related to the reasons above, and how intense abiotic- and climate factors contributed, was not obvious in the results. A change in the vegetation could be expected due to changes in land use. From the aerial photography I assume that abandoned grazing had a strong but not a sole influence on the increase of decoupled erosion areas (many new decoupled erosion areas were found on old grassland in the aerial photographs). A more exact correlation between grassland and decoupled erosion area distribution could be the goal of further research, where a GIS database could be considered.

5.3.2 Coupling relationship distribution in 2004, 1999 and 1959

In contrast to the changes within the decoupled subsystem, the percentage of area occupied by the coupled and decoupled system remained almost constant during the last 45 years. A 4.4% increase in the decoupled system (an increase of decoupled system for the entire catchment with 2.9%) was recognized during the last 45 years (Figure 5-27, Table 28, Table 29 and Table 30).

Table 28 Coupling relationship area distribution in 2004, 1999 and 1959

System	2004 [km^2]	1999 [km^2]	1959 [km^2]
Coupled	2.8	2.8	3.1
Decoupled	6.7	6.7	6.4

Table 29 Coupling relationship distribution (percentage) in 2004, 1999 and1959

System	2004 [%]	1999 [%]	1959 [%]
Coupled	29	29	32
Decoupled	71	71	68

Table 30 Coupling area distribution change

System	1959-2004[%]	1999-2004 [%]	1959-1999 [%]	1959 [%]
Coupled	-2.9	0.1	-3	32
Decoupled	2.9	-0.1	3	68

Reasons for only a small change in the areas distribution of the coupled- and decoupled system may be necessary for the change from one system to the other could have been found in the rate of catchment adjustment concerning coupled- and decoupled systems. In the Weraamaia catchment in New Zealand, developments of gully complexes maintained coupling processes with channels for periods up to 100 years. In contrast, slopes subjected to shallow landslides became decoupled from channels within 10 years (Kasai, 2005). This means coupled systems have been changed to decoupled systems within 10 years, where decoupled systems needed 100 years to change to a coupled system. If the rates of geomorphic change are comparable between the Illgraben and Weraamaia catchment, 45 years of aerial photography observations may be too short to see a clear trend concerning the coupling relationship. The Illgraben catchment differs from the Weraamaia catchment because of steeper slopes, its alpine setting and its high debris flow occurrence. The rates of change in the Weraamaia catchment were due mostly to fluvial processes, whereas in the Illgraben, mass movement processes occurred in addition to and may be generally more important than fluvial processes. The interactions between mass movement processes and fluvial processes in the Illgraben catchment are not well known. Therefore the influence of mass movement processes concerning the change rates for the Illgraben catchment are not yet recognized, but fast landscape changes due to debris flows were known from storm events observations, where debris flows formed new gullies during one intense rainfall event. In Trun (canton GR) a debris flow produced, a new gully across forest, grassland and the village during an intense rainfall event in November 2002 (Figure 5-25 and Figure 5-26). Consequently, a catchment with mass movement processes should have faster rates of change than a catchment where only fluvial processes occur. One could assume a shorter change rate from a decoupled- to a coupled system due to the high force of debris flows and a longer change rate from a coupled- to a decoupled system, because debris flows may flush away barriers (as rocks, new vegetation, etc.).

This would mean that catchments with regular debris flow activity may be distinguishable from catchments without debris flows through a higher change rate from coupled- to decoupled systems and a shorter change rate from decoupled- to coupled systems. This hypothesis could not be investigated herein, but it is not apparent in our 45 year observation interval.

Figure 5-25 Trun, November 2002 (WSL)

Figure 5-26 Trun, November 2002 (WSL)

A different hypothesis is that of a dynamic steady state between the coupled- and decoupled systems. Where the proportion of decoupled- to coupled systems remained constant, and changes that occurred in one system are balanced by the other system. A constant distribution between those two systems implies an unchanging total debris fan area and -channel volume, which leads to a steady state for the entire catchment. Due to the short observation interval (45 years) for the Illgraben catchment, this hypothesis could not be tested, but it perhaps could be it the intervening aerial photographs are processed and could be therefore an interesting topic for a further research.

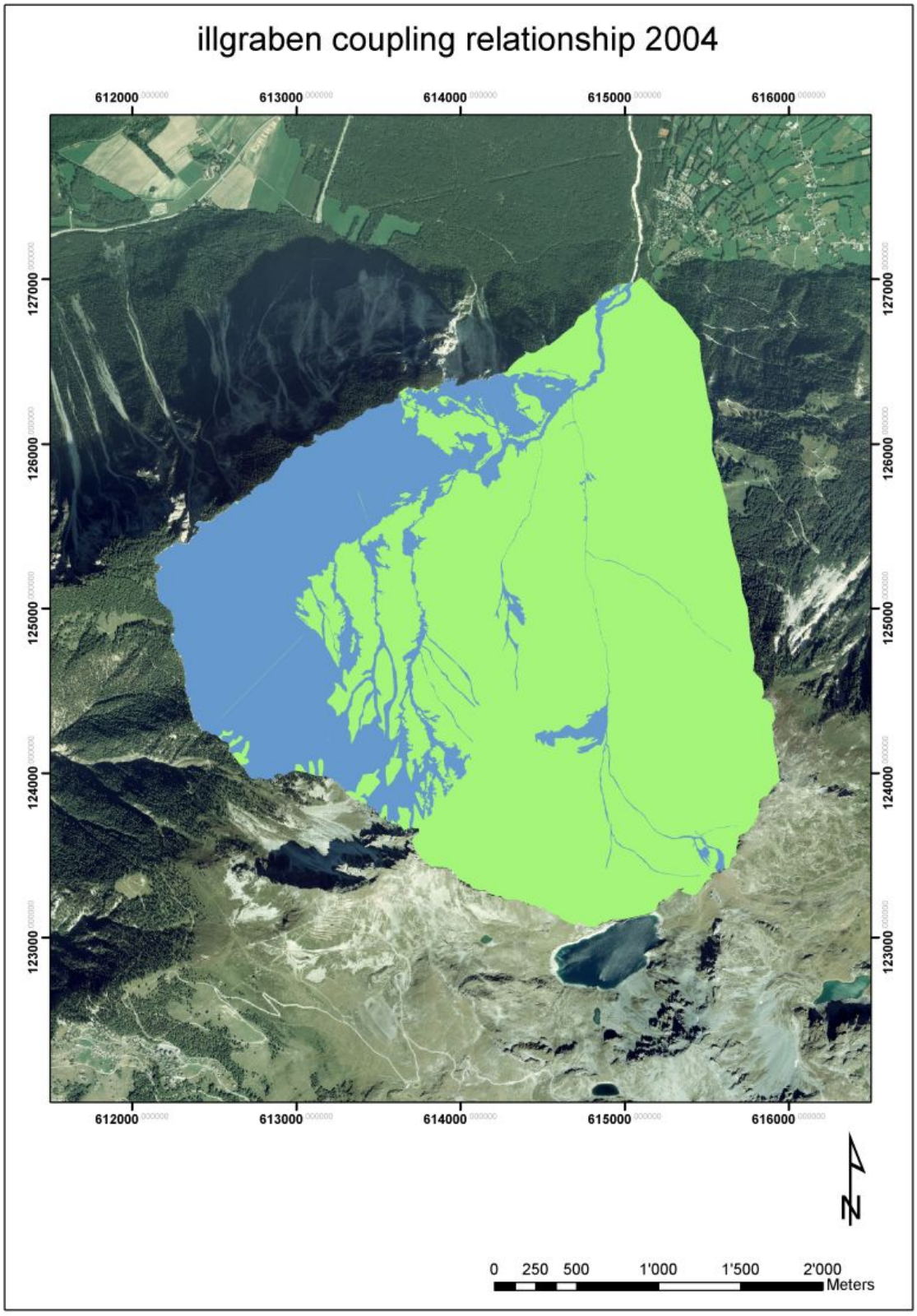

Figure 5-27 Coupling relations in the Illgraben 2004 (green = decoupled, blue = coupled)

5.3.3 Catchment slope angle distribution

The median slope angle distribution for the Illgraben catchment was determined to be 40°, additionally, 90% was less than 75° and 10% less than 26°. The coupled system has the steepest slope angle average (45°), followed by the grassland with 30° and decoupled erosion with 29° (Table 31 and Figure 5-28).

Table 31 Catchments slope angle distribution in 2004 out of the GIS Database and the DEM 25 (copyright by Swisstopo 2007)

	D 50	D 10	D 90
Coupled [°]	45	81	22
Catchment [°]	40	75	26
Decoupled erosion [°]	29	46	12
Grassland [°]	30	44	16

Where D 50 = median slope angle and D 10 and D 90 refer to the 10Th and 90th cumulative percentiles (Figure 5-28).

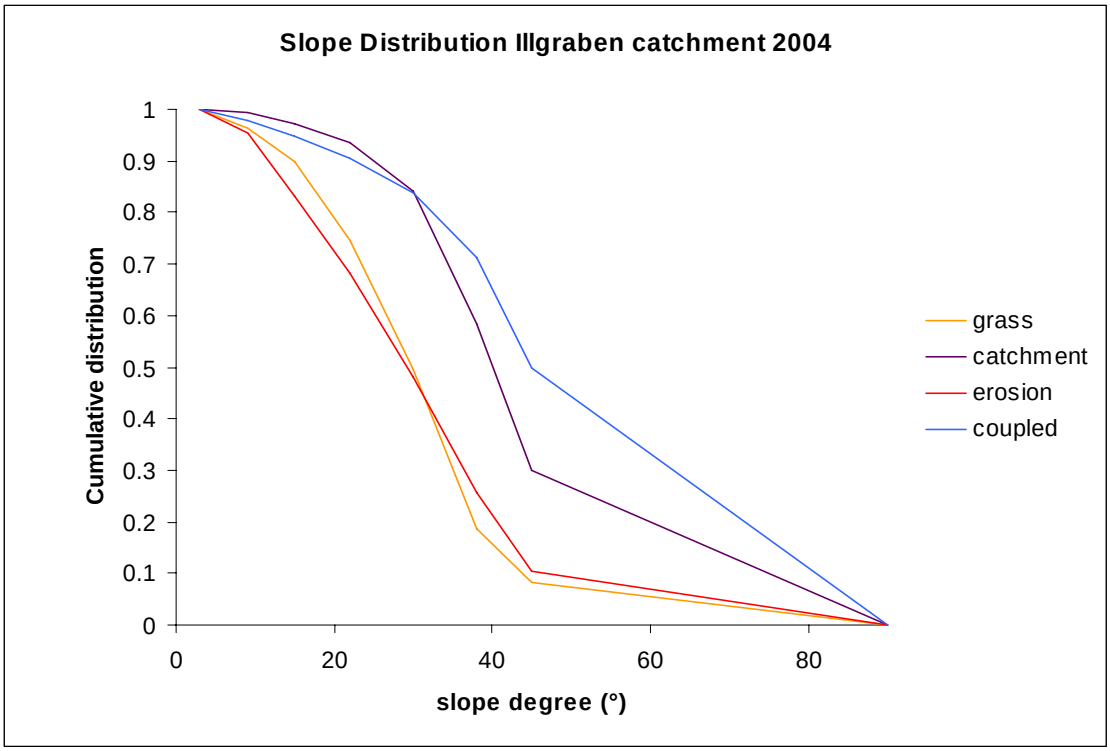

Figure 5-28 Mean slope angle distribution in the Illgraben catchment 2004

The results show steep hillslopes for the Illgraben catchment. Only 10% of the entire catchment areas has a slope angle smaller than 26°, while the coupled system has the steeper slopes than the decoupled subsystems. This distribution corresponds to the erosion rates out of those systems and subsystems, as well with correlation with slope angle and erosion rate from related studies. This relationship will be discussed further in the section 5.2.1.

5.4 Process rates and sediment budget

5.4.1 Process rates

The mean process rates (Table 32 and Table 33) varied intensely between the different subsystems of the decoupled system, the decoupled system itself, and the coupled system. Grassland had a process rate of 0.01 g/ (m^2*d), which was not measurable with the silt fence technique and was therefore almost negligible. Forest had a process rate one order of magnitude higher than grassland (0.51 g/ (m^2*d)). The process rate for the decoupled erosion (4 g/ (m^2*d)) was again one order of magnitude higher than the process rate of the forest and two orders higher than the process rate of grassland. The average of the entire decoupled process rate was 1.20 g/ (m^2*d).

Table 32 Process rates and related data for the individual silt fence plots and the coupled system

	A1	A2	B1	B2	C1	C2	D1	D2	E1	F1	G1	coupled system
sum [kg]	4	2	0	0	0	2	30	140	88	11	25	392000000
m period [d]	107	107	107	107	107	107	107	107	75	69	69	138
max sediment amount [kg]	1	1	0	0	0	1	5	27	40	4	6	-
m. period max amount [d]	6	16	6	6	6	6	6	5	7	7	7	-
m. period max amount [h]	144	384	144	144	144	144	144	120	168	168	168	-
area [m^2]	57	44	30	32	25	16	43	51	144	208	234	2800000
process rate [kg/(m^2*h)]	0.00	0.00	0.00	0.00	0.00	0.00	0.00	0.00	0.00	0.00	0.00	0.04
process rate [g/(m^2*h)]	0.03	0.02	0.00	0.00	0.00	0.05	0.27	1.07	0.34	0.03	0.06	42.27
process rate [g/(m^2*d)]	0.69	0.51	0.00	0.01	0.03	1.27	6.40	25.66	8.11	0.77	1.54	1014.49
area [m^2]	57	44	30	32	25	16	43	51	144	208	234	2800000
max process rate [kg/(m^2*h)]	0.00	0.00	0.00	0.00	0.00	0.00	0.00	0.00	0.00	0.00	0.00	-
max process rate [kg/(m^2*h)]	0.13	0.04	0.00	0.01	0.02	0.21	0.79	4.44	1.66	0.10	0.16	-
max process rate [kg/(m^2*h)]	3.21	0.99	0.02	0.13	0.43	5.11	18.87	106.46	39.68	2.51	3.79	-

Table 33 Process rates for subsystems (forest, grassland, decoupled erosion areas) and systems (decoupled and coupled)

	forest (deco)	grassland (deco)	erosion (deco)	entire decoupled	coupled
area [m^2]	4002000	1330000	1403000	6740000	2800000
# plots	2	2	7	11	1
sum plot area [m^2]	41	62	781	6740000	2800000
mean process rate [kg/(m^2*h)]	0.00	0.00	0.00	0.00	0.04
mean process rate [g/(m^2*h)]	0.02	0.00	0.18	0.05	42.27
mean process rate [g/(m^2*d)]	0.51	0.01	4.27	1.20	1014.49
max process rate [kg/(m^2*h)]	0.00	0.00	0.00	0.00	
max process rate [g/(m^2*h)]	0.09	0.00	0.73	0.21	
max process rate [g/(m^2*d)]	2.27	0.08	17.41	4.98	

Comparisons of the different process rates on the silt fence plot sites and possible explanations them will be discussed afterwards. First, the attention is directed towards the difference in process rates between the coupled- and decoupled systems. As mentioned above, the coupled system had a three order of magnitude higher process rate than the decoupled one, which made the erosion rates from the decoupled system almost negligible in comparison. The much higher rate for the coupled systems resulted from a higher slope angle, less vegetation, and larger grain size distribution than in the decoupled system. Also, influences such as melting permafrost, different temperature and precipitation behavior, etc., could have also contributed to an increase of the process rate. The individual influences will be discussed later. The most important fact related to the process rates is based on the catchment geomorphology, where the decoupled system was characterized by a predominance of slope erosion and the coupled system of gully erosion. Gully erosion was important because gully complexes produce a wide range of sediment particles in response to even moderate magnitude rainfall events (Betts, 2003) and a subsequent increase in forest and scrub cover as gully complexes areas stabilized (Kasai, 2005) the main source of sediment at the catchment scale (Valentin, 2005).

5.4.2 Process rates correlations

process rates ranking:
- Highest process rate = 1.
- Lowest process rate = 12.

slopes angles (s) measured on plot:
- s < 30° = +
- 30<= s < 40 = ++
- s =>40 = +++

plot grain size D 50 (pg):
- 4< pg = +
- 2.5 < pg <=4 = ++
- pg <=2.5 = +++

silt fence transport sample grain size D 50 (sg):
- sg >20 = +++
- 10 <= sg <20 = ++
- sg <10 = +

ground vegetation covers (V):
- completely V = +
- partially V = ++
- no to little V = +++

coupling relation (C):
- decoupled system = +
- coupled system = 0

Table 34 Correlation coefficient (least-squares) R^2 for the process rate compared with assumptions from the different absolute terms (slope angle, plot grain size, silt fence grain size, vegetation and coupling relation) for the respective plots, where the absolute terms were assessed on the basis of the weights listed above (not statistically tested). The assessment for the plot grain size and the silt fence grain size for the coupled system is derived from field monitoring (plot substrate) by eye and debris flow composition, where the slope angle for the coupled system was taken out of the slope distribution from the orthophoto analysis.

Plots	Slope angle (1)	Plot grain size (2)	Silt fence content grain size (3)	Vege-tation (4)	Coupling relation (5)	Sum (1-5)	Hypothetic process rate ranking	Measured process rate ranking
A1	+++	+	+++	++	+	10	4.-9.	8.
A2	+++	++	++	++	+	10	4.-9.	9.
B1	++	+++	+	+	+	8	11.	12.
B2	+	+++	+	+	+	7	12.	11.
C1	+++	+++	+	+	+	9	10.	10.
C2	+++	++	++	++	+	10	4.-9.	6.
D1	++	+	+++	+++	+	10	4.-9.	4.
D2	++	+	+++	+++	+	10	4.-9.	2.
E1	+++	+	+++	+++	+	11	2.-3.	3.
F1	+++	+	+++	++	+	10	4.-9.	7.
G1	+++	+	+++	+++	+	11	2-3.	5.
Coupled system	+++	+	+++	+++	+++	13	1.	1.

According to the assumptions about the different absolute terms, the plot with the highest process rate should have the highest sum out of the absolute term weightings (Table 34). This would mean that the coupled system had the highest process rate followed by G1+E1, F1+A1+A2+C2+D1+D2, C1, B1, B2. The highest measured process rate agreed with the assumption (coupled system) and also afterwards an agreement could be found almost everywhere (Ranking: coupled system, D2, E1, D1, G1, C2, F1, A1, A2, C1, B2, B1).

Only plots D2 and G1 have unanticipated ranks. This disagreement may be attribute to the weightings of the different absolute terms (different terms may influence the erosion rate with different weights), other attitudes than expected or an oversimplification (missing absolute terms etc.). More specific observation influences between the specific absolute terms and the estimated/measured process rates will be discussed in the following. Not all comparisons are based on statistical tests. Apart from plots D2 and G1 the assumptions correlated surprisingly well with the measured rates, which indicated the importance of slope angle, grain size distribution, vegetation and coupling relationship for the erosion processes in the Illgraben catchment.

Slope angle and erosion process rate
The slope angle did not have the expected influence as in related studies on the measured process rates. Geomorphologists have generally recognized a strong connection between the slope morphology and erosion rates (Montgomery, 2002). Classical conceptual models of landscape evolution incorporated the implicit assumption of a simple linear functional relation between erosion and greater relief or steeper slopes (Montgomery, 2003). Instead, those traditional assumptions were challenged by recent work documenting both strongly coupled feedback between erosional processes and tectonic forcing. Therefore slope angle was used to illustrate that the variability for connectivity, for a given slope angle, the energy for transport is insufficient (Fryirs, 2006). The linear relation between slope angle and erosion rate should have only limited relevance to long-term, landscape-scale erosion rates in the steep-topography of tectonically active mountain ranges (Montgomery, 2002). Even so, slope steepness, together with land use, is often the most important attribute that controls the rate of soil erosion (Verstraeten, 2006). The slope angles in the Illgraben have a high influence on the process rates, but those influences were not visible due to the fact that all plots had more or less the same slope angle or were in any case steep. The proportions of large slope angles (Figure 5-28) for the entire catchment must be a key influence for processes happening there (debris flow initiation, erosion, flow, rock fall, etc.), but it was not obvious how much the weighting for the slope angle was compared to that for the other absolute terms.

Relationship between Silt fence content grain size distribution and erosion process rate
The relationship between the silt fence transported grain size on the erosion process rate is clear. Larger grain sizes are heavier than smaller ones. Due to the fact that the content in the silt fences consisted mostly of sand, stones and small rocks, the relationship between silt fence content grain size and erosion process rate is expected.

Relationship between Plot grain size distribution and erosion process rate
Choppin and Richards (Choppin, 1990) found a relationship between the percent silt fraction and erosivity. The larger the percent of silt amount, the smaller the erosivity. For the sand- and clay fraction the relationship was the other way, a smaller sand- or clay fraction results in a smaller erosivity (Choppin, 1990). Because our silt content was so low we didn’t expected this to have any influence. However the transport rate increased with mean grain size. The reason for this is still unclear.

Vegetation and erosion process rate

From the measured erosion process rates, relations with the vegetation layer could be detected. Plots with a ground vegetation layer had a smaller process rate than plots without ground vegetation. This reflected results of similar studies, where the connection “the more ground vegetation, the less erosion” (Markart, 2004) and “a two or three orders higher magnitude of erosion rates on bare soils than on pastures” (Descroix and Mathys, 2003) was found. Besides the fundamental role of vegetation in reducing runoff and erosion, vegetation protects the ground further from gullying and fast changes in landscape (e.g. Dedkov and Moszherin, 1992).

Coupling relation and process rate

The link between the measured process rate and the coupling relation was out of the question. The coupled system has a much higher process rate than the decoupled one and produced therefore a much larger sediment amount. Due to the huge source of gullies in the coupled system, which are the main source of sediment at the catchment scale (Valentin, 2005); the decoupled system with its surface erosion was almost negligible.

5.4.3 Sediment budget

A simple sediment budget was calculated for the subsystems, the coupled- and decoupled systems from the process rates and the area distributions (Table 35 and Table 36). The decoupled subsystems were extrapolated to one year (365 days), while the coupled system was projected over 138 days corresponding to the duration of the debris flow season (the period between the first and the last debris flow in 2006). The entire catchment had a sediment rate of 394'900 t per year, whereas the coupled system delivered 392'000 t and the decoupled system 2'900 t. That means the coupled system delivered 99.3% of the sediment and the decoupled system the remaining 0.7%. The sediment budget contains an output rate (coupled system) and a storage rate (decoupled system). Therefore 99.3% of the sediment exchange exited the Illgraben catchment (in form of debris flows), where 0.7% formed a sediment storage.

Table 35 Sediment budget for system and subsystems

	forest (deco)	grassland (deco)	erosion (deco)	entire decoupled	coupled
area [m^2]	4'002'000	1'330'000	1'403'000	6'740'000	2'800'000
sediment [kg/h]	86	0	250	330	118'400
sediment [kg/d]	2'060	7	6'000	7'900	2'842'000
sediment [kg/y]	751'700	2'700	2'190'000	2'900'000	392'000'000

Table 36 Sediment budget for the entire catchment [t/y]

	Catchment	coupled	decoupled
Area [m^2]	9'500'000	2'800'000	6'700'000
Sediment [t/y]	394'900	392'000	2'900

Sediment equation: input – output = storage
The output component in the Illgraben catchment formed the coupled systems with its debris flows, where the storage component was determined by the decoupled system. Due to a missing input component and a much higher output- than storage component, the balance is negative, indicating, that the system lost more sediment than it received and stored.

Almost $4*10^5$ t sediment output from the Illgraben catchment per year is difficult to imagine. Easier to visualize is the estimate that 22% of the sediment input to the Rhone River comes from the Illgraben catchment, calculated from the yearly sediment output of the Rhone river ($1.8*10^6$ t/year) and the Illgraben catchment output 2006 (392'000 t) (Fritz Schlunegger, UniBern, personal communication).

5.5 Petrographic composition of coupled sediment output

Due to the sharp geological separation (northern catchment greywacke, dolomite, calcite and southern catchment quartzite, quartzite with rose quartz) a provenance analysis could be made using the debris flow material. The measurements indicated that more than 60% of the debris flow materials came from the southern catchment side, 14% from the channel bed, and the remaining 25% from the northern catchment side. Because the southern catchment side comprises just about 20% of the entire coupled system, which was about 6% of the entire catchment, only a small area produces most of the sediment outputs (in the form of debris flows). That means 60% of the material came from 6% of the entire catchment area (Table 37, Figure 5-29 and Figure 5-30). From the orthophoto and field observations, we determined that this active area is located directly under the Illhorn.

Table 37 Petrographic composition in the Illgraben catchment and amounts of the coupled subsystem in 2006

Coupled sediment output 2006 [t]:			392000
	Petrography	**Amount [%]**	**Coupled sediment output amount 2006 [t]**
Southern catchment:	Quartzite:	43.70	171304
	Quartzite with Rose quartz:	16.67	65346
	Total:	60.37	236651
Northern catchment:	Greywacke:	1.93	7565
	Dolomite:	3.03	11878
	Calcite:	20.47	80242
	Total:	25.43	99686
Channel bed:	Schist and Gneiss:	14.10	55272
	Total:	14.10	55272

The reasons for the high activity in the area located under the Illhorn are not yet known. From photographs and field observations it is clear that the material under the Illhorn is strongly eroded and readily mobilizable through precipitation or snowmelt. This high erodibility could be the result of the petrography (the presence of easily weatherable thin stratagraphic units interbedded with quartzite layers), steepness, exposition etc. Other processes such as melting permafrost, climate changes etc., may involve but were well beyond the scope of this study. An interesting result is the fact that less material comes of the northern catchment side than presumed. Through to the steep walls in the northern catchment, gravity must have played a higher role than precipitation for erosion activity. As long there is not a large rockfall (like in 1961), the continuous rockfall activity dynamic relatively supplies little material to the channel bed (about 25% of the entire coupled sediment output).
For a better understanding of the area under the Illhorn, and therefore for a better understanding of the Illgraben catchment, further research should be conducted. Already in autumn 2006 three temperature loggers were installed for checking a possible permafrost appearance. Due to the difficult accessibility and the high danger potential all further research activities will be challenging.

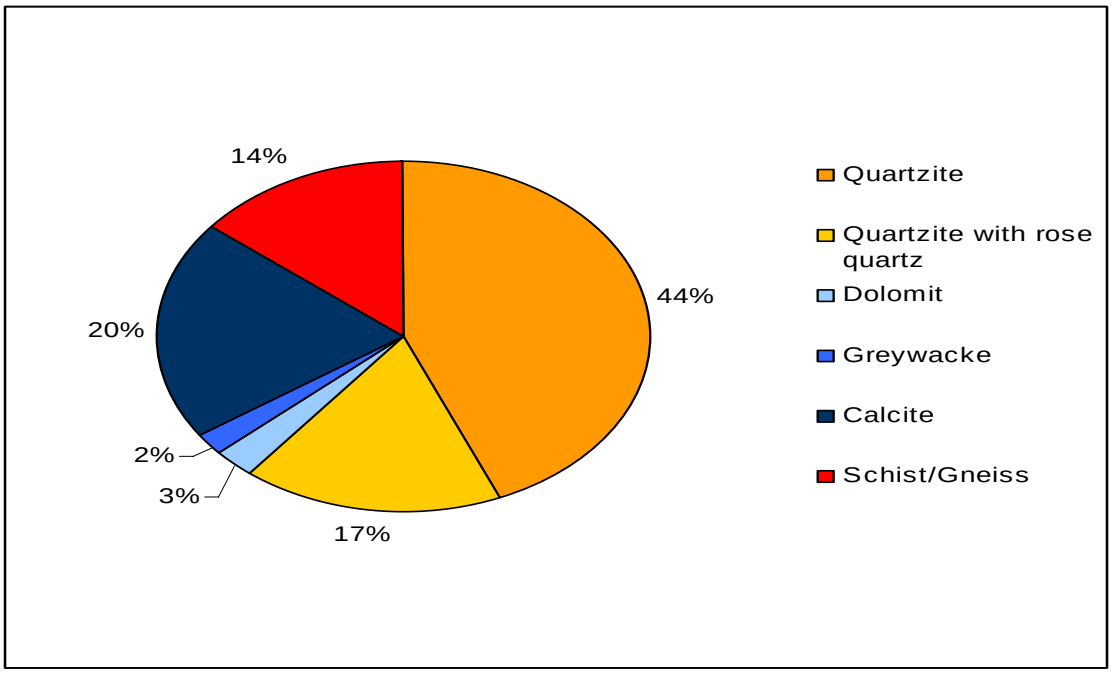

Figure 5-29 %- Petrographic composition of the coupled sediment output (debris flow composition). Red belongs to channelbed, orange and yellow to the southern catchment- and the blue colors to northern catchment side

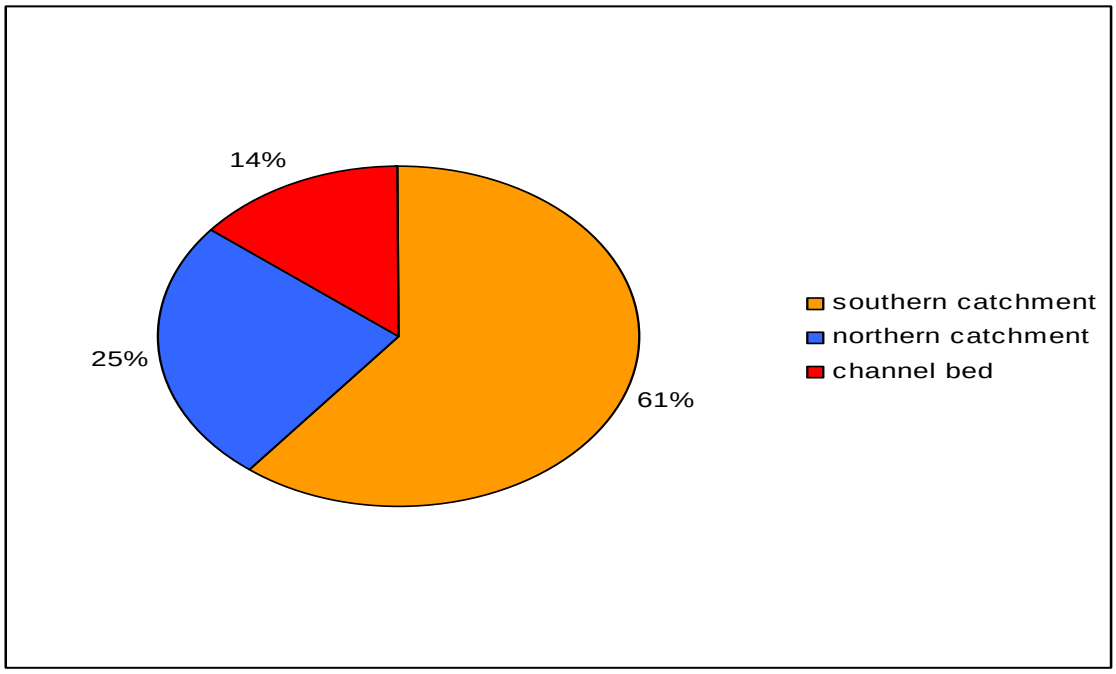

Figure 5-30 Petrographic derivation of coupled sediment output (debris flow materials)

5.6 Summary of results

5.6.1 The core results in few words

In this thesis erosion processes that occur in the Illgraben catchment were investigated. The methods used were primarily field measurements on hillslope erosion, aerial photograph analysis, and of occurred debris flow. As described before, erosion is influenced by different interrelated factors. For the research in the Illgraben catchment, different factors were determined and analyzed, others were assumed and some could not be considered (Figure 5-31).

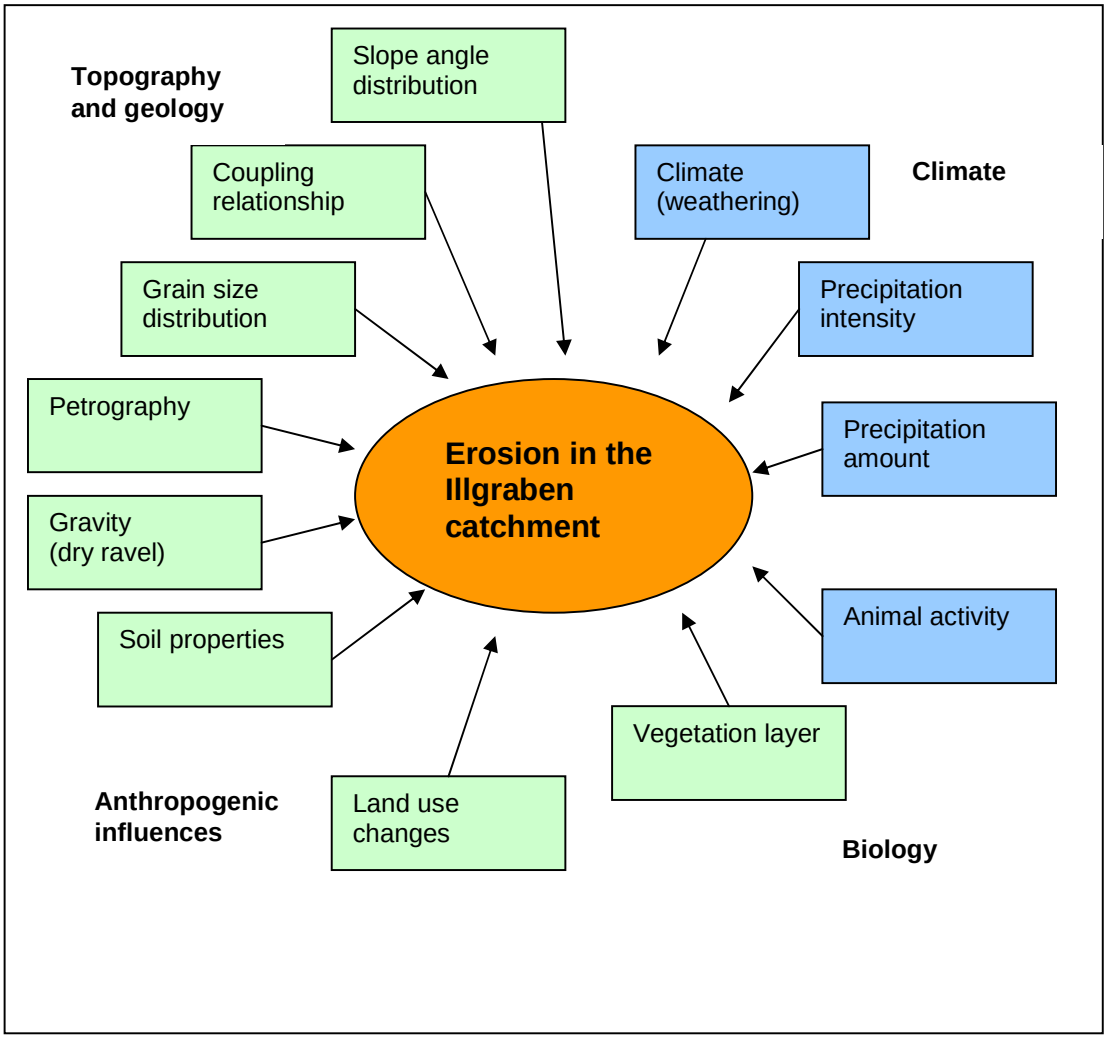

Figure 5-31 Some of the measured (green) and assumed (blue) factors that influence the erosion in the Illgraben catchment

Observations of aerial photography from 1959, 1999 and 2004 showed a trend towards an increase in forested areas and decoupled erosion areas at the expense of grassland areas during the last 45 years. These area changes took place within the decoupled subsystems and had no influence on the entire decoupled system area that stayed constant as the coupled system area.

A dynamic steady state is assumed in the Illgraben catchment between the coupled- and decoupled system and also between the catchment and the fan and between output material and material in the channel. Beside the constant proportion between the coupled- and decoupled system during the last decades since 1959, those two systems showed very interesting differences and behaviors. In the decoupled system every subsystem reacted with a different erosion process rate on precipitation, time and other influences. Grassland showed a rate (0.01 g/ ($d*m^2$)) that was one order of magnitude smaller than forest (0.51 g/ ($d*m^2$)) that was again one order of magnitude smaller than decoupled erosion areas (4.27 g/ ($d*m^2$)). On the average, the erosion process rate of the decoupled system with 1.2 g/ ($d*m^2$) was three units smaller than the one of the coupled system with 1014 g/ ($d*m^2$). This showed clearly that the coupled system represents the active part in the catchment, whereas processes in the decoupled system remained small to negligible. Even if the coupled system represents only approximately 30% of the entire catchment area, it delivers more than 99% of the yearly sediment budget as catchment output. In the remaining 70% (decoupled system) eroded material is stored. The almost 400'000 t of sediment output of the Illgraben catchment in 2006 not only formed impressive debris flows but also represented more than 20% of the yearly Rhone sediment load. Compared to the results of the petrographic debris flow analyses (60% of the debris flow material originates from the southern catchment, 25% from the northern catchment, and the remaining 15% from the channel bed), this large sediment output into the river Rhone is even more interesting. 60% of the debris flow material and therefore of the coupled sediment output were mobilized in around 20% of the southern catchment side or in around 6% of the entire catchment. This means that 60% of the 22% of the Rhone sediment load belongs to 0.6 km^2 (accord with 6%) catchment area, what means 10-13% of the Rhone sediment is derived from an area of 0.6 km^2.

Table 38 Summary of the core results of this thesis

Precipitation	There were only a few intensive rainfall events during the measurement period 2006
	During the measurement period, a precipitation intensivity higher than 2 mm per 10 minutes was only recorded five times (on five different days) at pluviometer 1.
	Those five days with a rainfall intensity higher than 2 mm per 10 minutes correlated exactly with the five occurred debris flows during the measurement period. All five events happened on day where the precipitation intensity reached the above mentioned threshold.
	Based on the daily precipitation distribution at the stations Grimentz, Sierre and Hérémence no increase towards a more intense rainfall pattern was detected. This means the distribution between the periods 1959-1999 is similar to the distribution of the period 1999-2004.
Field measurement on silt fence plots	The variable "precipitation amount" showed a better correlation with the sediment amount and –rate than the variable "precipitation rate".
	The upper plots (A1, A2, B1, B2, C1, C2, D1 and D2) showed no correlation with "precipitation amount" (with R2 between 0 and 0.11)
	The lower plots (E1, F1 and G1) showed a small correlation with the "precipitation amount" (with R2 between 0.51 and 0.67) duration.
	The variable "measurement interval" correlated better than "precipitation amount" for most plots, even if the R2 were low.

	Due to the weak correlation between the sediment variables with "precipitation amount" and "measurement interval", other processes must have occurred during the measurement period. Assumed processes were: gravity, animal activity and crossings over the plot sides as well as natural weathering.
	Plots with a smaller grain size distribution in the plot side had less erosion activity than the ones with a larger grain size distribution in the plot side.
Aerial photography	In 2004 the catchment was composed of 4.0 km^2 (42%) of forest, 1.3 km2 (14%) of grassland and 4.2 km^2 (44%) of erosion areas (coupled and decoupled erosion areas). The entire catchment measured 9.5 km^2.
	The biggest land use changes for the last 45 years happened within the decoupled system where the fraction of grassland, forest and decoupled erosion varied. The grassland decreased and the forest and decoupled erosion area increased.
	The decoupled area (68%) had in 2004 as well in 1999 and 1959 the twice size of the coupled area (32%). There was no change in the proportion of those two systems for the last 45 years.
	In 2004, the decoupled system had in 2004 a mean slope angle of 30°, whereas the coupled system showed a much higher mean with 45°.
Process rates	In the decoupled system, grassland had the smallest process rate with 0.01 g/ (d*m2), followed by forest with 0.51 g/ (d*m2) and decoupled erosion with 4.27 g/ (d*m2).
	The decoupled system had a process rate of ~1 g/ (d*m2), whereas the coupled system had a 1000 times higher process rate of ~1000 g/ (d*m2).
	Slope angle, grain size on plot side, vegetation layer etc. influenced the process rates for the individual subsystems and systems.
Sediment budget	The decoupled system would have moved due to calculation 2'900 t of sediment per year, while the coupled system would have moved 392'000 t per year. Sediment moved by the decoupled system is stored, whereas the sediment moved by the coupled system leaves the catchment in form of debris flows.
	More than 20% of the annual Rhone sediment load was mobilized in the Illgraben catchment
Petrographic composition	The petrographic composition of the debris flows (coupled system) showed that 60% belonged to the southern catchment side, 25% to the northern catchment side and the remaining 15% to the channel bed.
	60% of the debris flow material comes from the southern side (i.e. to the coupled system in the southern side). The coupled system covers about 20% of the southern side, what corresponds to 6% of the entire catchment area. That means that 60% of the coupled sediment output is generated in 6% of the entire catchment area.

Table 39 The most important differences between the coupled- and decoupled system

	coupled system	**decoupled system**
Area (2004) km^2	2.8	6.7
Approx. process rate [g/(d*m^2)]	1'000	1
Approx. sediment budget [t/y]	392'000	2'900
Component of the sediment equation	output component	storage component
Erosion related to	precipitation intensity and climate	climate
Processes	Debris flow, gullying, natural weathering	slope erosion, natural weathering

6 Conclusions and perspectives

6.1 Thematic conclusions

The goal of the present thesis was to measure local erosion processes at defined sites with different land use within the Illgraben catchment and to receive a general view of the erosion behavior and processes that take place in the catchment. Even though it was not possible to gain a comprehensive knowledge of all the processes and mechanisms that are involved, a few new and interesting results could be found and a better understanding of the "black box" Illgraben catchment was obtained. Some of the original hypotheses were confirmed, whereas others did not apply. Like always, when a new method is applied, additional questions and assumptions arise beside results and new knowledge, and ask for further studies (also see section 6.3).

6.1.1 Verification of hypotheses

In this section, the focus is directed on the different hypotheses established in section 1.2 and if they apply or not in the catchment. An extensive discussion of the different topics and results can be found in the previous chapter 5 (results and discussion).

1. ***A strong influence of the grain size distribution, slope angle and the vegetation layer on erosion processes.***

This hypothesis applied for the measured silt fence plot sites, where plot sites with a vegetation layer, a smaller grain size distribution and a lower slope angle were characterized by a smaller erosion process rate (not statistically tested).

2. ***Differences in the erosion process rates between the decoupled subsystems forest, grassland and erosion.***

This hypothesis applied for the measured silt fence plot sites. Plots located in the subsystem grassland had a negligible process rate with 0.01 g/ ($d*m^2$) that was one order of magnitude smaller than the one of the subsystem forest with 0.5 g/ ($d*m^2$). The process rate of the subsystem forest was one order of magnitude lower than the one of the erosion (4.3 g/ ($d*m^2$).

3. ***Higher erosion rates for intensive precipitation events than for low precipitation events on the silt fence plot sites.***

This hypothesis applied partially for the investigated silt fence plots. A small correlation between the measured sediment amount and the precipitation intensity was detected only on the lower silt fence plots (E1, F1 and G1). In contrast, the amount collected in the upper fences (A1, A2, B1, B2, C1, C2, D1 and D2) was not influenced by precipitation. Too small precipitation events during the measurement season, a high soil infiltration capacity and other factors could have contributed.

4. ***Different processes in the coupled and decoupled systems.***

This hypothesis applied for the Illgraben catchment with its landscape connectivity. Results showed that the behavior of the coupled system is strongly related to precipitation intensity, whereas the decoupled system showed more relations towards the climate and including natural weathering processes. Moreover, the coupled system was more affected by gully erosion processes while the decoupled system showed only slope erosion processes.

5. ***Higher erosion rates and sediment outputs in the coupled system than the decoupled one.***

This hypothesis applied for the Illgraben catchment. The process rate of the coupled system was roughly three orders of magnitude larger than the one of the decoupled system (1000 g / (d*m^2) and 1 g / (d*m^2) respectively).

6. ***A high sediment output from the coupled areas in the northern catchment part.***

This hypothesis did not apply to the Illgraben catchment. The petrographic analysis (by David Schnydrig, UniBe) investigated the origin of the debris flow components mobilized in the coupled system. The analysis showed that over 60% of the debris flow material originated from the southern catchment side, 15% to the channel bed and only the remaining 25% to the northern catchment side.

7. ***An increase of the coupled system associated with a decrease of the decoupled system during the last 45 years.***

This hypothesis did not apply to the Illgraben catchment. Aerial photography from 1959, 1999 and 2004 and the periods in between showed an almost constant distribution between those two systems. That means the proportion between the coupled- and decoupled system stayed constant over the last 45 years.

8. ***An increase of the decoupled erosion subsystem during recent years.***

This hypothesis applied for the decoupled system. The decoupled erosion subsystem increased by 7.7% of the entire catchment area (which corresponds to 0.75 km^2) during the last 45 years. This increase was associated with the increase of the forest subsystem and the decrease of the grassland subsystem.

6.2 Possibilities and limits of the applied methods

The main methods used here were the silt fence measurement technique, aerial photograph analysis and the interpretation of the debris flow data that were collected at the force plate. The central idea examined was the landscape connectivity between a coupled- and decoupled system. Due to the very large differences detected in those two systems, the importance of landscape connectivity investigation was emphasized. The application of this landscape division was based on aerial photography observations for the separation in different systems and subsystems. The detection of area changes and the determination of slope angle distributions. Furthermore, the field measurements with the silt fence technique allowed for the study of erosional behavior and conditions on the different subsystems in the decoupled system. Finally, with the interpretation of the debris flow data the coupled system could be characterized. The analysis of the aerial photography with GIS was a simple method that contributed many basics of this thesis and showed nicely how the system changed in space and time during recent years. For a more detailed temporal analysis of the surface area changes, more aerial photography should be considered. The silt fence measurement technique was applied in an alpine mountain catchment for the first time and proved to be a good method for the investigation of the decoupled system. It was characterized by a low cost, easy measurement and a quick set up and disassembly. Its application in the decoupled system gave an interesting overview on the erosion behavior. To get a more precise view about this behavior during individual events and the various sites, more silt fence plots should be installed and the measurement period should cover a longer time scale. If the responses of slopes to individual precipitation events are of interest, silt fence measurements must be carried out immediately after every event. Because there were sometimes several rainfall events during one measurement interval, the individual rates could not always be distinguished in my investigation period. But due to the low number of precipitation events during the measurement period, and only few events with intensive rainfall, this did not represent a major problem in this thesis.

6.3 Perspectives

Through the application of different observation methods on erosion processes in the Illgraben catchment in this thesis, we better understand some interactions and discovered important factors. The division into coupled- and decoupled systems as well the following independent observations clearly showed large differences in landscape connectivity. The most important results out of this thesis for further researches were the determination of the active debris flow initiation zone and the different relations with precipitation in the systems. Now that we know the location of the debris flow initiation zone and its high importance for the sediment delivery, further research can focus on properties that can be found there as well on the initiation itself. Besides the scientific motivation the knowledge of this active zone could be used for efficient danger reductions or at least observations. Even though erosion in mountain catchments is not a new research topic, many processes are poorly understood. The application of landscape connectivity for an erosion analysis is new and brings various new perspectives and knowledge. But as always when new methods are applied and new knowledge arises and therefore many new questions are generated and the system becomes more and more complex. Therefore, the results of a new method required many new assumptions that could form a basis for further studies. Many of those assumptions were based on a catchment non-specific behavior, where other ones were more catchment specific. But catchment specific or not, every assumption shapes a new research topic and forms, as a part of a puzzle, a better comprehension of the entire system. Further research emerging from this thesis could be carried out in:

- Circumstantial analysis of the soil properties in the determined active debris flow initiation zone (weathering condition, possible permafrost occurrence, water saturation, grain sizes etc.)
- Breakdown of the debris flow initiation in the determined active debris flow. When and where does the flow process change into a mass movement process?
- Exploration of the assumed dynamic catchment steady state. Is a catchment steady state possible, how could this steady state be controlled, do other catchments show analog proportional behavior in their landscape connectivity for recent years, etc?
- Considerations regarding the Illgraben process rates and process rates of other catchments. Are the process rates of the subsystems and systems in the Illgraben catchment similar compared to other catchments or do they show other behaviors?
- Analysis of possible initiation factors that change a coupled system into a decoupled one and vice-versa. Also investigations on the lifetime of a decoupled- and coupled system.
- Research on the possible future behavior of the Illgraben catchment, mainly of the catchment output.
- Analysis of further aerial photography material that could be used as a better information on the processes that happened during the period between 1959 and 1999.
- Examination of the influence of land use changes in the Illgraben on the increase of the decoupled erosion areas.

Considering all the possible additional research topics listed above and many unidentified ones, it becomes apparent that there is still plenty of work to do.

7 References

Arattano, M., Deganutti, A.M. and Marchi, L., 1997. Debris flow monitoring activities in an instrumented watershed on the Italian Alps. In: C.-L. Chen (Editor), 1st International Conference on Debris flow Hazard Mitigation: Mechanics, Predictions and Assessment. American Society of Civil Engineers (ASCE), San Francisco, California, pp. 506-515.

Arattano, M. and Marchi, L., 2000. Video-derived velocity distribution along a debris flow surge. Physics and Chemistry of the Earth, 25(9): 781-784.

Avni, Y., 2004. Gully erosion incision inducting on going desertification in the arid regions of the Middle East, examples from the Negev highlands, southern Israel. Sichuan Science and Technology Press, China: 143-162.

BAFU, 1999. Hydrologisches Jahrbuch der Schweiz 1999, Bern.

Bätzing, W., 1996. Landwirtschaft im Alpenraum- Ansätze für eine Synthesedarstellung, Landwirtschaft im Alpenraum- unverzichtbar, aber Zukunftslos. Europäische Akademie Bozen (eds), Berlin, pp. 224-242.

Berti, M., Genevois, R., Lattusen, R., Simoni, A. and Tecca, P.R., 2000. Debris flow monitoring in the Acquabona watershed on the Dolomites (Italien Alps). Physics and Chemistry of the Earth, 25(9): 707-715.

Berti, M., Genevois, R., Simoni, A. and Tecca, P.R., 1999. Field observations of a debris flow event in the Dolomites. Geomorphology, 29(3-4): 265-274.

Betts, H.D., Trustrum, N.A., DeRose, R.C., 2003. Geomorphic changes in a complex gully system measured from sequential digital elevation models, and implications for management. Earth and Planetary Science Letters, 28: 1043-1058.

Bogaart, P.W., Van Balen, R.T., Kasse, C., Vanderberghe, J., 2003. Process based modeling of fluvial system response to rapid climate change. Quanternary Science Review, 22: 2077-2095.

Braton, S.B., 1979. Environment and Management, 3. Springer, New York.

Brierley, G. and Fryirs, K., 2005. Geomorphology and river management: application of the River Styles framework. Blackwell, Oxford.

Brierley, G., Fryirs, K., Jain, V., 2006. Landscape connectivity: the geographic basis of geomorphic applications. Area, 38.2: 165-174.

Bryan, R.B., 2000. Soil erodibility and processes of water erosion on hillslope. Geomorphology, 32: 385-415.

Bryan, R.B., Brun, S.E, 1999. Laboratory experiments on sequential scour/ deposition and their application to the development of banded vegetation. Catena, 37(1-2): 147-163.

Choppin, N.J., Richards, J.G., 1990. Use of vegetation in Civil Engineering. Butterworths, London, 292 pp.

Chorley, R.J., 1978. The hillslope hydrological cycle. Hillslope Hydrology. Wiley, Chichester.

Corominas, J., 1995. Evidence of basal erosion and shearing as mechanisms contributing the development of lateral ridges in mudslides, mudflows and other flow-like gravitational movements. Eng. Geology, 39: 45-70.

Crosta, G., 1998. Regobalization of rainfall thresholds: an aid to landslide hazard evaluation. Environmental Geology, 35(2-3): 131-145.

Dedkov, A.P. and Moszherin, V.I., 1992. Erosion and sediment yield in mountain regions of the world, Erosion, Debris Flows and Environment in Mountain Regions. IAHS, Chengdu.

Descroix, L. and Mathys, N., 2003. Processes, spatio temporal factors and measurements of current erosion in the french southern alps: a review. Earth Surface Processes and Landforms, 28: 993-1011.

Finkner, S.C., Nearing, M.A., Forster, G.R. and Giley, J.E., 1989. A simplified equation for modeling sediment transport capacity. Transactions of the ASAE, 32(5): 1545-1550.

Forster, G.R., 1982. Modeling the erosion process. In: C.T. Haan (Editor), Hydrologic modeling of small watersheds. American Society of Agricultural Engineers, St. Joseph, Mich. USA, pp. 297-380.

Frei, C. and Schär, C., 2000. Detection Probability of Trends in Rare Events: theory and Application to Heavy Precipitation in the Alpine Region. Journal of climate, 14.

Frei, C., Schär, Ch., Lüthi, D., Davies H.C., 1998. Heavy Precipitation Processes in a Warmer Climate. Geophysical Research letters, 25(9): 1431-1434.

Fryirs, K.A., Brierley, G.J., 2001. Variability in sediment delivery and storage along river courses in Bega catchment, NSW, Australia: implications for geomorphic river recovery. Geomorphology, 38: 237-265.

Fryirs, K.A., Brierley, G.J., Preston, N.J., Spencer, J., 2006. Catchment-scale (dis)connectivity in sediment flux in the upper Hunter catchment, New South Wales, Australia. Department of Physical Geography, Macquarie University.

Fuhrer, J., Beniston, M., Fischlin, A., Frei, Ch., Goyette, S., Jasper, K., Pfister, Ch., 2006. Climate risks and their impact on agriculture and forests in Switzerland. Climatic Change 79: 79-102.

Geo7, 2000. Geomorphologische Analyse des Illgrabens, Geo 7, Bern.

Goudie, A.S., 2006. Global warming and fluvial geomorphology. Geomorphology, 79: 384-394.

Harvey, A.M., 2002. Effective timescale of coupling within fluvial systems. Geomorphology, 44: 175-201.

Hooke, J., 2003. Coarse sediment connectivity in river channel systems: a conceptual framework and methodology. Geomorphology, 56: 79-94.

Hürlimann, M., Rickenmann, D. and Graf, C., 2003. Fild an monitoring data of debris flow events in the Swiss Alps. Canadian Geotech, 40: 161-175.

Hutchinson, J.N., 1988. Morphological and geotechnical parameters of landslides in relation to geology and hydrogeology. Landslides and Processes, 1. Wiley, 3-35 pp.

IPCC, 2001. The Climate Change 2001- the scientific basis. Cambridge University Press, Cambridge.

Kasai, M., Brierley, G., Page, M.J., Marutani, T., Trustrum, N.A., 2005. Impacts of land use change on patterns of sediment flux in Weaamaia catchment, New Zealand. Catena, 64: 27-60.

Kaufmann-Havoy, R., 2005. NFP 48: Landscapes and Habitats of the Alps, Bern.

Klein Tank, A.G.M. and Können, G.P., 2003. Trends in indices of daily temperature and precipitation extremes in Europe 1946-1999. Journal of Climate, 16: 3665-3680.

Markart, G., Kohl, B., 1995. Starkregensimulation und bodenphysikalische Kennwerte als Grundlage der Abschätzung von Abfluss- und Infiltrationseigenschaften alpiner Boden-/Vegetationseinheiten, Institut für Lawinen- und Wildbachforschung, Forstliche Bundesversuchsanstalt Wien, Wien.

Markart, G., Kohl, B., Starnberger, R., Gallmetzer, W., 2004. Erosionsentwicklung auf begrünten alpinen Steilhängen- Prozessanalyse auf Kleinflächen. BFW.

Mathys, N., Klotz, S., Esteves, M., Descroix, L., Lapetite, J.M., 2005. Runoff and erosion in the Black Marls of the French Alps: Observation and measurements at the plot scale. Catena, 63: 261-281.

McArdell, B.W., Bartelt, P. and Kowalski, J., in review. Field observations of basal forces and fluid pore pressure in a debris flow. WSL. Geophysical research letters.

Merritt, E., 1984. The identification of four stages during microrill development. Earth Surface Processes and Landforms, 9: 493-496.

Milliman, J.D. and Syvitski, P.M., 1992. Geomorphic/tectonic control on sediment discharge to the ocean: the importance of small mountainous rivers. Journal of Geology, 100: 525-544.

Mitasova, H., Hofierka, J., Zlocha, M. and Iverson, R.L., 1996. Modeling topographic potential for erosion and deposition using GIS. Int. Journal of Geographical Information Science, 10(5): 629-641.

Montgomery, D.R., 2003. Predicting landscape-scale erosion rates using digital elevation models. Surface Geosciences, 335: 1121-1130.

Montgomery, D.R., Brandon, M.T., 2002. Topographic controls on erosion rates in tectonically active mountain ranges. Earth and Planetary Science Letters, 201: 481-489.

Morgan, R.P.C., 2005. Soil Erosion and Conservation. Blackwell

Nilaweera, N.S., Nutulay, P., 1999. Role of tree roots in slope stabilization. Bulletin of Engineering, Geology and the Environment, 57: 337-342.

Phillips, C.J. and Davies, R.H., 1991. Determing rheological parameters of debris flow material. Geomorphology, 4(2): 101-110.

Poesen, J., Lavee, H., 1994. Rock fragments in top soils: significance and processes. Catena, 23(1-2): 1-28.

Rickenmann, D. and Koch, T., 1997. Comparison of debris flow modeling approaches. In: C.-L. Chen (Editor), 1st International Conference on Debris flow hazard Mitigation: Mechanics, Predictions and Assessment. American Society of Civil Engineers (ASCE), San Francisco, California, pp. 575-585.

Rickenmann, D. and Weber, D., 2000. Flow resistance of field and experimental debris flow in torrent channels, 2nd International Conference on Debris flow hazard mitigation: Mechanics, Predictions and Assessment, pp. 245-254.

Riebe, C.S., Kirchner, J.W., Granger, D.E., Finkel, R.C., 1991. Minimal climatic control on erosion rates in the Sierra Nevada, California. Geology, 29: 447-450.

Robichaud, P.R., Brown, R.E., 2002. Silt Fences: An Economical Technique for Measuring Hillslope Soil Erosion, United States Department of Agriculture, Forest Service, Rocky Mountain Research Station.

Schlunegger, F., 2002. Impact of hillslope-derived sediment supply on drainage basin development in small watersheds at the northern border of the central Alps of Switzerland. Geomorphology, 46: 285-305.

Schuerch, P., Densmore, A.L., McArdell, B.W., Molnar, P., 2006. The influence of landsliding on sediment supply and channel change in a steep mountain catchment. Geomorphology, 78: 222-235

Selby, M., 1993. Hillslope materials and processes, 1. Oxford University Press.

Sidle, R.C. and Onda, Y., 2004. Hydrogeomorphology: overview of an emerging science. Hydrological Processes, 18: 597-602.

Suwa, H., 1989. Field observation of debris flow, Japan-China (Taipei) Joint Seminar on Natural Hazard Mitigation, Kyoto, Japan, pp. 343-352.

T&C and WSL, 2005. Technischer Bericht Notfallkonzept Illgraben. PROGE Notfallkonzept Illgraben, Visp, pp. 21.

Tasser, E., 2001. Südtirols Almen im Wandel. Europäische Akademie Bozen 28.

Tasser, E., Mader, M., Tappeiner, U., 2003. Effects of land use in alpine grasslands on the probability of landslides. Basic Applied Ecology, 4: 271-280.

Tognacca, C., 2000. Murgangsenstehung im Gerinne. Mitteilung der Versuchsanstalt für Wasserbau, Hydrologie und Glaciologie, 164: 259.

Valentin, C., 2005. Gully erosion: Impacts, factors and control. Catena, 63: 132-153.

Verstraeten, G., 2006. Regional scale modeling of hillslope sediment delivery with SRTM elevation data. Geomorphology, 81: 128-140.

Werner, P., 1985. La végétation de finges et de son Rhône sauvage. Bull. Murithienne, 103: 39-84.

Wischmeyer, W.H. and Smith, D.D., 1978. Predicting rainfall erosion losses- a guide to conservation planning. Agriculture Handbook, 537. U.S. Department of Agriculture, Washington D.C.

Zhang, S., 1993. A comprehensive approach to the observation and prevention of debris flows in China. Natural Hazards 7: 1-23.

A Appendix

A.1 Orthophotos

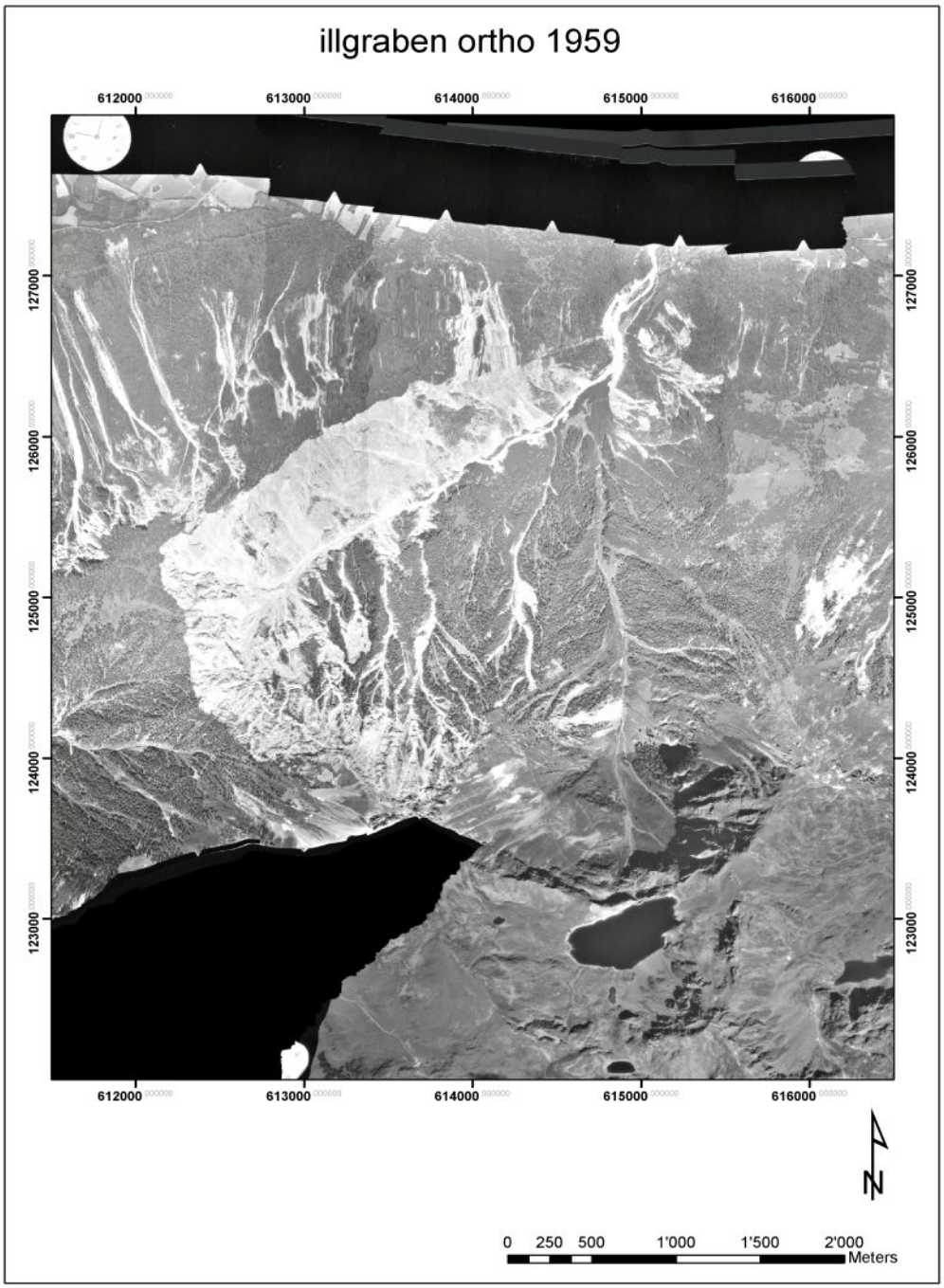

Figure A-1 Illgraben orthophoto 1959 (David Schnydrig and Corina Gwerder, 2006)

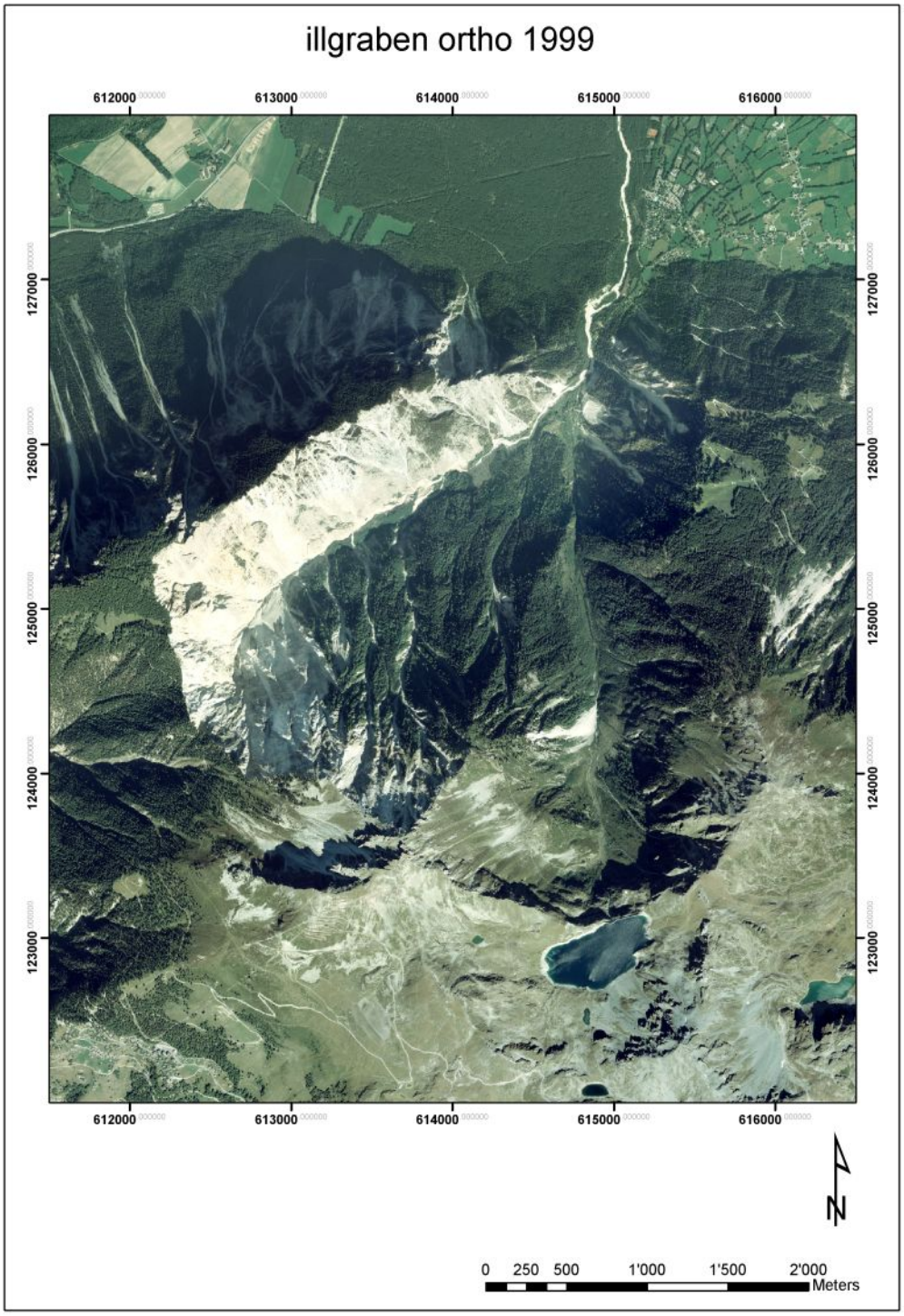

Figure A-2 Illgraben Orthophoto 1999 (Swiss Image, copyright Swisstopo 2007)

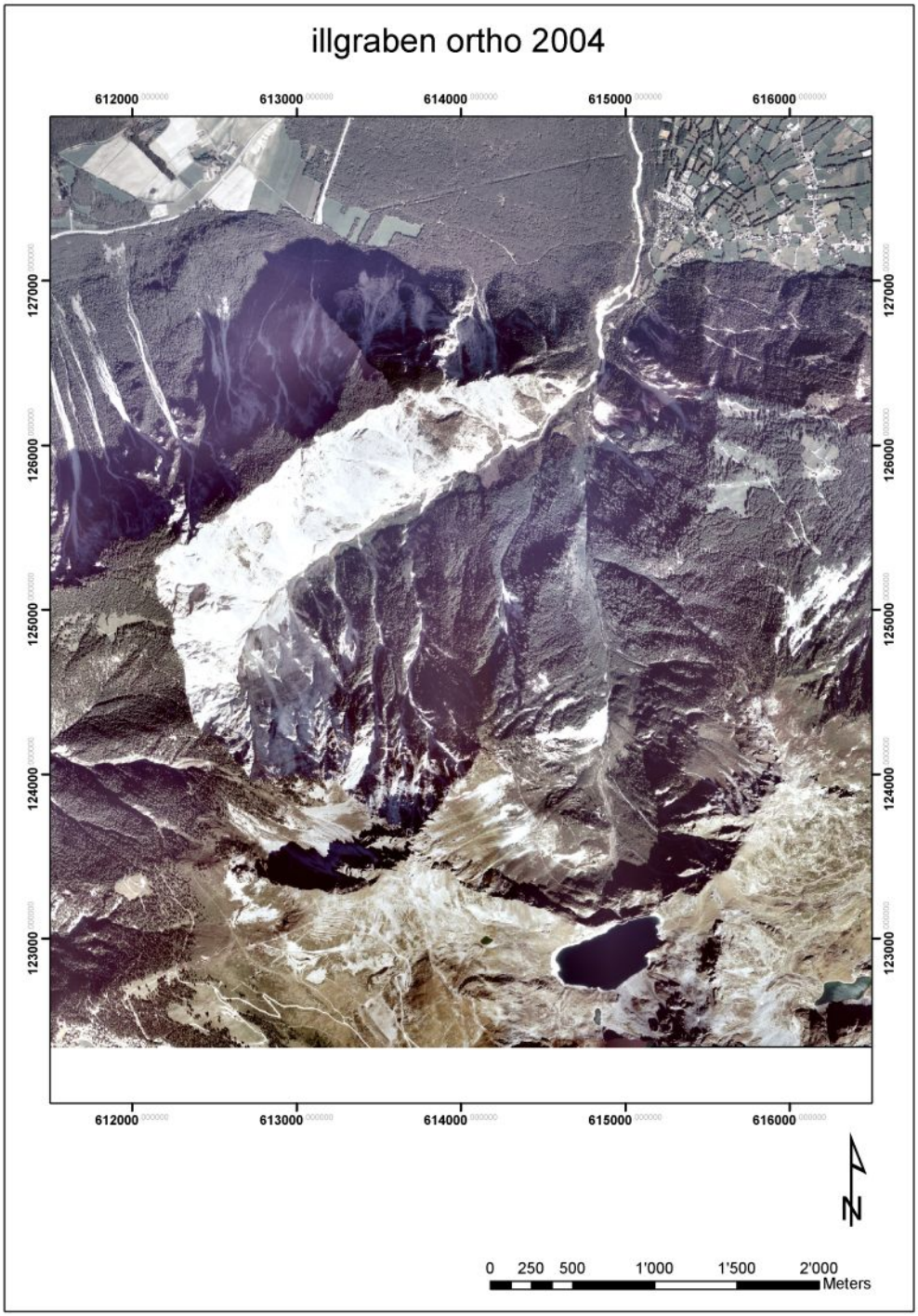

Figure A-3 Illgraben orthophoto 2004 (David Schnydrig and Corina Gwerder, 2006)

A.2 Debris flow events between 1932 and 2004 in the Illgraben

Table 40 Debris flows between 1932-2000 (T&C and WSL, 2005)

Date	year	size	process	comment
29. Jun.	1932	3	Debris flow	
4. Sep.	1944	2	Debris flow	
25. Jul.	1945	1	Debris flow	
8. Aug.	1945	2	Debris flow	
19. Aug.	1945	1	Debris flow	
28. Jul.	1948	3	Debris flow	
24. Jun.	1953	2	Debris flow	
6. Jun.	1961	4	Debris flow	
9. Jun.	1961		Debris flow	**
11. Jul.	1961		Debris flow	**
19. Jul.	1961		Debris flow	**
1. Jun.	1962		Debris flow	**
2. Jun.	1962		Debris flow	**
8. Jun.	1963		Debris flow	**
18. Jun.	1963		Debris flow	**
28. Jun.	1963		Debris flow	**
12. Aug.	1963		Debris flow	**
20. Mai	1964		Debris flow	**
30. Mai	1964		Debris flow	**
2. Jun.	1964		Debris flow	**
14. Jun.	1964		Debris flow	**
17. Jun.	1964		Debris flow	**
4. Mai	1965		Debris flow	**
7. Jun.	1965		Debris flow	**
8. Jun.	1965		Debris flow	**
18. Jun.	1965		Debris flow	**
4. Jul.	1965		Debris flow	**
25. Jul.	1965		Debris flow	**
31. Jul.	1982	1	MG (Rhyner)	
6. Jun.	1985	1	MG (T&C and WSL)	
6. Jul.	1986	2	Debris flow	Date unsure, Ph. ZenR.
7. Jun.	1987	1	Debris flow	
29. Aug.	1988	1	Debris flow	
16. Aug.	1989	2	Debris flow	Date unsure, Ph. ZenR.
13. Aug.	1990	1	Debris flow	
12. Jul.	1991	3	Debris flow	
3. Okt.	1995	3	Debris flow	Perhaps. 23.10.
21.Aug.	1997	2	Debris flow	Date unsure
30. Okt.	1998	1	Debris flow	
16. Aug.	1999	3	Debris flow	
3. Jun.	2000	1	Debris flow	
28. Jun.	2000	2	Debris flow	

* estimated volume divided into 4 classes:

1:	< 25'000 m^3	3:	75'000 – 250'000 m^3
2:	25'000 – 75'000 m^3	4	> 250'000 m^3

** Source area by a rock fall material (size not known).

An additional source of debris flow is attributed to a large landslide / rock avalanche in 1961.

Table 41 Debris flows between 2000-2004 (T&C and WSL, 2005)

Date	Volume [m^3]	Q_{max} [m^3/s]	H_{max} [m]	V_{front} [m/s]	Precipitation [mm/12h]	Initiation and comment
03.06.2000 17:18	10'000	19[b]	2.50	2.7	Not available	Field observation
28.06.2000 13:58	90'000	92	2.90	4.1	Not available	Calibration event for the Illgraben protection concept
24.07.2000 07:40	20'000	6	1.42	1.1	Not available	
06.06.2001 06:34	32'000	43	1.93	3.4	14.3	precipitation
09.06.2001 01:09	7'500	15	1.00	3.0	11.4	precipitation
15.06.2001 20:42	10'500	18	0.96	3.8	7.4	precipitation
28.06.2001 05:22	36'000	52	1.58	6.3	17.4	precipitation
07.07.2001 09:43	45'000	114	2.65	6.1	14.2	precipitation
21.07.2002 12:15	< 5'000	---	1.50	---	20.5	Very small event
31.07.2002 12:07	20'000	62	2.57	3.1	---	Unknown initiation, granular flow
10.08.2002 10:50	71'000	100	1.78	8.6	31.6	precipitation
29.06.2003 00:00	unbekannt	---	1.00	---	---	Unknown initiation
19.05.2003 17:50	90'000	94	3.26	3.5	13.3	precipitation
08.06.2003 19:36	< 5'000	---	0.70	---	9.6	precipitation
12.08.2004 17:55	34'000	31	1.50	3.0	8.6	precipitation
24.08.2004 10:44	36'000	17	1.30	2.3	23.4	precipitation
26.10.2004 13:28	< 5'000	5	0.90	3.2	16.8	Precipitation, had a second wave

A.3 Illgraben Geological map

Figure A-4 Illgraben geological map (WSL)

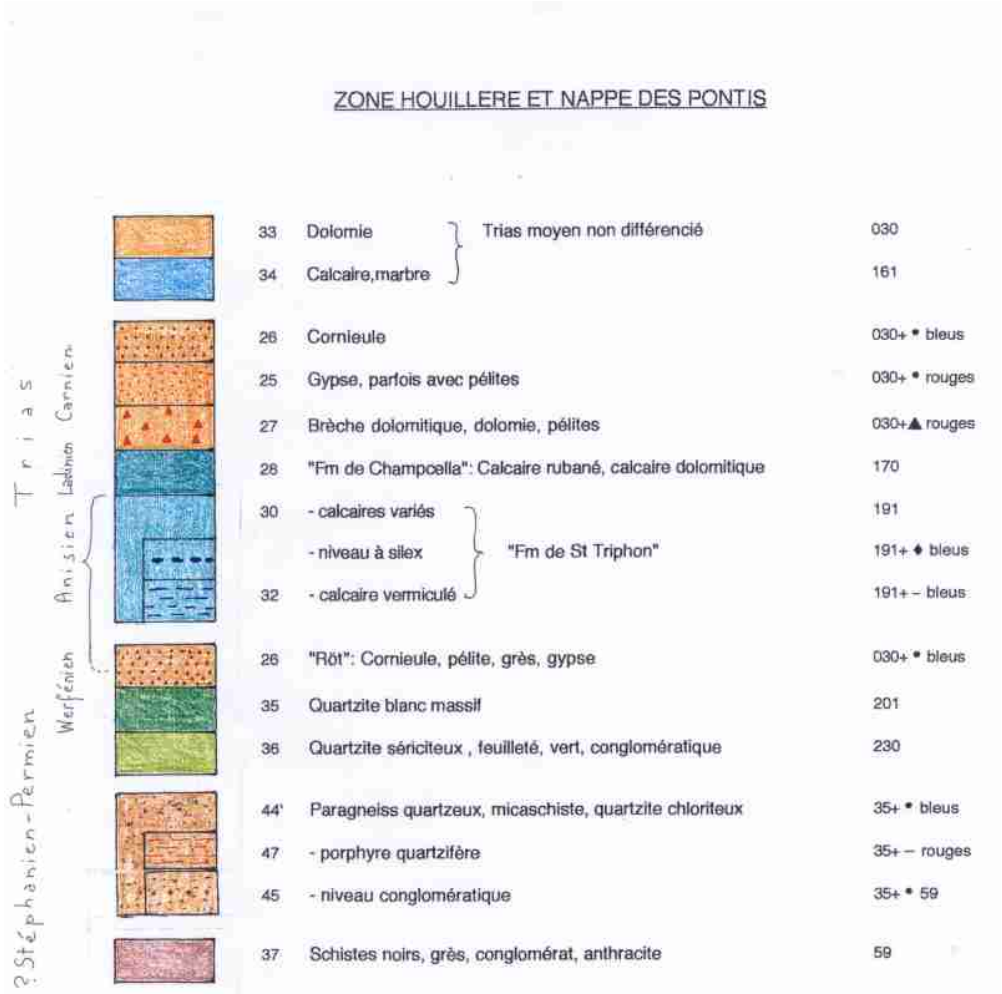

Figure A-5 Legend of the geological map Illgraben (WSL)

A.4 Silt fence plot measurements for the entire measurement period

A.4.1 Plot precipitation amount

Table 42 Plot precipitation [mm]

date	A1	A2	B1	B2	C1	C2	D1	D2	E1	F1	G1
26.6.-11.7.06	15.75	22.5	20	19.5	18	5	17.5	14.5			
11.7.-13.7.06	0	0	0	0	0	0	0	0			
13.7.-20.7.06							6	6.25	-	-	-
13.7.-26.7.06	8.5	11.5	12.5	12	12	3.5					
20.7.-26.7.06							1.5	1			
26.7.-06.8.06							32	28.5			
28.7.-02.8.06									10		
02. 8.-06.8.06									24.75	29.75	30
26.7.-11.8.06	35	29	35	35	35	15.5					
06.8.-11.8.06							1	1.25	0	0.5	0.75
11.8.-16.8.06							12.5	13.5	11.5	12	12.5
11.8.-23.8.06	21	21.5	29	26.25	24.25	8.75					
16.8.-23.8.06							2.25	2.25	2.75	3	3
23.8.-30.8.06	30	33	35	35	35	16	29.25	29	29	34	34
30.8.-07.9.06	0	0	0	0	0	0.5	0.5	0.25	0.25	0	0
07.9.-20.9.06	12.25	12	14.75	14.75	13	4	7.5	10	11	10.75	10.75
20.9.-27.9.06	6	6	6.5	6.25	6.25	4	4.75	5.75	4.75	5	5
27.9.-04.10.06							18	18	17	20	20
27.9.-11.10.06	23.5	25	29	26.5	26.5	11	-				
04.10.-11.10.06							5	5.5	4.75	4.5	4.75

A.4.2 Plot precipitation rate

Table 43 Plot precipitation rate [mm/h] (number of hours with rain at Pluviometer 3 forms the rain duration)

date	A1	A2	B1	B2	C1	C2	D1	D2	E1	F1	G1
26.6.-11.7.06	0.51	0.73	0.65	0.63	0.58	0.16	0.56	0.47			
11.7.-13.7.06	0.00	0.00	0.00	0.00	0.00	0.00	0.00	0.00			
13.7.-20.7.06							0.50	0.33			
13.7.-26.7.06	1.42	1.92	2.08	2.00	2.00	0.58					
20.7.-26.7.06							0.50	0.33			
26.7.-06.8.06							0.84	0.75			
28.7.-02.8.06									2.00		
02. 8.-06.8.06									4.27	5.13	5.17
26.7.-11.8.06	0.88	0.73	0.88	0.88	0.88	0.39					
06.8.-11.8.06							0.5	0.63	0.00	0.25	0.38
11.8.-16.8.06							0.54	0.59	0.50	0.52	0.54
11.8.-23.8.06	0.60	0.61	0.83	0.75	0.69	0.25					
16.8.-23.8.06							0.19	0.19	0.23	0.25	0.25
23.8.-30.8.06	0.91	1.00	1.06	1.06	1.06	0.48	0.89	0.88	0.88	1.03	1.03
30.8.-07.9.06	0.00	0.00	0.00	0.00	0.00	0.17	0.17	0.08	0.08	0.00	0.00
07.9.-20.9.06	0.45	0.44	0.55	0.55	0.48	0.15	0.28	0.37	0.41	0.40	0.40
20.9.-27.9.06	0.38	0.38	0.41	0.39	0.39	0.25	0.30	0.36	0.30	0.31	0.31
27.9.-04.10.06							1.00	1.00	0.94	1.11	1.11
27.9.-11.10.06	1.07	1.14	1.32	1.20	1.20	0.50					
04.10.-11.10.06							1.25	1.38	1.19	1.13	1.19

A.4.3 Sediment amount on silt fence plots

Table 44 Sediment amount measurements on silt fence plots in [kg]

date	A1	A2	B1	B2	C1	C2	D1	D2	E1	F1	G1
26.6.-11.7.06	1.1	0.45	0.0021	0.0255	0.0055	0.5	2.75	13			
11.7.-13.7.06	0	0	0	0	0	0	0	0			
13.7.-20.7.06							2.35	6.15			
13.7.-26.7.06	0.6	0.6	0.0045	0.0049	0.0641	0.15					
20.7.-26.7.06							4.9	12.2			
26.7.-06.8.06							4.45	27.2			
28.7.-02.8.06									1.8		
02. 8.-06.8.06									4.6	0.165	2.75
26.7.-11.8.06	0.5	0.7	0	0	0	0.5					
06.8.-11.8.06							1.9	9.95	0.55	0.1	0.5
11.8.-16.8.06							0.8	6.3	0.6	1.3	3.5
11.8.-23.8.06	0.25	0	0	0	0	0.35					
16.8.-23.8.06							0.8	6.3	2.1	0.5	2.05
23.8.-30.8.06	0	0.1	0	0	0	0.06	2.45	9	40	3.65	5.8
30.8.-07.9.06	0.85	0.4	0	0	0	0	0.8	4.7	3.1	0.5	0.4
07.9.-20.9.06	0.5	0	0	0	0	0.3	4.8	24.5	28.1	3	6.2
20.9.-27.9.06	0.1	0.1	0	0	0	0.2	2.1	6.5	3.1	0	0.8
27.9.-04.10.06							1.2	7.2	2.6	0	1.2
27.9.-11.10.06	0.3	0.05	0	0	0	0.15					
04.10.-11.10.06							0.35	2.25	1.05	0.35	1.7

A.4.4 Sediment rates on silt fence plots

Table 45 Sediment rates on silt fence plots per measurement day [kg/d]

date	[d]	A1	A2	B1	B2	C1	C2	D1	D2	E1	F1	G1
26.6.-11.7.06	15	0.07	0.03	0.00	0.00	0.00	0.03	0.18	0.87			
11.7.-13.7.06	2	0.00	0.00	0.00	0.00	0.00	0.00	0.00	0.00			
13.7.-20.7.06	7							0.34	0.88			
13.7.-26.7.06	13	0.05	0.05	0.00	0.00	0.00	0.01					
20.7.-26.7.06	6							0.82	2.03			
26.7.-06.8.06	11							0.40	2.47			
28.7.-02.8.06	5									0.36		
02. 8.-06.8.06	4									1.15	0.4	0.69
26.7.-11.8.06	16	0.03	0.04	0.00	0.00	0.00	0.03					
06.8.-11.8.06	5							0.38	1.99	0.11	0.02	0.10
11.8.-16.8.06	5							0.16	1.26	0.12	0.26	0.70
11.8.-23.8.06	12	0.02	0.00	0.00	0.00	0.00	0.03					
16.8.-23.8.06	7							0.11	0.90	0.30	0.07	0.29
23.8.-30.8.06	7	0.00	0.01	0.00	0.00	0.00	0.01	0.35	1.29	5.71	0.52	0.83
30.8.-07.9.06	8	0.11	0.05	0.00	0.00	0.00	0.00	0.10	0.59	0.39	0.06	0.05
07.9.-20.9.06	13	0.04	0.00	0.00	0.00	0.00	0.02	0.37	1.88	2.16	0.23	0.48
20.9.-27.9.06	7	0.01	0.01	0.00	0.00	0.00	0.03	0.30	0.93	0.44	0.00	0.11
27.9.-04.10.06	7							0.17	1.03	0.37	0.00	0.17
27.9.-11.10.06	14	0.02	0.00	0.00	0.00	0.00	0.01					
04.10.-11.10.06	7							0.05	0.32	0.15	0.05	0.24

A.5 Rainfall data and sediment rates on individual plots (E, F and G)

A.5.1 Summary E, F and G

Table 46 Summary of Plot E1

	Sed.rate [kg/d]	# h with rain at P3	P3 max [mm/h]	Precipitation Rate [mm/h] R-plot/P3	Precipitation Amount [mm] R-plot
28.07-02.08.06	0.36	7	1.2	1.43	10
02.08-06.08.06	1.15	30	3.2	0.83	24.75
06.08-11.08.06	0.11	2	0.6	0	0
11.08-16.08.06	0.12	23	1.8	0.5	11.5
16.08-23.08.06	0.3	12	2.4	0.23	2.75
23.08-30.08.06	5.71	33	6	0.88	29
30.08-07.09.06	0.39	3	0.4	0.08	0.25
07.09-20.09.06	2.16	27	1.6	0.41	11
20.09-27.09.06	0.44	16	0.8	0.30	4.75
27.09-04.10.06	0.37	18	7.2	0.94	17
04.10-11.10.06	0.15	4	4	1.19	4.75

Table 47 Summary of Plot F1

	Sed.rate [kg/d]	# h with rain at P3	P3 max [mm/h]	Precipitation Rate [mm/h] R-plot/P3	Precipitation Amount [mm] R-plot
02.08-06.08.06	0.4	30	3.2	5.13	0.99
06.08-11.08.06	0.02	2	0.6	0.25	0.5
11.08-16.08.06	0.26	23	1.8	0.52	12
16.08-23.08.06	0.07	12	2.4	0.25	3
23.08-30.08.06	0.52	33	6	1.03	34
30.08-07.09.06	0.06	3	0.4	0	0
07.09-20.09.06	0.23	27	1.6	0.4	10.75
20.09-27.09.06	0	16	0.8	0.31	5
27.09-04.10.06	0	18	7.2	1.11	20
04.10-11.10.06	0.05	4	4	1.13	4.5

Table 48 Summary of Plot G1

	Sed.rate [kg/d]	# h with rain at P3	P3 max [mm/h]	Precipitation Rate [mm/h] R-plot/P3	Precipitation Amount [mm] R-plot
02.08-06.08.06	0.69	30	3.2	1	30
06.08-11.08.06	0.10	2	0.6	0.38	0.75
11.08-16.08.06	0.70	23	1.8	0.54	12.5
16.08-23.08.06	0.29	12	2.4	0.25	3
23.08-30.08.06	0.83	33	6	1.03	34
30.08-07.09.06	0.05	3	0.4	0	0
07.09-20.09.06	0.48	27	1.6	0.4	10.75
20.09-27.09.06	0.11	16	0.8	0.31	5
27.09-04.10.06	0.17	18	7.2	1.11	20
04.10-11.10.06	0.24	4	4	1.19	4.75

A.5.2 Summary of the measurement intervals for E, F and G

Table 49 Interval 28.7.-02.8.06

Rain events	Precipitation interval	# hours with rain	Max. intensity [mm/h]	Precipitation amount [mm]	Precipitation rate [mm/#h]
31.7.-01.8.06	21-01	2	1.2	1.6	0.8
01.8.06	05-11	5	0.6	1.4	0.28

Table 50 Interval 02.8.-06.8.06

Rain events	Precipitation interval	# hours with rain	Max. intensity [mm/h]	Precipitation amount [mm]	Precipitation rate [mm/#h]
3.8.06	02-18	11	3.2	17	1.55
4.8.06	02-06	4	0.8	2	0.5
4.8-5.8.06	16-09	14	2.4	14	1

Table 51 Interval 11.8.-16.8.06

Rain events	Precipitation interval	# hours with rain	Max. intensity [mm/h]	Precipitation amount [mm]	Precipitation rate [mm/#h]
11.8-12.8.06	23-07	6	1.4	5.8	0.97
13.8.06	00-16	12	1.8	11.4	0.95
14.8.06	10-11	1	0.2	0.2	0.2
15.8.-16.8.06	23-03	4	0.8	1.6	0.4

Table 52 Interval 23.8.-30.8.06

Rain events	Precipitation interval	# hours with rain	Max. intensity [mm/h]	Precipitation amount [mm]	Precipitation rate [mm/#h]
24.8.06	11-13	2	0.4	0.6	0.3
26.8-27.8.06	16-05	8	1.8	6.6	0.825
28.8.06	15-00	9	6	10.8	1.2
29.8-30.8.06	14-08	14	2.8	13.8	0.99

Table 53 Interval 07.9.-20.9.06

Rain events	Precipitation interval	# hours with rain	Max. intensity [mm/h]	Precipitation amount [mm]	Precipitation rate [mm/#h]
09.9.06	23-00	1	1	1	1
10.9.06	18-19	1	0.6	0.6	0.6
11.9.06	20-21	1	0.4	0.4	0.4
15.9.06	09-20	4	1.4	3.4	0.85
17.9.06	05-16	10	1.6	5.6	0.56
17.9.-18.9. 06	22-08	8	1	5	0.625
18.9.06	16-17	1	0.2	0.2	0.2
19.9.06	04-05	1	0.2	0.2	0.2

Table 54 Interval 27.9.-04.10.06

Rain events	Precipitation interval	# hours with rain	Max. intensity [mm/h]	Precipitation amount [mm]	Precipitation rate [mm/#h]
30.9.06	05-00	4	0.2	0.8	0.2
01.9.-02.9.06	11-04	10	2.2	9	0.9
03.10.06	14-18	4	7.2	12.4	3.1

A.5.3 Abridged version of six individual measurement intervals

Table 55 Measurement interval between 28.7.-2.8.06

	28.7.06	29.7.06	30.7.06	31.7.06	01.8.06	0.2.8.06
01:00	/				1.2	
02:00	/					
03:00	/					
04:00	/					
05:00	/					
06:00	/				0.2	
07:00	/					
08:00	/				0.2	
09:00	/				0.2	
10:00	/				0.6	
11:00	/				0.2	
12:00	/					
13:00						/
14:00						/
15:00						/
16:00						/
17:00						/
18:00						/
19:00						/
20:00						/
21:00						/
22:00				0.4		/
23:00						/
00:00						/

Table 56 Measurement interval between 02.8.-06.8.06

	02.8.06	03.8.06	04.8.06	05.8.06	06.8.06
01:00	/			1.6	
02:00	/			2.4	
03:00	/	0.6	0.8	1.4	
04:00	/		0.4	1.8	
05:00	/	3.2	0.4	0.8	
06:00	/	1.6	0.4		
07:00	/	1			
08:00	/	2.8		0.4	
09:00	/	2.6		0.8	
10:00	/	0.2			
11:00	/				
12:00	/	0.6			
13:00					/
14:00					/
15:00		3.2			/
16:00					/
17:00		1.0	0.4		/
18:00		0.2			/
19:00			0.4		/
20:00			0.4		/
21:00			0.8		/
22:00			0.6		/
23:00			1.2		/
00:00			1		/

Table 57 Measurement interval between 11.8.-16.8.2006

	11.8.06	**12.8.06**	**13.8.06**	**14.8.06**	**15.8.06**	**16.8.06**
01:00	/		0.8			0.2
02:00	/	0.2	0.4			0.8
03:00	/					0.2
04:00	/	1.2	0.2			
05:00	/	1				
06:00	/	1.4				
07:00	/	0.4				
08:00	/		0.8			
09:00	/		1.8			
10:00	/		1.4	0.2		
11:00	/		0.6			
12:00	/		1			
13:00			0.2			/
14:00			1.6			/
15:00			1.4			/
16:00			1.2			/
17:00						/
18:00						/
19:00						/
20:00						/
21:00						/
22:00						/
23:00						/
00:00	0.2				0.4	/

Table 58 Measurement interval between 23.8.-30.8.06

	23.8.06	24.8.06	25.8.06	26.8.06	27.8.06	28.8.06	29.8.06	30.8.06
01:00	/							
02:00	/				0.4			0.2
03:00	/				1.4			0.2
04:00	/				0.4			
05:00	/				0.6			0.2
06:00	/							
07:00	/							
08:00	/							0.8
09:00	/							
10:00	/							
11:00	/							
12:00	/	0.4						
13:00		0.2						
14:00								/
15:00							0.6	/
16:00						0.4	1.8	/
17:00				0.6		1.6	2	/
18:00				1.8		1.8	2.8	/
19:00				1.2		1.8	2.6	/
20:00				0.2		6	2.8	/
21:00						1.6	1.6	/
22:00						1	0.8	/
23:00						1.6	0.4	/
00:00						0.4	0.4	/

Table 59 Measurement interval between 7.9.-20.9.06

	07.9	08.9	09.9	10.9	11.9	12.9	13.9	14.9	15.9	16.9	17.9	18.9	19.9	20.9
01	/													
02	/													
03	/											0.2		
04	/											0.6		
05	/											1	0.2	
06	/										0.2	0.4		
07	/										0.2	0.4		
08	/											0.2		
09	/										0.4			
10	/										0.4			
11	/								1.4		0.4			
12	/										1			
13											0.4			/
14											0.6			/
15											1.6			/
16											0.4			/
17												0.2		/
18									0.4					/
19				0.6					1					/
20									0.6					/
21					0.4									/
22											0.2			/
23														/
00			1								0.2			/

Table 60 Measurement interval between 27.9-04.10.06

	27.9.06	28.9.06	29.9.06	30.9.06	01.10.06	02.10.06	03.10.06	04.10.06
01:00	/					0.4		
02:00	/							
03:00	/					0.2		
04:00	/					0.2		
05:00	/							
06:00	/			0.2				
07:00	/							
08:00	/							
09:00	/							
10:00	/							
11:00	/							
12:00	/				0.6			
13:00								/
14:00								/
15:00				0.2	0.2		3.6	/
16:00							7.2	/
17:00							1.4	/
18:00							0.2	/
19:00								/
20:00					1			/
21:00					2.2			/
22:00					2			/
23:00				0.2	1.8			/
00:00				0.2	0.4			/

A.6 Documentation

A.6.1 Silt fence plots installations

Figure A-6 Installations 1 (Corina Gwerder)

Figure A-7 Installations 2 (Corina Gwerder)

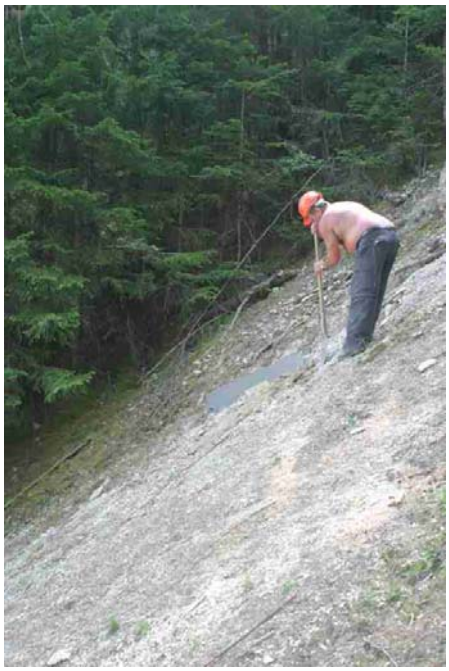

Figure A-8 Installations 3 (Corina Gwerder)

Figure A-9 Installations 4 (Corina Gwerder)

A.6.2 Helpers

Figure A-10 My installation-, supporting- and measurement-team (Christian, Alexandre, Leslie, Kari, Annemarie, Path, Corinna, Chistoph, François)

Figure A-11 My installation-, supporting- and measurement-team (Margrit, Thomas, Kurt, Nicolas, Lydia, David, Brian, Fritz, Peter)